MAGISTERARBEIT

Titel der Magisterarbeit

Vertical profiles of Sulphur dioxide in the Venusian lower atmosphere

Verfasser

Alen Đuričić, Bakk. rer. nat.

Angestrebter akademischer Grad

Magister der Naturwissenschaften (Mag. rer. nat.)

Wien, März 2012

Studienkennzahl lt. Studienblatt: A 066 861

Matrikelnummer: 0200035

Studienrichtung lt. Studienblatt: Astronomie

Betreuerin: Univ. Prof. Dr. Maria G. Firneis

Contents

Acknowledgements 4
Summary 5
Abstract (in German) 9
Exploration of Venus 10
1.1 The very first explorations 10
1.2 The exploration during the cold war 12
1.3 The exploration after the cold war 16
1.4 Near Infrared Windows 19
1.5 The timeline of the spacecrafts sent to Venus 22
The Venusian atmosphere 25
2.1 General overview 25
2.2 Comparison of Earth and Venus 30
2.3 Sulphur bearing compounds 32
2.4 Water Vapor and D/H Ratio 36
2.4 Carbon Monoxide 37
2.5 Hydrogen Halides 39
Sulphur dioxide in the Earth's Atmosphere 40
3.1 Sulphur dioxide emissions 40
3.2 Anthropogenic emissions 44
3.3 The Sulphur Cycle 46
Vertical profile of sulphur dioxide 50
4.1 Vertical data points 50
4.2 Model A and model B 53
4.3 Linear vertical profile 54
4.4 Exponential vertical profile 56
4.5 Cubic Spline vertical profile 58
Calculations with the vertical profile 60
5.1 Plotting the density profile 60
5.2 Plotting the temperature and pressure profile 61
5.3 Calculating the mass of the atmosphere 63
5.4 Sulphur dioxide in the atmosphere 64

5.5 Vertical profiles with the transformed mixing ratio 66
Calculating the total amount of sulphur dioxide 69
6.1 The numerical calculations 69
6.2 Using the linear vertical profile 70
6.3 Using the exponential vertical profile 70
6.4 Using the cubic spline vertical profile 71
6.5 Comparing the results 72
6.6 Proving the accuracy 72
Estimating the destruction rate 75
7.1 Weathering on Venus' surface 75
7.2 Discussing the results 78
Appendix 1 80
Appendix 2 83
Appendix 3 87
Appendix 4 91
Appendix 5 95
Appendix 6 98
Appendix 7 101
Appendix 8 105
Appendix 9 109
Appendix 10 113
Appendix 11 117
Appendix 12 120
Appendix 13 123
Appendix 14 134
Appendix 15 145
Appendix 16 156
Reference List 157
Picture Reference List 163
Curriculum Vitae 165

Acknowledgements

I am grateful for the support of Univ. Prof. Dr. Maria G. Firneis (Institute for Astronomy, University of Vienna). Her encouragement and guidance made this master thesis possible and I am thankful for all her comments, proposals and corrections.

Lastly, I would like to thank my family for the support and the possibility to study Astronomy in Vienna.

Summary

The Venusian atmosphere is a fascinating subject. A lot is known about our neighbor planet, but still a lot remains unknown. In this work the vertical profile of sulphur dioxide in the Venusian lower atmosphere is the main topic. From the very first in-situ measurements from Russian and US spacecrafts it is known that sulphur dioxide is present in the atmosphere in considerable abundance.
With the decades and many missions it was possible to obtain a pretty good overview about the vertical profile of sulphur dioxide.

In this work the data from this multiple missions are taken and together they form a data set with error bars. Two different models have been proposed in this study, because the abundance at the surface level is still not known very well. The Vega missions delivered two completely different values, a 25 ppm abundance and a 0 ppm value at ground level. And so model A and model B are proposed and used in the whole work.

Altitude (km)	Mixing Ratio (ppm)	Reference	Source
0	0/25		Vega 1 & 2
12	22 ± 3	Bertaux et al. 1996	Vega 1 & 2
22	38	Bertaux et al. 1996	Vega 1 & 2
35	130 ± 40	Bézard et al. 1993	Earth based IR spectrometry
42	130 ± 40	Bézard et al. 1993	Earth based IR spectrometry
52	110	Bertaux et al. 1996	Vega 1 & 2
69	0.5	Na et al. 1994	UV sounding rocket

The vertical profile of each of these models is calculated three times with different plots. It is important to compare them and consider the major differences.
The three approximation types used are:

1) Linear functions
2) Exponential functions
3) Cubic Spline

The results do not vary much and this means that they result in a good vertical profile for sulphur dioxide on Venus.

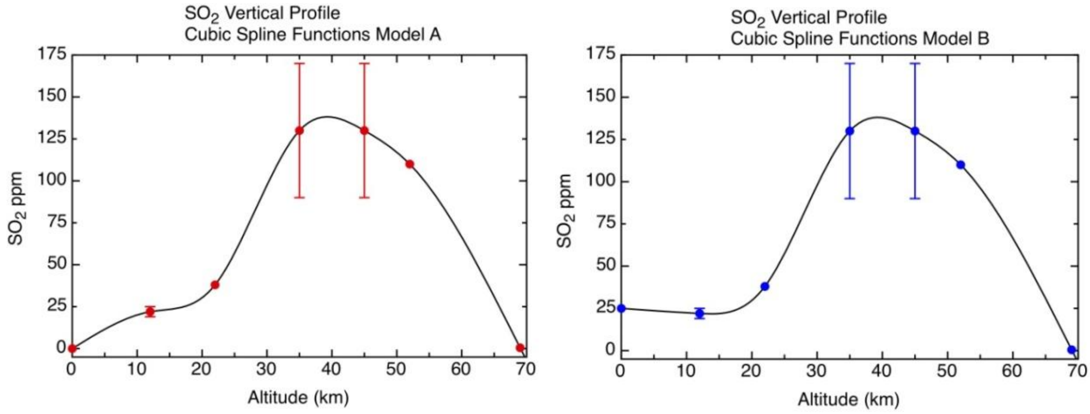

All plots and calculations are presented in chapter 4.

After the setup of the vertical profile it was possible to calculate the total mass of sulphur dioxide. To do so the necessity arose to create also a plot of the density profile. This was done in chapter 5 and also calculated with a cubic spline fit. Here it has to be said that the data set of the density profile was very good and obtained from the probes for each 5 kilometers in altitude and the plot type does not play a big role, because the differences are marginal.

Similar to the density profile a temperature profile and a pressure profile was calculated and plotted against the altitude.

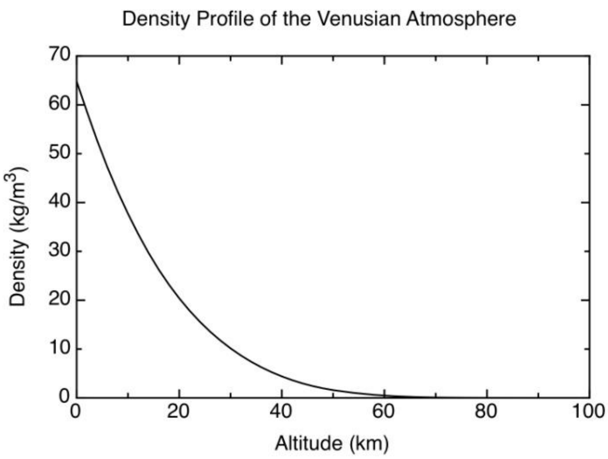

The atmosphere was separated into 70 shells and the total mass of each shell was calculated with the density profile and the volume of each shell. According to the vertical profile the percentage of sulphur dioxide in each shell is calculated and summed up.

All results are presented in chapter 5 and again they give a quite small range for all three plot types. Model A and model B do vary, but the difference is in a ten to twenty percent range and this is understandable because of the much larger abundance of model B at ground level.

	Linear Profile (10^{16}kg)	Exponential Profile (10^{16}kg)	Cubic Spline Profile (10^{16}kg)
Model A	2.236±0.40	2.104±0.31	2.267±0.41
Model B	2.831±0.40	2.617±0.39	2.782±0.41

After the results were obtained, the accuracy of the numerical calculations had to be certified. Although the three plot types give very similar results it seems to be better to ameliorate it with a numerical calculation with an increased number of shells. For this attempt in chapter 6 calculations are carried out with a 280 shell set up with the approximation of the cubic spline model A and model B
The results of the enhanced numerical calculations are very similar to the results from the 70 shells calculations. The difference is less than 1 percent and this is neglect able.

The total amount of sulphur dioxide in the present Venusian lower atmosphere has not been published before in literature. It is important to have known the edge of the present abundance and to consider the destruction rate of sulphur dioxide. This can help find out the strength of the volcanic activity at Venus.

The biggest part of the destruction rate of sulphur dioxide is the production of anhydrite on the surface of Venus. Other reactions are not that strong and the low mixing ratios of other sulphur bearing species show that they are not present in roleplaying abundances.

My research has shown that the destruction rate is far too high. The production rate must be at least 10 times higher than the one known from terrestrial volcanoes and this is not plausible, because Venus is far less geologically active than Earth.

To obtain todays abundances in the Venusian atmosphere two solutions must be considered. Either the destruction rate of sulphur dioxide has slowed down with the rising amount of anhydrite or the present abundance is a relic from newer volcanic activity.

Abstract (in German)

Die folgende Arbeit beschäftigt sich mit dem unteren Teil der Venus Atmosphäre, wobei der Hauptaugenmerk auf der Untersuchung des Schwefeldioxids liegt.
Durch die vielen russischen und US Missionen ist es gelungen sich ein gutes Bild der Atmosphäre zu machen. Durch diese Daten war es möglich vertikale Profile für Schwefeldioxid zu erstellen. Es wurden lineare, exponentielle und kubische spline Funktionen zur Modellerstellung der Atmosphäre verwendet und verglichen.

Weiters war es möglich die gesamte Masse des Schwefeldioxids in der Venus Atmosphäre durch numerische Rechnungen zu bestimmen und auf Ihre Zuverlässigkeit zu prüfen.
Es wurden 2 Modelle, die sich durch die Häufigkeit von Schwefeldioxid auf der Oberfläche der Venus unterscheiden, erstellt.
Die Werte liegen ungefähr bei $2.5 * 10^{16}$ kg und die Abweichungen der verschiedenen Modelle sind sehr gering.

Nachdem die Gesamtmasse von Schwefeldioxid, in der Venus Atmosphäre, bekannt war lag es daran die Rate zu berechnen wie viel Schwefeldioxid zerstört wird um auf die Produktion und somit direkt auf den aktiven Vulkanismus schließen zu können.
Es war sofort ersichtlich, dass die von Fegley et al. (Fegley et al. 1989) vorgerechnete Produktion von Calciumsulfit und somit die Zerstörung von Schwefeldioxid sehr stark ist und diese unmöglich im Rahmen einer geologisch längeren Zeitskala funktioniert, da sonst heute nicht so viel Schwefeldioxid beobachtbar wäre. Entweder wird durch immer mehr Calciumsulfat die Produktion von diesem verlangsamt oder das Schwefeldixoid, das heute noch in der Atmosphäre vorhanden ist, ist durch neueren starken Vulkanismus entstanden. Es gibt keinerlei Hinweise, dass die vulkanische Aktivität in den letzten wenigen Millionen Jahren zugenommen hat, deswegen muss die Zerstörung von Schwefeldioxid sehr stark verlangsamt worden sein.

Chapter 1

Exploration of Venus

1.1 The very first explorations

Venus has always been a special celestial body. Known as the morning and evening star, it was already observed by ancient cultures.
The very first tablets of Venus observations are Babylonian and they are attributed to King Ammi-saduqa, who reigned during 1582 – 1562 BC. The tablets contain the first and last visibility of Venus. This means that the Babylonians did know that the morning and the evening star are a single celestial body and not two.

After the fall of Babylon Pythagoras of Samos was the first, who realized this fact again. It is not known if Pythagoras had copies of the Babylonian tablets. Copies of them were probably very common and some were found at the library of Niniveh. They have been made in the 7th century BC and are now in the British museum.

The Persian universal scholar Avicenna was the first one, who observed a Venus transit in 1032 and he claimed that Venus is closer to Earth than to the sun.
Contemporary critics doubt that Avicenna could see the transit, due to his observation location.
The first officially quoted transit is credited to IbnBajjah, an Andalusian scientist in the 12th century. He affirmed that he saw 2 dark dots on the sun. These two dark dots have been identified as Mercury and Venus (Murdin P. 2000).

The next step on exploring Venus was done when the telescope was invented. Galileo Galilei could see the phases of Venus, when he observed it with a telescope. The phases of Venus were a controversial subject in the early 17th century, because they are only explainable, when Venus revolves around the sun. This was against the concept of the geocentric model and a good argument for a heliocentric model.

Venus had more secrets to be unfolded. The Russian astronomer Mikhail Lomonosov was the first who predicted an atmosphere in 1761. Further studies have been made by Johann Schröter, Chester Smith Lyman and Giovanni Cassini. (Marov M.Y., 2005)

First analysis of the atmosphere was possible when UV observations were done in the early 20th century. Frank E. Ross found spots, which were present only in the UV and not in the visible and infrared spectral range. He claimed that this hinted to a very dense atmosphere and that possible clouds cover the planet (Nicholson, 1961).

In 1963 the radar observation allowed to find out that the rotation of Venus is retrograde and that the rotation period is about 243 days. In the next decade it could be shown that the surface of Venus is far more complex than the one of the Moon or Mercury. The two, first observed, huge highlands on Venus have been named Alpha Regio, Beta Regio and the third radar feature are mountains called Maxwell Montes.

The earth based observation lost its importance with the start of the Soviet and US spacecraft programs in 1961. The earth based exploration became very interesting again when Allen and Crawford discovered the near infrared windows in 1984 (Allen and Crawford 1984).

Figure 1.1: The Babylonian Venus tablet from King Ammi-saduqa

1.2 The exploration during the cold war

The dueling Soviet and US programs during the cold war led to big efforts in the exploration of Venus. From 1961 until 1985 every launch window, which appears every 19 month, was used. Most of the Soviet missions have not been successful, but the dedication for the exploration of Venus was high.
The first mission was the Soviet Venera 1 spacecraft in 1961. Contact was lost after seven days.

The first US mission started with the Mariner 1 spacecraft. Mariner 1 was destroyed during the launch. After this first loss the US Mariner program managed to get into an Venusian orbit with Mariner 2. It was the first spacecraft in a planetary orbit (except the Earth orbit). Mariner could affirm that the Venusian surface temperature is far higher than expected. Up to 1962 many people believed that the Venusian surface could look very similar to the Earth's one. Since Venus and the Earth have very similar masses, the escape velocities do not vary a lot and so it was predicted that oxygen was one of the main chemical substances in the lower atmosphere. Even terrestrial plants and animals were an issue in this controversy. Temperatures above 400° C destroyed these illusions.

The Soviet missions had to face many problems with their carrier rockets. Many spacecrafts did not leave the earth orbit at all, but after 1973 all Soviet missions have been successful.

Venera 3 was the first spacecraft, which hit the surface of another planet, but the communication broke down before terrestrial transmissions started and no data were delivered to earth. The first really functional Soviet mission was Venera 4 in 1967. The lander sent data from the Venusian atmosphere for nearly 100 minutes, but no data from the surface were obtained. The descending procedure was thought to last shorter, because it was not known up to this time, how dense the atmosphere really was. The batteries of Venera 4 ran out at an altitude of 25 kilometers.

The second US mission was a fly by with Mariner 5 in 1967. Mariner 5 could detect that the surface pressure was just below 100 bars. The very next Soviet missions did not know that and so the Venera 5 and 6 landers have been built for pressures up to 25bar, which is too low. This was in the next launch window, only 2 years after Mariner 5.

Nevertheless Venera 5 and 6 brought an achievement and they could send data from 18 km and 10 km altitude, which were the lowest altitude data ever received.

Venera 7 was built for pressures up to 180 bars and so it was the first lander, which sent data from the Venusian surface. It was a highly successful mission and the lander could deliver data for 23 minutes from the surface. Venera 8 was the follower mission and the lander was equipped with a photometer, which could prove that the atmosphere is very clear below the massive cloud deck. This meant that future missions should be fitted with cameras.

Venera 9 started in 1975 and it was equipped with cameras, which should take pictures from the ground for the first time in Venus exploration. The lander worked well and pictures from the surface were obtained. Another very interesting fact about the Venusian lower atmosphere was gained. Venera 9 could show that the cloud deck is separated into three totally different layers.

Venera 10 was similar to the Venera 9 spacecraft and it was launched in the same launch window. The remarkable discovery obtained was that Venera 10 could detect wind speeds up to 3 m/s at the surface. Venera 10 also had panorama cameras on board, just like Venera 9. Both landers had to face the problem, that they could not open the second lens cover and so both spacecraft could only make panorama pictures of 180° instead of 360°.

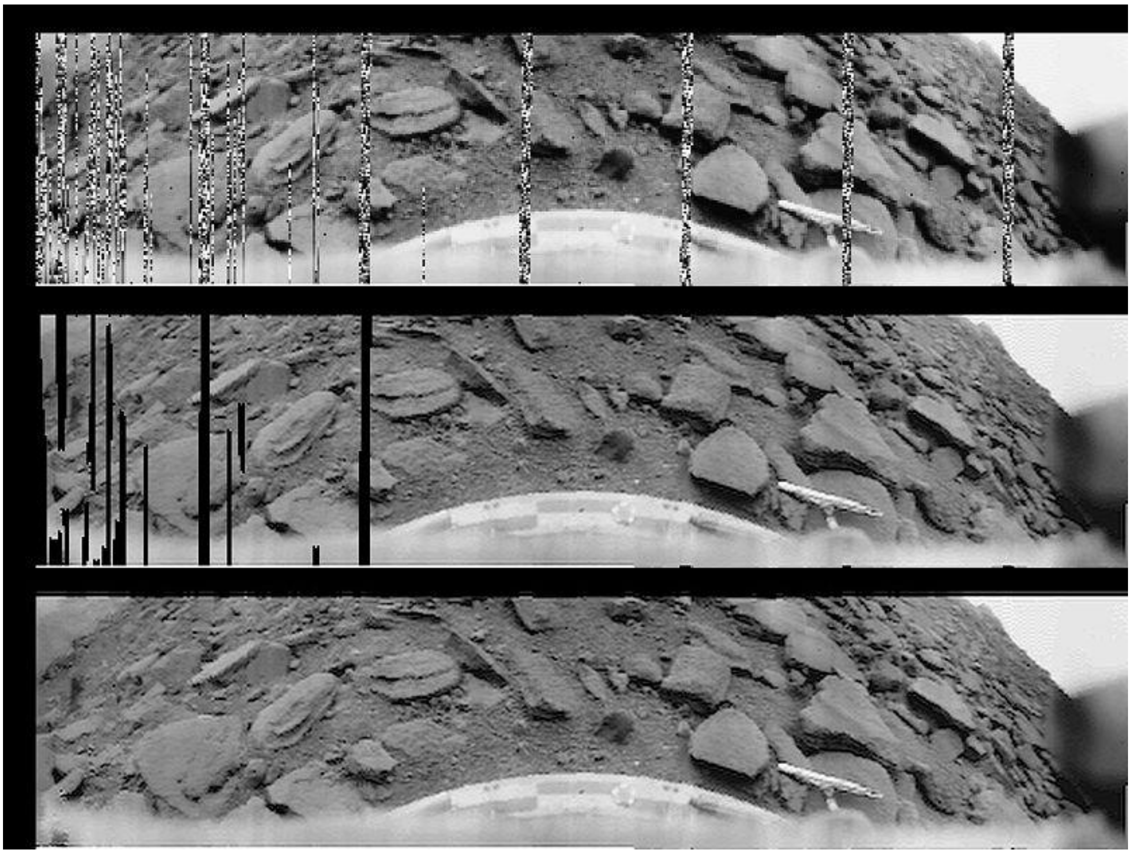

Figure 1.2: The first pictures from the surface of Venus made by Venera 9 in 1975.

In 1978 the US spacecrafts Pioneer Venus 1 and 2 reached the Venus orbit. Pioneer Venus 1 was an orbiter and Pioneer 2 a multiprobe, carrying a large probe and three small probes. The Pioneer 2 bus released the probes and entered the Venusian upper atmosphere a short time later. The bus did not have any parachute or heat shield and it was not planned to land at all. The bus gathered information about the upper atmosphere and transmitted it back to earth until it burned up.

The large probe and the three small probes explored the Venusian lower atmosphere at four different places and they were not build for a landing. One of the small probes, which did not have a parachute, reached the surface intact and sent information for more than one hour.

Pioneer Venus 1 entered into orbit and worked for a very long time. Shortly before the spacecraft ran out of fuel it was directed to Venus to burn up during the atmospheric entry in 1992.

It should be noted that all Soviet missions did not fail anymore since the start of Venera 9 and 10 in 1975. Further missions have been successful, although single instruments did not work always. The landers managed to send data back to Earth and record durations have been achieved with Venera 11, 12 and 13.

Venera 11 and 12 started in 1978 and the landers survived for 95 and 110 minutes on the surface. This was far more than expected. The missions were not perfect, because the color cameras and the drill for the surface did not work. For the exploration of the atmosphere they have been absolutely successful. They carried mass spectrometers and gas chromatographs and helped to find out the composition and the abundances of the chemical substances in the lower atmosphere.

Venera 13 and 14 had pretty the same research mission like Venera 11 and 12. The landers worked for 127 and 57 minutes and they obtained the very first color images from the surface of Venus.

The Venera program ended with the last two orbiters Venera 15 and Venera 16. These space crafts orbited in polar orbits in 1983 and they mapped the northern regions of Venus. Venera 15 and 16 could discover new surface features, which we now know as Coronae and Arachnoids.

In 1985 another Soviet program, which was a cooperation with other countries, including Austria, started two space crafts to Venus. Their names were Vega 1 and 2.

The program was a two-part mission. The first part of the mission was to deploy two landers for Venus and for the first time two balloons, which should float in the Venusian atmosphere for maximal 60 hours. The second part of the mission was to make a flyby on Venus and to head on for Halley's Comet.

The helium balloons had been ejected at a height of 50 kilometers and they had floated upwards in the Venusian atmosphere and after that they had moved for one-third around the circumference of Venus. This helped very much to understand the dynamics of the Venusian winds within the atmosphere. The measurements of temperature and pressure play a decisive role in further research.

The main instruments of the landers were gas chromatographs and mass spectrometers, and they were able to deliver very good measurements of the composition of the Venusian lower atmosphere. The vertical profiles of many elemental species were achieved.

Only Vega 2 could gather information from the surface too, because the Vega 1 surface experiments were started unintended too early during the descent phase. A wind blast at 20 kilometer height could have been the trigger. Vega 2 worked for 56 minutes on the surface.

1.3 The exploration after the cold war

The great era of Soviet Venus programs ended with the end of the cold war and the last US mission was the Magellan orbiter in 1990. After the end of cold war in 1991 both sides abandoned the Venus programs. Their competition of exploring Venus ended with Magellan.

Magellan started in 1990 and it was an orbiter, which worked for 4 years in the Venus orbit. For the first time a high frequency radar map of Venus was created. Up to then, the radar maps did not have appropriate resolutions. Magellan mapped 98% of Venus and the resolution was about 100 meters. Magellan helped to understand the Venusian geology. The maps revealed far less craters than expected and this means that the Venusian surface has been very young in relation to other terrestrial planets.

Continental drift features known from Earth were not found on Venus, although the planets are similar. This means that Venus is not geologically active anymore. Other features like the Coronae, which were already found with Venera 15 and 16, could be studied better. It was clarified that they are volcanic features and a still active volcanism was proposed for Venus.
Another interesting fact was carried out with Magellan data. It seems that there is no wind erosion at Venus, although the wind dynamics in the cloud deck are immense.
In 1994 Magellan was destroyed with a planned atmospheric entry.

After a decade of no measurements with space crafts, the European ESA started Venus Express, a Venus orbiter, which entered the Venusian orbit in 2006. Venus Express is studying the Venusian atmosphere since then and new atmospheric features like the double vortex at the poles have been discovered.

Figure 1.3: The Venusian double vortex at the pole observed with Venus Express

Venus Express was able to detect lightning in the Venusian atmosphere. It was detected by Venera 11 and 12 even before, but there was no certain proof until then, because the Cassini-Huygens mission could not detect any lightening during the two flybys to Saturn, when studying Venus.
The operative mission of Venus Express was extended until 2012. After that new missions are already planned and in progress.

In the 21st century Europe has entered the exploration stage of Venus after the strong dominance of the Soviet and US missions. Also the Japanese JAXA sent a spacecraft to Venus in May 2010. Akatsuki failed to enter the Venusian orbit and now it is in a heliocentric orbit. Although the mission did not start as planned, another good trial to enter Venusian orbit could be done in 2016.

NASA, ESA and Roscosmos proposed already new missions to Venus. The NASA mission proposal is the Venus In Situ Explorer (VISE), which should start in 2013 and study the surface and mineralogy of Venus. The main goal of VISE is to gather a core sample and to analyze it in situ.

The Roskosmos project is Venera-D. After the long and successful Soviet exploration of Venus, Russia is following up in these footsteps. Venera-D is an ambitious project and the main goals are to acquire better maps than those obtained by Magellan. A more powerful radar will be used to map the surface of Venus again. A lander is also planned, and since the Soviet landers were the most successful ones and the duration of their survival on Venus was spectacular now a long duration lander must be the next goal. Venera-D should start in 2016.

ESA has proposed the Venus Entry Probe, which was renamed to European Venus Explorer (EVE). It is a complex mission, which should analyze the atmosphere of Venus and gather more information from the surface with a lander probe.

The whole mission consists out of three independent parts. An orbiter, a balloon and a lander are planned. The aspiring thing about this mission is to use a balloon again. Only the Vega 1 and 2 missions did that before, but they have shown that is worthwhile. The balloon should float at a height of 50-60 kilometers and study the dynamics of the Venusian cloud deck. The lifetime of the balloon is planned at least for 7 days and it should make at least one full circle around Venus too.

1.4 Near Infrared Windows

Venus was explored by orbiters and landers for a quite long time, but the observations from earth also play a big role since the detection of the near infrared windows by Allen and Crawford in 1983 (Allen and Crawford 1984).

They have been found by coincidence, because at first they have been misinterpreted as spread sunlight from the day side of Venus. Later it was clear that it must result from thermal radiation, which proceeds through different optical depths from the Venusian cloud cover.

These features have been found at wavelengths near to 1.74 and 2.3 µm and they allowed new insights on the Venusian lower atmosphere.

Not much time later some more near infrared windows have been found and they were associated with the altitude of these features.

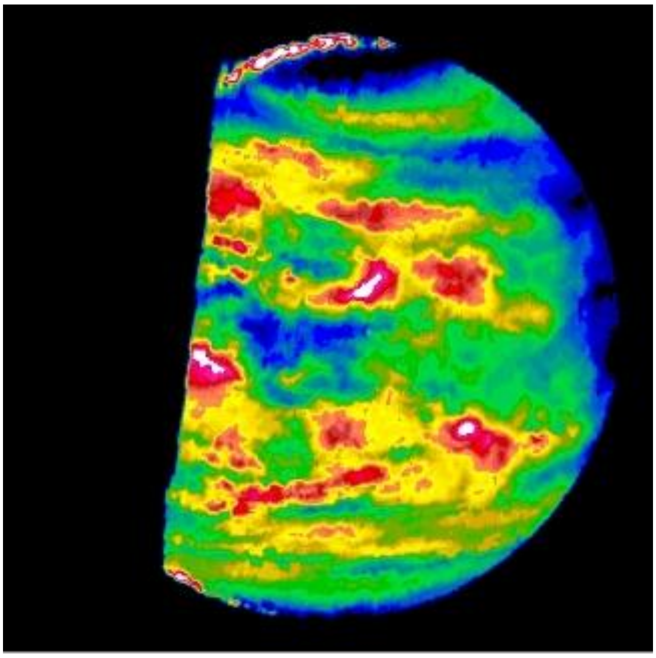

Figure 1.4: Image of Venus at 2.3 µm, taken from Galileo NIMS (Carlson et al, 1990)

Figure 1.4 shows the night side of Venus in a 2.3 µm filter. The blue features are massive cloud decks and the brighter features are less cloudy decks. The first observation was done by Allen and Crawford and this one is from the Galileo spacecraft with a far better resolution. More observations have been done at different wavelengths. Allen and Crawford have provided the following near infrared windows.

Window Region (µm)	Altitude
1.01	Surface (>90%)
1.10	Surface (~60%) plus 0 to 15 km
1.18	Surface (~40%) plus 0 to 15 km
1.27	15 to 30 km
1.31	30 to 50 km
1.74	15 to 30 km
2.3	26 to 45 km

Table 1.1: Near Infrared Window Region attributed to the height of the features (F.W. Taylor et al.)

The near infrared windows allowed studying the composition of the Venusian lower atmosphere too, because some elemental species have bands in these regions. The water vapor bands can be detected at the 1.10, 1.18, 1.74 and 2.3 µm regions. Mixing ratios of CO, HF, HCl, OCS and SO_2 were detectable too and they could be analyzed if there are topological variations.

The near infrared windows made it possible to explain the dynamics in the Venusian lower atmosphere. It was possible to study single features for the first time. The features, which have been found at 1.74 and 2.3 µm have a rotation period of 5.5 days, which is a little bit longer than the period of the super rotation. This means that single cloud layers move at their specific speed and are not connected to the known rotation of 4 days of the cloud cover.

1.5 The timeline of the spacecrafts sent to Venus

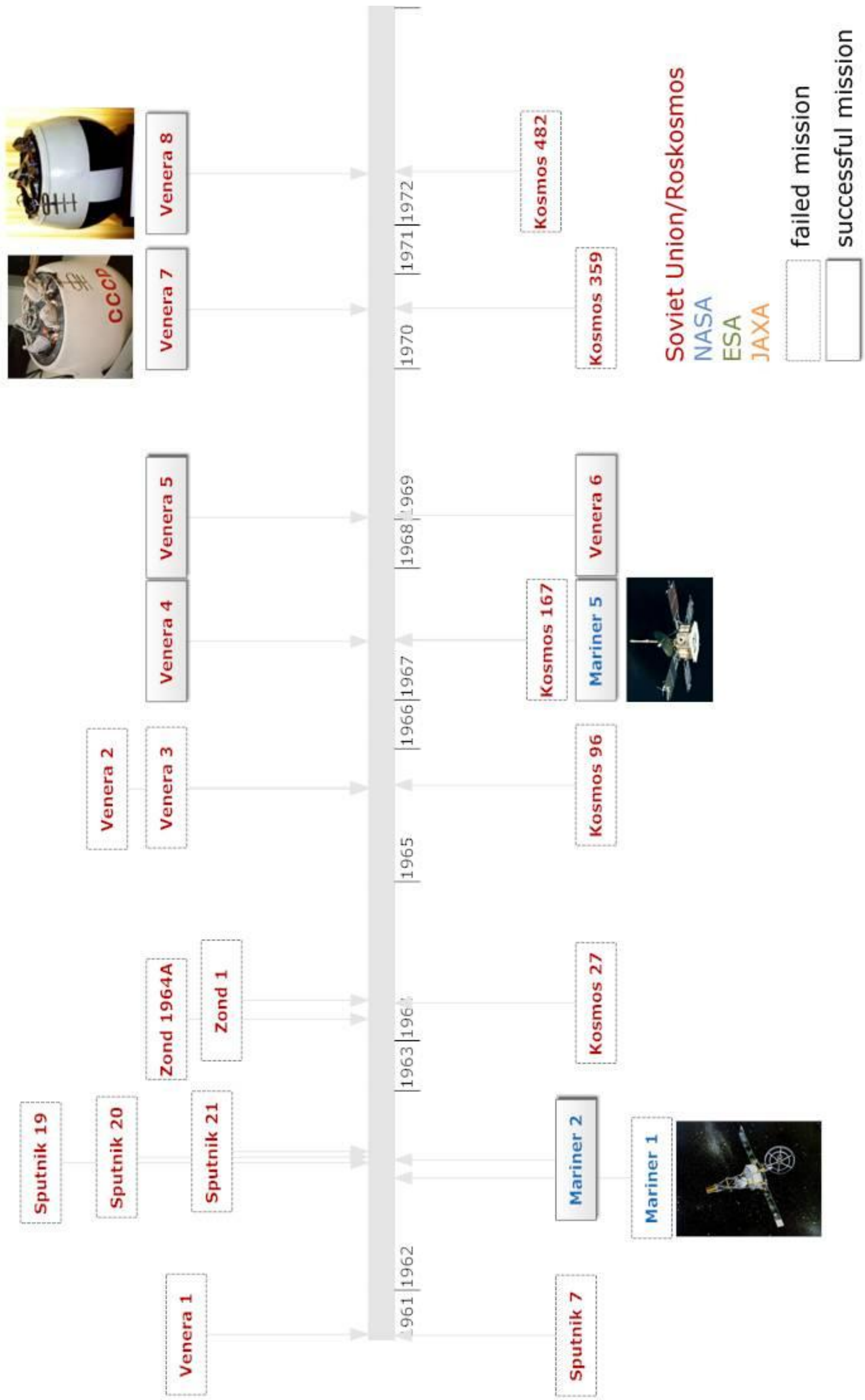

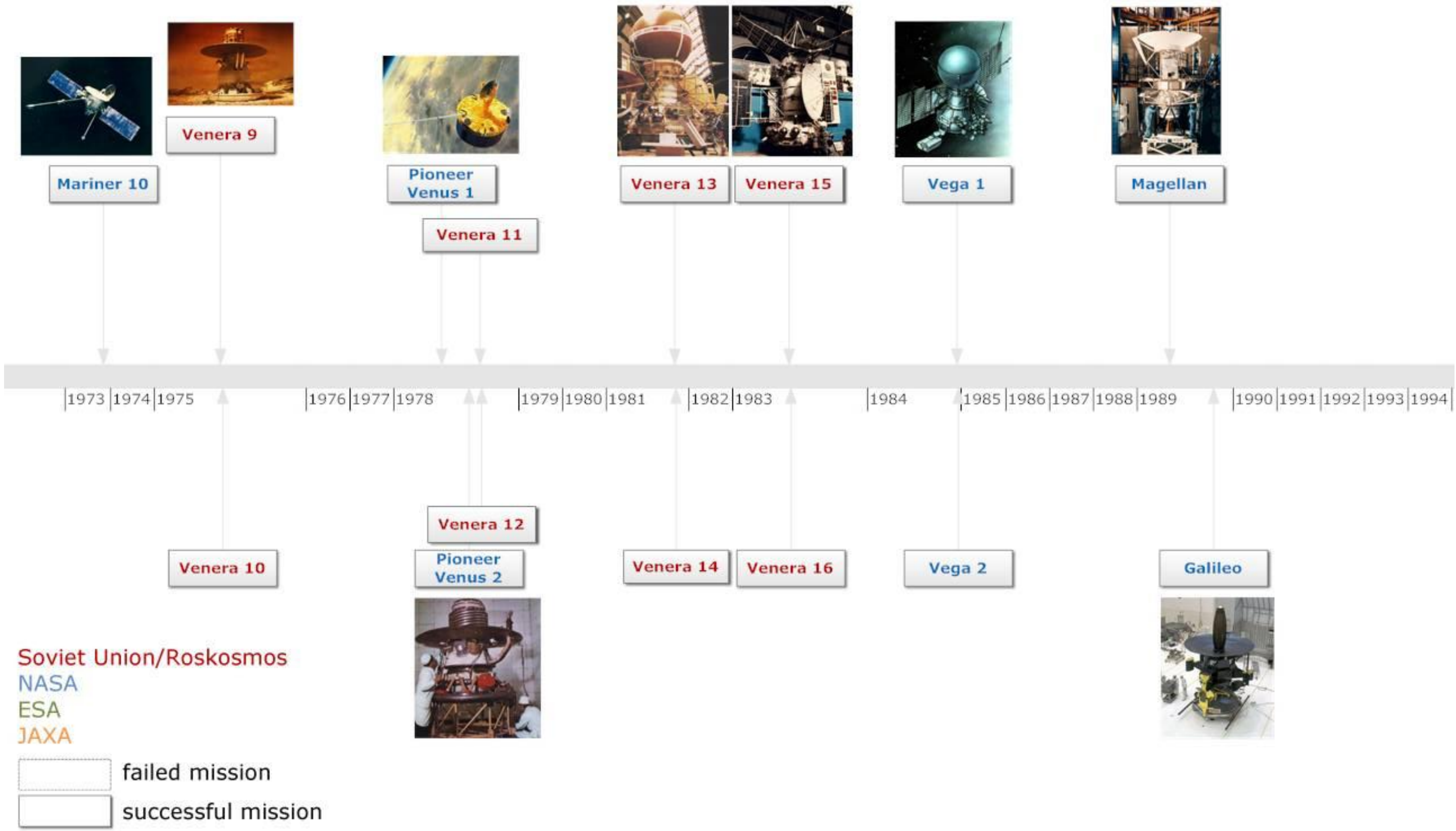
Mariner 10
Venera 9
Pioneer Venus 1
Venera 11
Venera 13
Venera 15
Vega 1
Magellan
1973
1974
1975
1976
1977
1978
1979
1980
1981
1982
1983
1984
1985
1986
1987
1988
1989
1990
1991
1992
1993
1994
Venera 10
Venera 12
Pioneer Venus 2
Venera 14
Venera 16
Vega 2
Galileo
Soviet Union/Roskosmos
NASA
ESA
JAXA
failed mission
successful mission

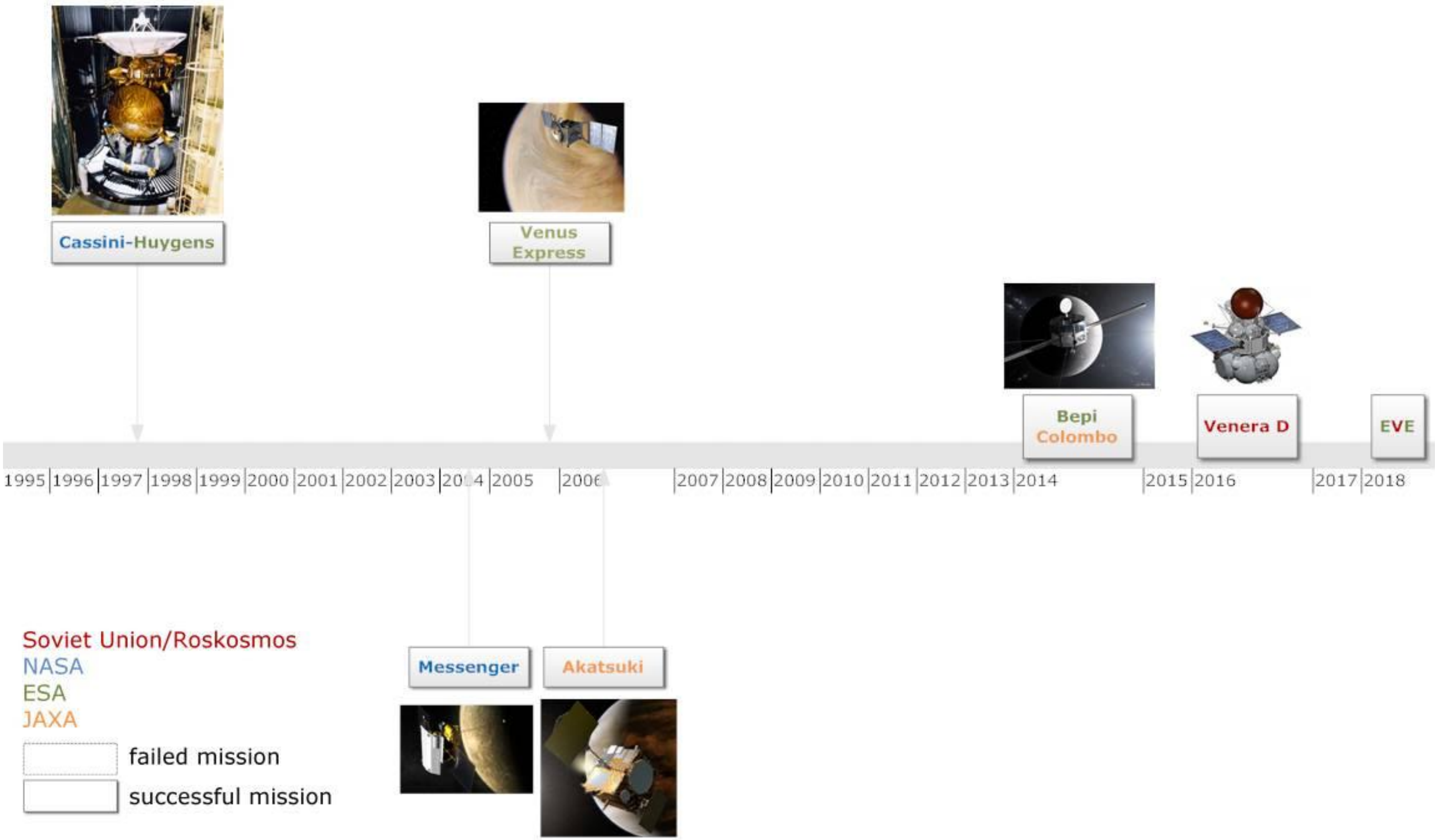

Cassini-Huygens
Venus Express
Bepi Colombo
Venera D
EVE
1995 1996 1997 1998 1999 2000 2001 2002 2003 2004 2005 2006 2007 2008 2009 2010 2011 2012 2013 2014 2015 2016 2017 2018
Messenger
Akatsuki
Soviet Union/Roskosmos
NASA
ESA
JAXA
failed mission
successful mission

Chapter 2

The Venusian atmosphere

2.1 General overview

The Venusian atmosphere is dominated by carbon dioxide. The atmosphere consists out of 96.5% carbon dioxide and 3.5% nitrogen. There are trace amounts of other elemental species. Sulphur dioxide makes the biggest part of these. In literature a value of 150 ppm can be found, but this value has to be discussed (Basilevsky et al. 2003). It is too high but sulphur dioxide is still the most present trace amount. Water vapor, argon, carbon monoxide and hydrogen halides are the other minor species.

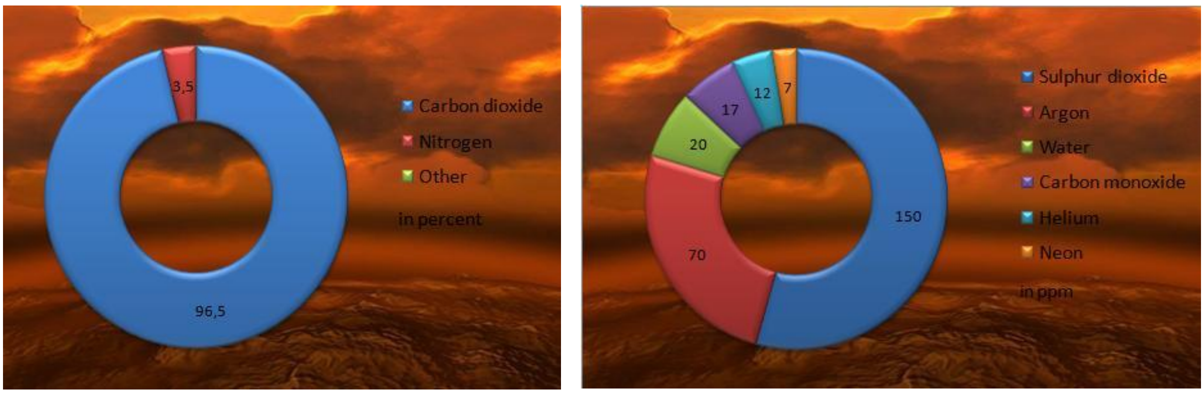

Figure 2.1: The composition of the Venusian atmosphere

The Venusian atmosphere is very complex and the layers are different than those known from Earth. The cloud deck is massive and almost 30 km thick and below the clouds there is a sulphuric acid haze. Below the haze the atmosphere is abruptly transparent. Although the density is very high the opacity is very low and from the surface the view is similar to the view on Earth.

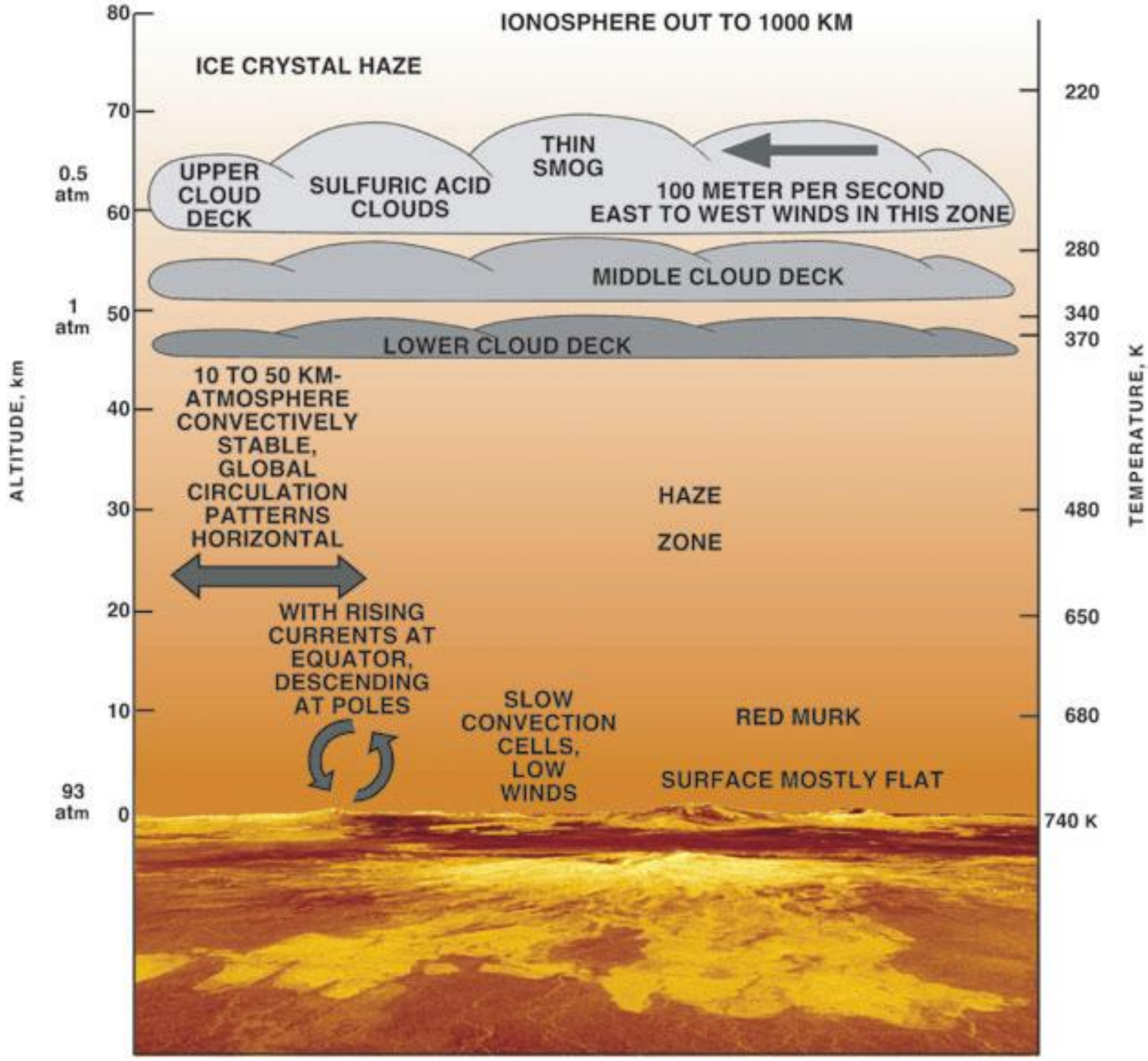

Figure 2.2: The Venusian lower atmosphere and their features (after Basilevsky et al. 2003)

The pressure on the surface is 93 times higher than on Earth. 93 bars are the highest pressure on a terrestrial planet and this is the main reason for the short life time of entry probes.

The temperature rises also very fast with descending altitude. While the temperature and even the pressure in the cloud regions are very moderate, the temperature rises up to 740 K at the surface. Venus has the hottest surface from all terrestrial planets. Although Mercury is much closer to the Sun the surface temperature is not as high as on Venus. The intensity of the solar radiation on Venus is just one quarter of the solar radiation on Mercury, but the greenhouse effect in the Venusian atmosphere is enormous.

The Venusian atmosphere is a very dense one and the whole troposphere is almost 65 km high. The troposphere is dominated by the winds. On the surface they are pretty weak with just a few meters per second but in the highest parts of the troposphere they reach velocities of 100 meter per second. Those winds blow from East to West, this means they are retrograde to the rotation of Venus. On Earth the winds blow in the direction of the rotation of Earth. The cloud deck rotates with a period of just 4 days around Venus.

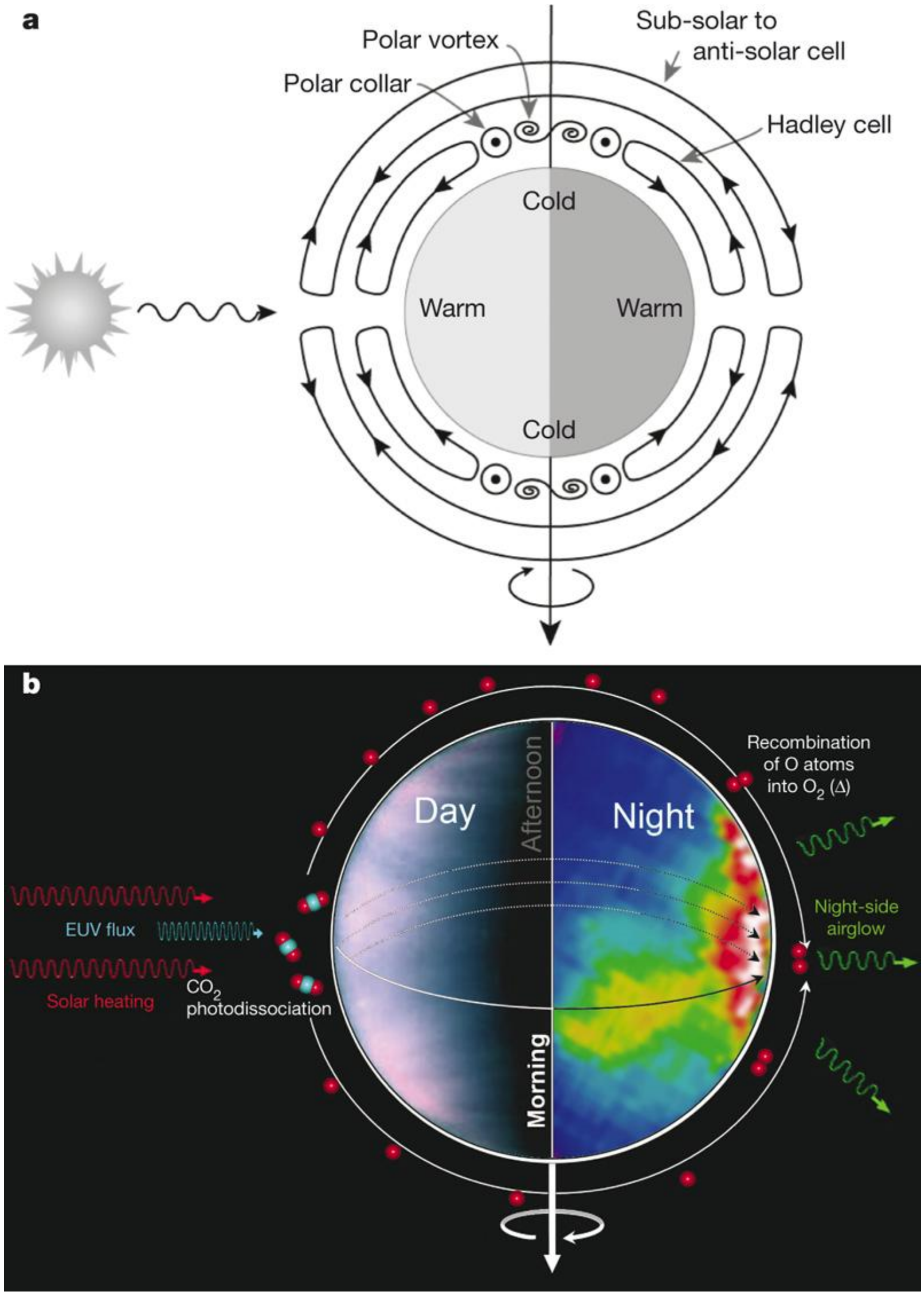

Figure 2.3: Dynamics in the Venusian lower atmosphere (after Svedham et al. 2007)

The solar radiation causes a strong convection in the atmosphere. Carbon dioxide is mostly heated on the equator and so it flows in the direction of the poles. This phenomenon is present on all Venus and these cells are called Hadley cells. They flow reaches latitudes of about 60°in the northern and southern hemisphere and then the cold carbon monoxide air drops and flows backwards to the equator.

At the edge of the Hadley cell another feature, which is called the polar collar, can be found. The polar collar is about 50° C colder than the carbon monoxide air in the Hadley cell in the Polar Regions. The collars extend from 60° to 70° latitude.
The clouds are even at greater altitudes in the polar collars. They can reach altitudes up to 70 to 72 kilometers and this is about 5 to 7 kilometers higher than the general cloud deck.

The Polar Regions are dominated by the double vortices, which are present at the North and the South Pole. The double vortex is not created by two features but is a single feature with two centers of rotation. These centers are interconnected with a cloud structure in the form of a S.

The double vortices move retrograde to the rotation of Venus. This means that they rotate in the direction of the whole super-rotation of the atmosphere.
The results from Venus Express show that the double vortex at the South Pole extends down to 50 kilometer altitude (Piccioni et al. 2007). It may also reach deeper and the same behavior is expected on the North Pole.

In the upper atmosphere there is another movement. A total flow from the sub-solar to the anti-solar point is only known in the regions above 100 kilometers altitude.
The oxygen airglow on the night side can also be explained by this movement.

Carbon dioxide in the upper atmosphere is photo-dissociated through the influence of solar radiation and Oxygen moves from the sub-solar to the anti-solar point.
The oxygen atoms (O) recombine with oxygen atoms (O) and dioxygen (O_2) is created. The airglow is very strong and it is visible in the 1.27 µm spectral window.

2.2 Comparison of Earth and Venus

Bulk Parameters	Venus	Earth
Mass (10^{24} kg)	48.685	59.736
Volume (10^{10} km^3)	92.843	108.321
Equatorial radius (km)	6051.8	6378.1
Polar radius (km)	6051.8	6356.8
Mean density (kg/m^3)	5243	5515
Surface gravity (m/s^2)	8,87	9,8
Escape velocity (km/s)	10,36	11,19
Atmosphere	Venus	Earth
Surface pressure (bars)	92	1.014
Surface density (kg/m^3)	65	1.217
Scale height (km)	15,9	8,5
Total mass of atmosphere (10^{18} kg)	480	5,1
Average temperature (K)	737	288
Wind speeds at the surface (m/s)	0,3 - 1	0 - 100
Mean molecular weight (g/mole)	43.45	28.97

Table 2.1: Terrestrial and Venusian bulk parameters and atmospheric parameters (after NASA fact sheet (Appendix 16))

Physical bulk parameters of Venus and Earth do not vary much and from outer space they may look like two twin planets. What happened that one of them turned into a blue water rich planet and the other to a stony desert with a huge carbon dioxide atmosphere?

The general theory is that Venus was probably very similar to Earth and there were water oceans just like on Earth but Venus lost its water to space. Venus and Earth did also have pretty much the same carbon dioxide amount but on Earth it was possible to bind it in the crust and on Venus the whole atmosphere is made out of carbon dioxide gas (Svedhem et al. 2007).

The high temperature on the surface made the binding of carbon dioxide to the crust impossible and more carbon dioxide was set free into the atmosphere. This faced the temperature to rise and the effect self-amplified.

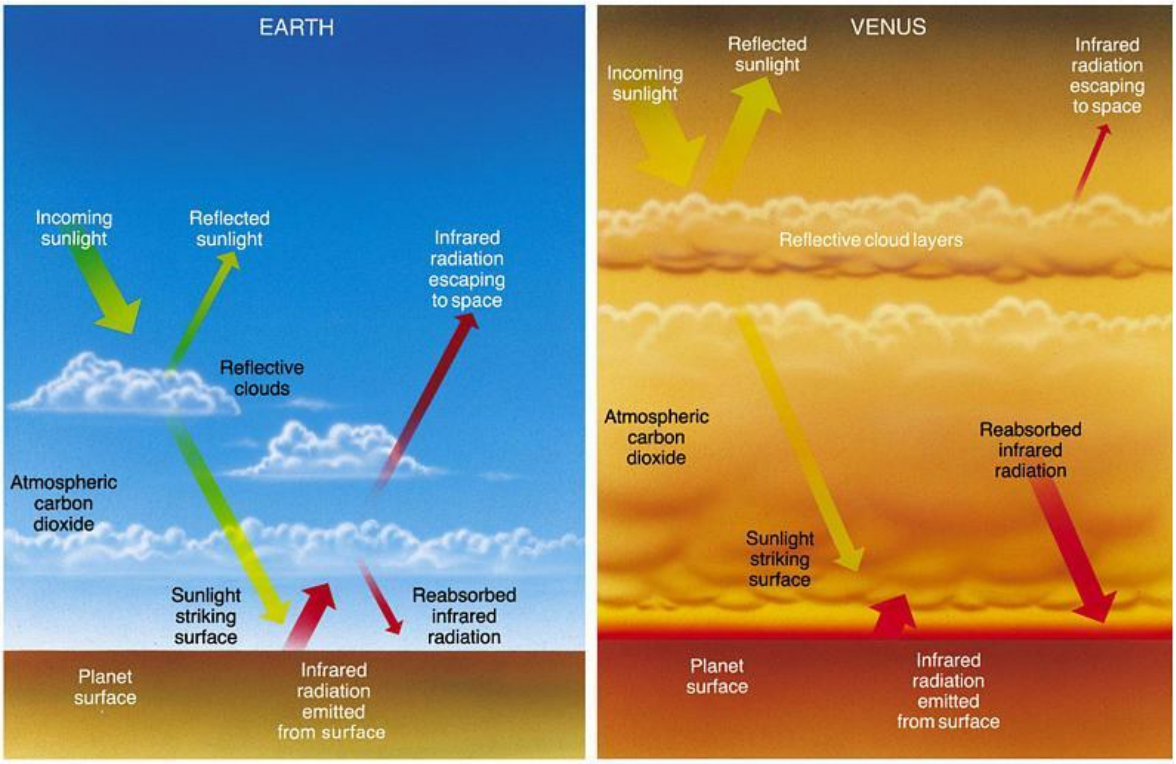

Figure 2.4: The Terrestrial and Venusian greenhouse effect

The least difference between the two planets made their atmospheric evolution so different. Venus is just a bit closer to the sun and the somewhat higher surface temperature was the big difference in the starting conditions.

The incoming sunlight was emitted as infrared radiation from the surface and reabsorbed in the strong carbon dioxide clouds. On Earth the clouds are not that dense and also not made out of reflective carbon dioxide, so the infrared radiation from the surface could escape to space again.

More and more carbon dioxide was heated out of the crust and set free. The more carbon dioxide was set free to the atmosphere, the more the temperature rose. The surface temperature conditions and the huge carbon dioxide amount in the Venusian atmosphere is the end product of a very long evolution of the greenhouse effect.

To reconcile the reason why these so similar planets evolved so differently, is just the fact that Venus was committed to a slightly stronger radiation and the carbon dioxide in the crust was set free and started the vicious circle.

2.3 Sulphur bearing compounds

The common sulphur bearing elemental molecules in the Venusian lower atmosphere are:

SO_2 (Sulphur dioxide)

OCS (Carbonyl sulfide)

H_2SO_4 (Sulphuric acid)

Sulphur dioxide is the most present species and it is very variable with the altitude. The first detection of sulphur dioxide in the Venusian atmosphere was made by Barker in 1979 by UV-Observations from Earth. The mixing ratios above the cloud deck vary from 0.5 ppm to 0.02 ppm (Barker 1979), which stand in pretty good agreement with newer observations.

The cloud top measurements showed a continuous decline of the mixing ratio on a short time scale. The Pioneer Venus mission delivered observations from 1978 to 1986 and the data were confirmed by several observations obtained with the International Ultraviolet Explorer and the Hubble Space Telescope (Na et al. 1990, 1992, 1994).

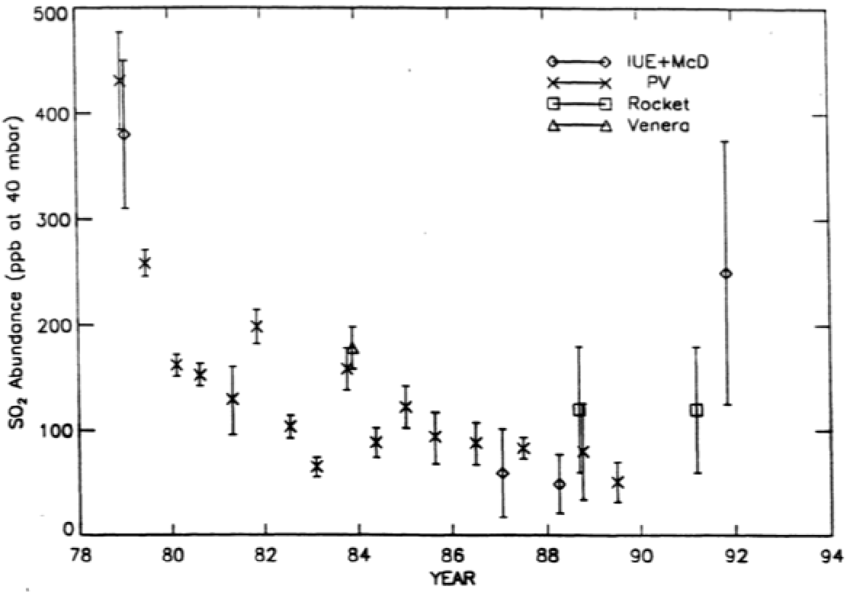

Mixing ratio of SO_2 at the cloud top level in the Venus atmosphere derived from the IUE, rocket, Pioneer Venus, Venera-15, and ground-based observations.

Figure 2.5: The mixing ratio of sulphur dioxide at 69 km height obtained from various observations (from Esposito et al. 1997)

Na et al. 1993 have discussed the decrease of the sulphur dioxide mixing ratio above the clouds and proposed that Venus may be volcanically active and the decrease is caused by a former sulphur dioxide injection from a volcanic eruption.
Belyaev et al (Belyaev et al. 2011) confirmed the variations in the cloud tops with measurements from SPICAV and VEX.

To obtain the sulphur dioxide mixing ratio below the clouds an in-situ mission was in need. Pioneer Venus (NASA) and the Venera 12 & 13 (USSR) missions were the first ones to obtain the data with their gas chromatographs in 1978.

The first observations describe a unified model. The sulphur dioxide mixing ratio has a peak directly below the cloud deck and it is strongly decreasing towards the ground. The fast decrease of sulphur dioxide is still difficult to explain but it might be in a strong connection to the mixing ratios of carbon monoxide and carbonyl sulfide.

Carbon monoxide and sulphur dioxide are decreasing from 44 km down to 10 km altitude, while carbonyl sulfide is increasing in the same altitude region. It is notable that the carbonyl sulfide and carbon monoxide mixing ratios vary contrary to each other with latitude as well.

In 1984 further investigations by the Vega 1 & 2 space crafts were performed. For Vega 1 & 2 it was possible to affirm the strong vertical gradient of sulphur dioxide.

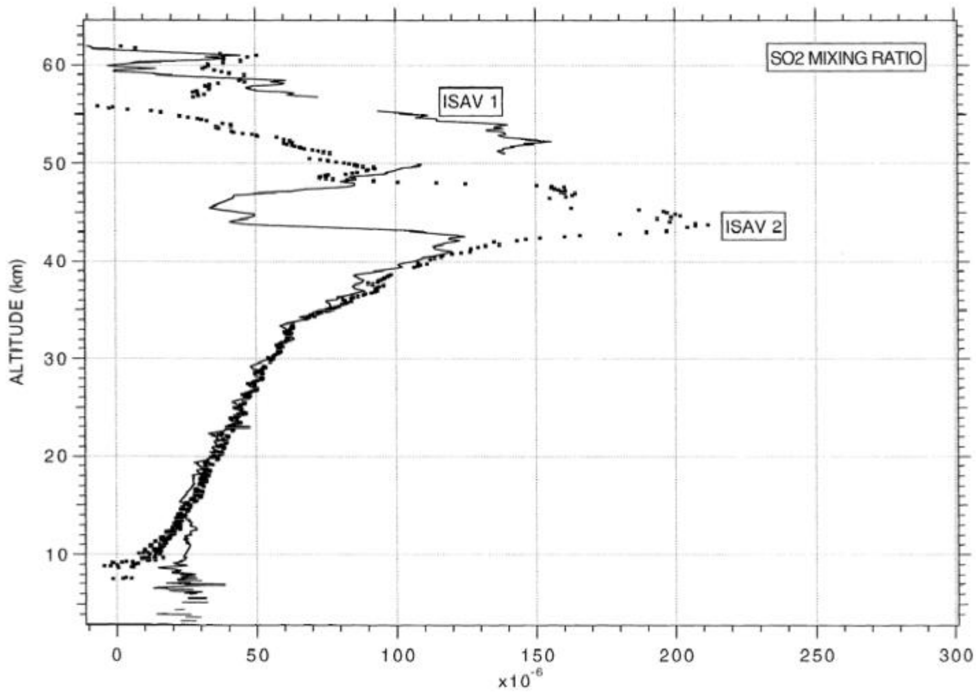

Figure 2.6: The ISAV 1 & 2 measurements of the mixing ratio of sulphur dioxide versus the altitude (from Bertaux et al. 1996)

In the range between 42 and 15 kilometers altitude the measurements from ISAV 1 and 2 are very identical but in the higher regions only the ISAV 2 data seems to fit to mixing ratios obtained by earlier in-site missions.

Below 15 kilometers the two profiles start to differ again. The reason could be a topographic difference in the mixing ratio of sulphur dioxide, since the Vega 2 lander reached ground level 2100 kilometers southeast from the Vega 1 lander. There is no equivalent data from the lowest region of the Venusian atmosphere that could be compared to the Vega 1 & 2 measurements.

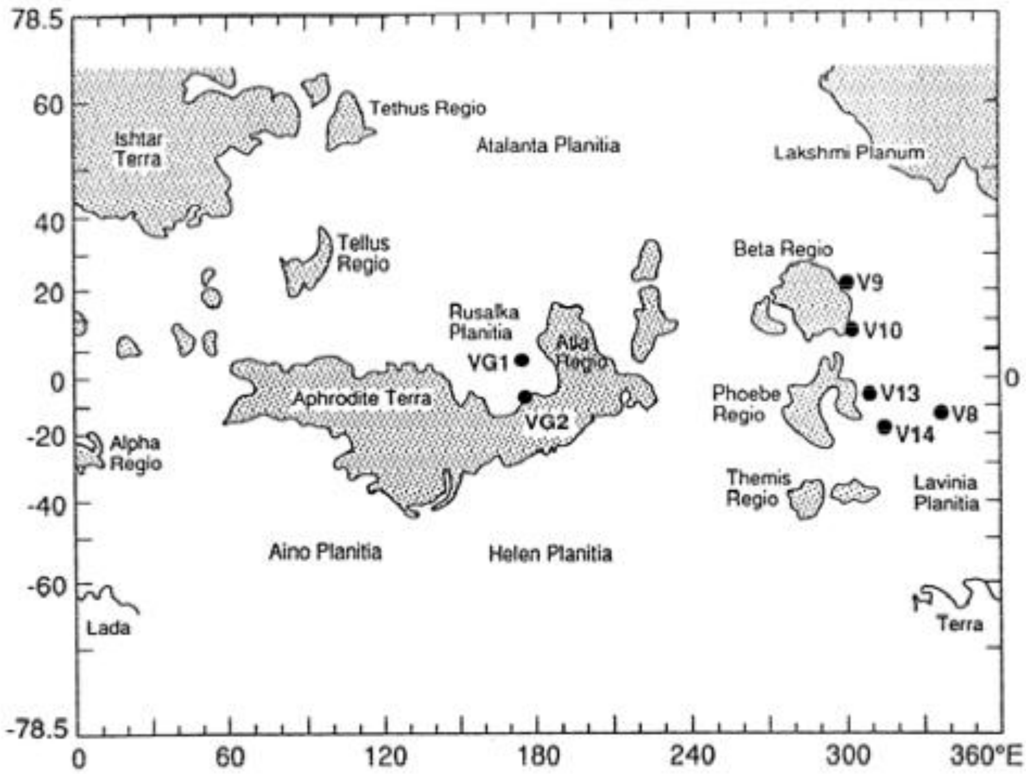

Figure 2.7: Vega 1 & 2 landing sites (from Bertaux et al. 1996)

The Vega 1 lander, touched down 700 meters lower than the Vega 2 lander, which landed 100 meters above the mean radius (6051,8 km) of Venus. Both mixing ratios decrease toward the ground and the sulphur dioxide mixing ratio obtained from Vega 2 seems to reach even nearly zero.

For the further investigation of the vertical profile of sulphur dioxide in the Venusian lower atmosphere, 2 models will be set up. They vary only in the mixing ratio at the surface. The first model has a surface mixing ratio of 0 ppm and the second one 25 ppm.

Altitude (km)	Mixing Ratio (ppm)	Reference	Source
0	0/25		
12	22 ± 3	Bertaux et al. 1996	Vega 1 & 2
22	38	Bertaux et al. 1996	Vega 1 & 2
35	130 ± 40	Bézard et al. 1993	Earth based IR spectrometry
42	130 ± 40	Bézard et al. 1993	Earth based IR spectrometry
52	110	Bertaux et al. 1996	Vega 1 & 2
69	0.5	Na et al. 1994	UV sounding rocket

Table 2.2: Sulphur dioxide mixing ratio obtained by various measurements. Overview is given also in de Bergh et al. 2006

In the dataset, the additional mixing ratios are provided by Earth based Infrared spectrometry and a UV Sounding Rocket. It is notable that the mixing ratio from the Earth based spectrometry stands in good agreement with the Vega results. The Vega missions delivered equal values at an altitude of 42 km.

2.4 Water Vapor and D/H Ratio

None elemental substance has caused so much struggle like water. The numerous entry probes showed very different results. The mixing ratios did vary from 20 to 1000 ppmv. A decrease of the mixing ratio with a decreasing altitude is something that was certain but the abundances were too different according to the 1000 ppm value, which was recorded by the Venera 14 (Hunten et al 1989)

Pioneer Venus recorded a 100 ppmv mixing ratio, which was constant with varying altitudes.

The controversial results made it important to keep on investigating the water abundance in the Venusian atmosphere.

Crisp et al. made further investigations with spectra obtained with the Anglo American Telescope and the mixing ratios were more plausibly explained with 40±20 ppmv (Crisp et al. 1991).

Bell et al. worked with the Cooled Grating Array Spectrograph and the results were split into 2 different results (Bell et al. 1991). From the dark spot spectra the mixing ratio was about 40 ppmv and the bright spot spectra delivered mixing ratios of about 200 ppmv.

The explanation of the big difference is the thermal dissociation of sulphur acid into water and sulphur trioxide. The thermal dissociation of sulphur acid occurs below the cloud deck and yields a higher abundance of water.

De Bergh et al. were the first to analyze the D/H ratio (de Bergh et al. 1991).
The ratio is about 120±40 times higher than the value on Earth. This means that there is a high production rate of Deuterium in the Venusian atmosphere. The explanation is pretty simple. In the higher parts of the Venusian atmosphere water is photo dissociated and the heavier Deuterium stays in the atmosphere while water escapes into space.

2.4 Carbon Monoxide

The carbon monoxide abundance is a pretty moderate one and various investigations have shown mixing ratios of 20 – 30 ppmv (Pollack et al 1993).

The more interesting fact is that the mixing ratio of carbon monoxide is changing with latitude. The abundance is increasing towards the poles (Collard et al. 1993)
More recent investigations with Venera Express affirmed this observations (Tsang et al. 2009).

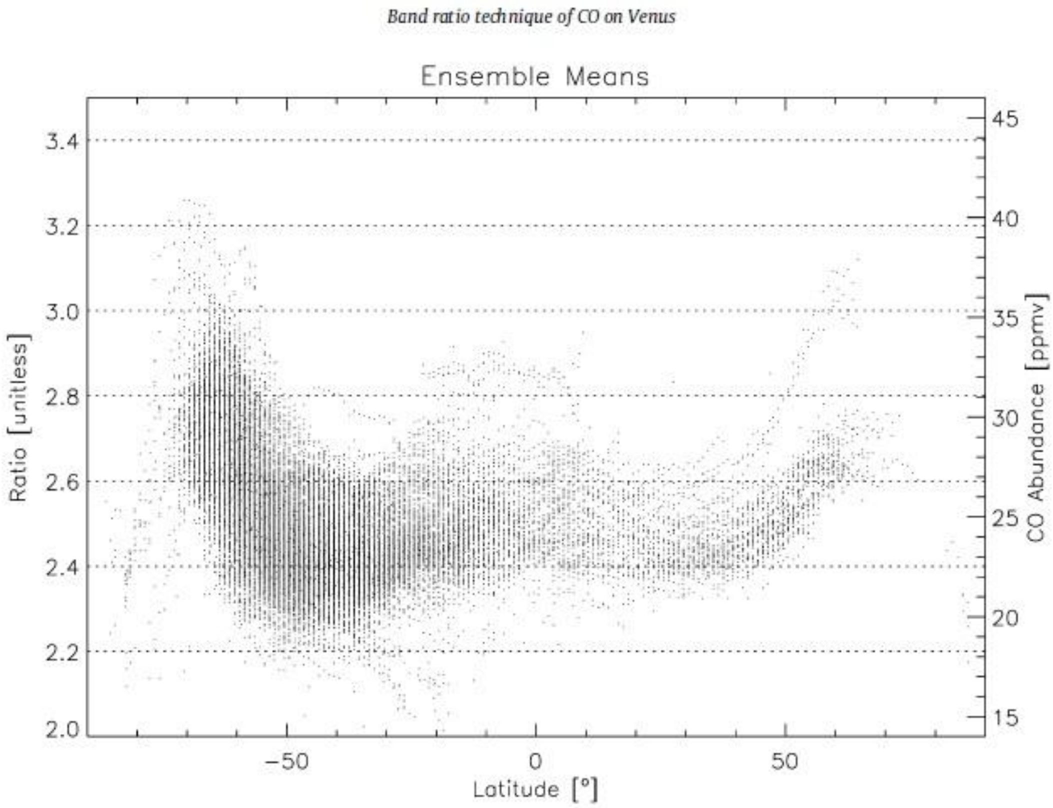

Figure 2.8: The carbon monoxide mixing ratio obtained by Venera Express (Tsang et al. 2009).

It is evident that there is a transport towards both polar vortices and this might be explained with the general atmospheric circulation.

2.5 Hydrogen Halides

Hydrogen halides like hydrochloric acid (HCl) and hydrogen fluoride (HF) have been found through near infrared spectroscopy in 1967 by Connes et al. (Connes et al. 1967). The first mixing ratio in the cloud tops was calculated to be around 0.6 ppm for hydrochloric acid and only 5 ppb for hydrogen fluoride.

More recent observations in the 1990's have shown that the values are still the same (Pollack et al. 1993). Pollack's observation from the Anglo-Australian Observatory has delivered mixing ratios of 0.48 ± 0.12 ppm for hydrochloric acid and 1 – 5 ppb for hydrogen fluoride.

Regrettably there are no measurements from the Venera missions in existence. The mass spectrometers and gas chromatographs were not able to detect such a small amount like 0.5 ppm hydrochloric acid or even less hydrogen fluoride.

Since the mixing ratio of both did not vary in the 25 years of observation, it is assumed that the mixing ratio is in an equilibrium state and contrary to sulphur dioxide, which is dominated by the volcanic outgassing.

Chapter 3

Sulphur dioxide in the Earth's Atmosphere

3.1 Sulphur dioxide emissions

Sulphur dioxide is one of the most puzzling elemental species in the Earth's and Venusian atmosphere. Their origins and their cycles in the atmosphere are similar, but they do have some differences too. Especially the origin of sulphur dioxide in the Earth's atmosphere is different, because it does not have only a volcanic origin. Anthropogenic production of sulphur dioxide plays a big role in the atmospheric models.

It was realized very soon that huge injections from the industry cause changes in the terrestrial climate, and although the anthropogenic emissions are becoming lesser, they are still huge in the relation to the output of the Earth's volcanoes.

- Anthropogenic sources of sulphur emissions
  - Energy Supply (coal burning)
  - Industry
  - Traffic & Transport
  - Biomass burning

- Natural sources of sulphur emissions
    - Volcanoes
    - Soils and Vegetation
    - Biogenic emissions from oceans
    - Natural biomass burning

Volcanoes do not only produce emissions during their active phase. The passive outgassing should not be forgotten. Although active volcanoes do produce a lot of sulphur dioxide and eject it in the atmosphere the passive outgassing is more constant and even larger than the active one.

The Total Ozone Mapping Spectrometer (TOMS) from NASA detected the sulphur dioxide from 55 global explosive terrestrial eruptions in 14 years. 52 Megatons were produced and this provides an average yearly output of 4 Megatons (Bluth et al. 1993.) This output can be taken as a lower boundary, because there exist also calculations, which predict a far bigger output.

Stoiber (Stoiber et al. 1972) did calculate the output with data from selected Central American volcanoes and the output was higher by a factor 2. The value obtained is 10 Megatons per year and it must be noted that very active eruptions have been omitted, and so the value was lowered.

Another totally different approach was achieved by Lambert (Lambert et al. 1988). The global Polonium output was measured and with a SO_2/Po ratio, which was known for a number of volcanoes, the total yearly flux of sulphur dioxide was calculated to be about 50 Megatons.

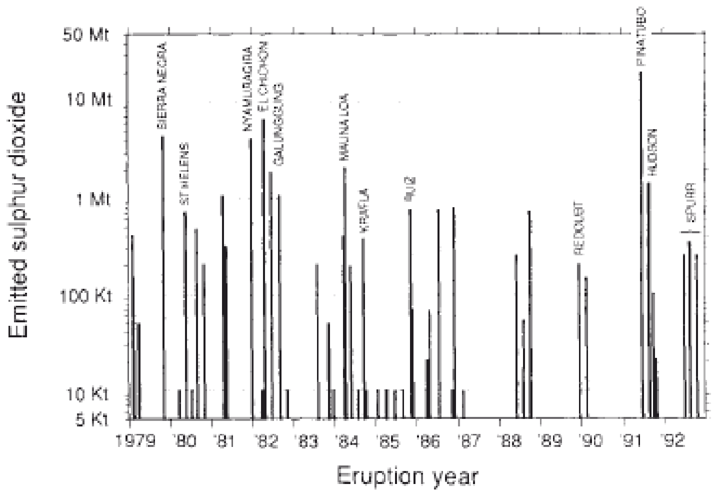

Figure 3.1: Volcanic eruptions from 1979 – 1993 (Bluth et al. 1993)

It is notable that one single event like Pinatubo in 1991 ejected 20 Megatons of sulphur dioxide. The Tambora Eruption in 1815 was the most explosive event in the modern history and it ejected approximately 200 Megatons of sulphur dioxide.

It is also very important to differentiate between arc and non-arc tectonics. Volcanoes in subduction zones (arc) do outgas far less sulphur dioxide than volcanoes at rifts or hot spots (non-arc).

Volcano	Momotombo	Kilauea Summit	Surtsey
Tectonic Style	Convergent-plate	Hot Spot	Divergent-plate
T (°C)	820	1170	1125
H_20	97.1	37.1	81.13
CO_2	1.44	48.9	9.29
SO_2	0.50	11.8	4.12
H_2	0.70	0.49	2.80
CO	0.01	1.51	0.69
H_2S	0.23	0.04	0.89
HCl	2.89	0.08	-
HF	0.26	-	-

Figure 3.2: Elemental species in volume percent concentrations (Symonds et al. 1994)

Non-arc eruptions outgas a lot more sulphur dioxide than arc eruptions, but arc volcanoes are far less on Earth then arc type ones. A ratio 1:2 is given by Bluth (Bluth et al. 1993). The calculated flux of 4 Megatons per year is split into 1.1 Megatons per year from non-arc eruptions and 2.6 Megatons per year from arc eruptions.

It has to be mentioned that there exists exceptions as well. Etna is a convergent plate volcano; this means it is an arc type volcano. It should be expected that the sulphur dioxide outgassing is pretty low, but Etna is one of the biggest sulphur dioxide producers.

Etna's volume percent concentration of sulphur dioxide is 47.7%. Measurements from 1975 by Haulet (Haulet et al. 1977) have shown that Etna had a flux of 3,740 tons per day. It has to be noted that in 1975 there was no major event from the very active Etna. This means it is an average value and this is about 1.4 Megatons per year. This is half of the production of all arc-type volcanoes together.

It should not be forgotten that 4 Megatons per year are just an average value, because eruptions on Earth are very infrequent. The observation window for this calculation is 14 years, which is quite long enough to give a good estimation of an average active output rate. In this time window the active output is dominated by the two eruptions of Pinatubo and El Chichón, without them the flux would be just 2 Megatons per year. Although the active output is very infrequent, the value of 4 Megatons per year is the most reasonable value.

The passive outgassing is the second kind of outgassing. This means that volcanoes do have emissions even when they are not active. The outgassing value of each volcano is pretty small, but the number of passive volcanoes and the fact, that they do have emissions frequently gives it an important role with a remarkable value.

Since the direct measurement of passive outgassing with TOMS is not possible, extrapolations have to be done and Stoiber (Stoiber et al. 1987) estimated the value for sulphur dioxide to be about 9 Megatons per year. This is more than twice of the active outgassing value.

The yearly global sulphur dioxide emissions are summed up from 4 Megatons, from active volcanism and 9 Megatons from passive volcanism. Together it gives a yearly flux of about 13 Megatons sulphur dioxide produced by volcanoes.

The anthropogenic percentage is far bigger. In older publications the total flux of sulphur dioxide produced by mankind is overrated with 190 Megatons per year (Möller et al. 1984), in newer publications (Graf et al. 1997) it is estimated with 78 Megatons sulphur per year, this yields a flux of ≈156 Megatons sulphur dioxide per year.

The molar mass of O_2 and sulphur is almost the same, therefore the amount of sulphur has to be doubled to obtain the correct value of sulphur dioxide.

It could be also lower with 72 Megatons sulphur (144 Megatons sulphur dioxide) per year, the error bars are given with ±8% (Smith et al. 2000).

3.2 Anthropogenic emissions

Most of the anthropogenic sulphur dioxide is produced by coal burning. This yields about 56% of the global flux. The rest is split up into petrol oil (24%), industrial processes like smelting ore (15%) and biomass burning (3%).
The trend is receding, it seems that mankind has reached the peak of sulphur dioxide production in the 1980’s and since 2000 the flux has been lowered for almost 10 Megatons (Smith et al. 2004).

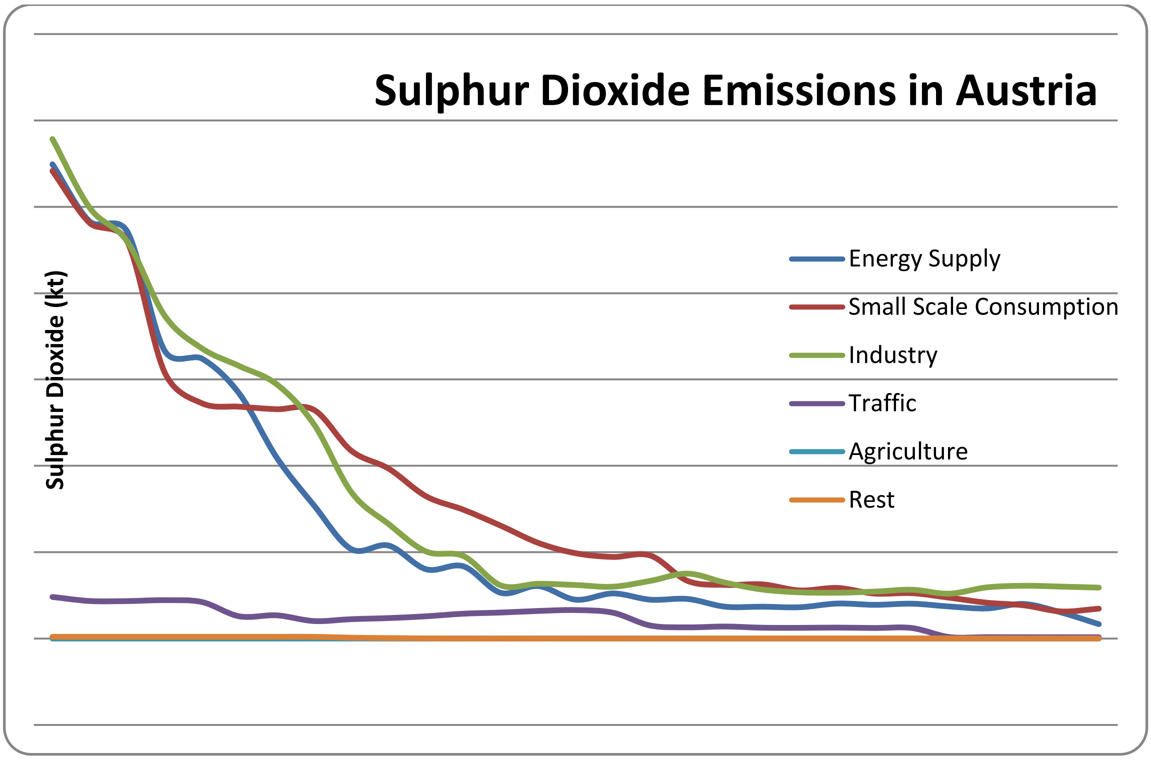

Figure 3.3: The sulphur dioxide emissions in Austria (provided by Umweltbundesamt) have been lowered to just one sixth part in three decades.

Generally in Europe the sulphur dioxide emissions have been lowered since the 80's by an ambitious value. The biggest sulphur dioxide producers are India, Central and Eastern Asia and the global ocean bunkers.

New techniques like the fluidized bed combustion, the Claus process and the Stretford process help to remove sulphur or they prevent the creation of sulphur dioxide. It can be assumed that the global anthropogenic production of sulphur dioxide will be lowered very much in the near future.

The anthropogenic production of sulphur dioxide is between 150 and 200 Megatons per year, this means that sulphur dioxide with volcanic origin has a percentage of only 7 – 12%.

The only organic sulphur producer, which reaches a reasonable value, is dimethyl sulfide (DMS). DMS is produced by marine phytoplankton and it gets oxidized to sulphur dioxide. It does emit around 90% of all sulphur produced by organic forms. The soils and vegetation and natural decays produce only 10% of the whole organic sulphur production.

Viney (Viney et al. 1990) have calculated the amount of the production of DMS in the sea. DMS is reduced from 290 to 55 µg Sm^{-2} per day. This is about 0.04 Megatons sulphur per year, if the production of DMS is assumed constant within all terrestrial seas. 0.8 Megatons sulphur dioxide are produced by marine phytoplankton.

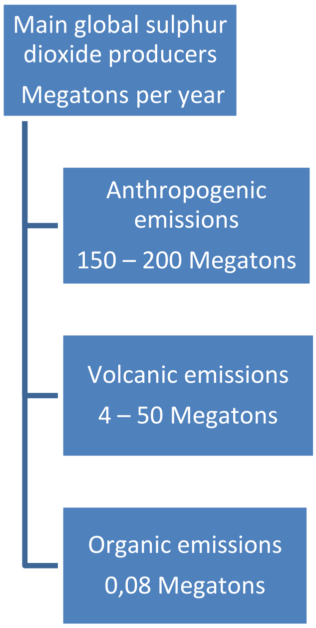

3.3 The Sulphur Cycle

In the Earth's atmosphere only a few sulphur species are common. H_2S, DMS ($(CH_3)_2S$), COS and CS_2 are the main species and in the atmosphere most of the sulphur oxidizes to SO_2 where the following reactions happen fast:

$$SO_2 + O \rightarrow SO_3 \quad (1.01)$$

$$SO_3 + H_20 \rightarrow H_2SO_4 \quad (1.02)$$

The first reaction 3.1 is a photochemical reaction, driven by sunlight. Sulphur trioxide combines with water rapidly and is mostly wet deposited by acid rain. The residence time of sulphur dioxide in the Earth's atmosphere is very short with only 24 hours. The two given reactions are fast and so the regional abundance of sulphur dioxide is very irregular.

DMS, COS and CS_2 are products of biogenic reactions. In the oceans DMS is the biggest sulphur provider but COS and CS2, which are created by soils, vegetation and industry, should not be disregarded.

COS is a very stable substance and has a very long residence time of 2 years. If COS leaves the troposphere into the stratosphere it combines with aerosols very easily and due to the very long residence time it is one of the leading sources for sulfate aerosols.

Leman (Leman et al. 2004) showed that COS is very interesting from the astrobiological point of view too. COS is a driver for the formation of peptides and the formation is very quick. Only in minutes complex peptides can be created and it is assumed that COS plays a big role in the origin of life.

The big difference between sulphur dioxide in the Earth's atmosphere and the Venusian atmosphere is the lack of water in the Venusian atmosphere. Sulphur dioxide which is produced by volcanoes on Venus cannot combine with water or oxygen, because there is very small amount of it in the lower atmosphere. This means that the residence time of sulphur dioxide is far longer on Venus and the abundance is much higher than in the Earth's atmosphere.

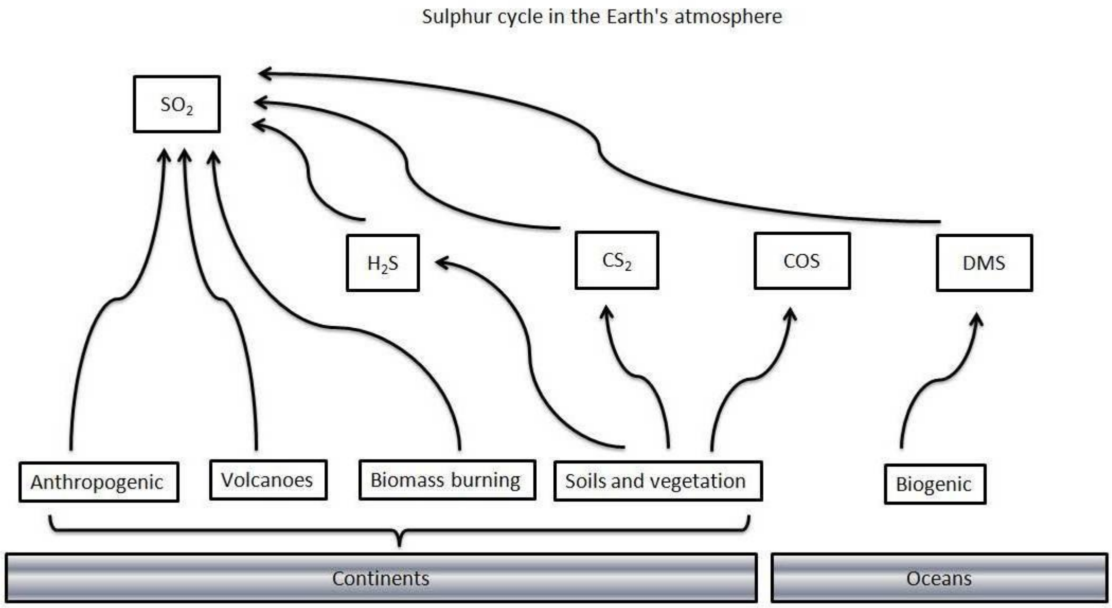

Figure 3.4: The sulphur cycle in the Earth's atmosphere

All sulphur bearing species, except COS, combine with oxygen and create sulphur dioxide. Sulphur dioxide follows the reactions 3.1 and 3.2 and is wet and dry deposited within 24 hours.

SO2 [kt]	1980	1981	1982	1983	1984	1985
Energy Supply	109,86	96,60	94,30	66,69	64,84	56,73
Smalls Scale Consumption	108,23	96,18	91,95	61,67	54,49	53,69
Industry	115,67	99,70	91,95	74,80	67,18	63,09
Traffic	9,65	8,72	8,70	8,90	8,48	5,17
Agriculture	0,04	0,04	0,04	0,04	0,04	0,05
Rest	0,41	0,41	0,41	0,41	0,41	0,41
Total	**343,86**	**301,65**	**287,34**	**212,52**	**195,44**	**179,13**

	1986	1987	1988	1989	1990	1991
Energy Supply	41,93	30,82	20,70	21,53	16,04	16,72
Smalls Scale Consumption	53,11	52,94	43,48	39,33	32,95	29,84
Industry	58,87	49,57	33,86	26,47	20,13	19,08
Traffic	5,40	4,07	4,51	4,76	5,18	5,78
Agriculture	0,04	0,04	0,05	0,05	0,00	0,00
Rest	0,41	0,41	0,22	0,14	0,07	0,06
Total	**159,77**	**137,87**	**102,81**	**92,27**	**74,37**	**71,47**

	1992	1993	1994	1995	1996	1997
Energy Supply	10,58	12,15	8,99	10,44	9,00	9,16
Smalls Scale Consumption	26,13	22,16	19,78	18,91	19,23	13,35
Industry	12,28	12,67	12,38	11,99	13,34	15,02
Traffic	6,05	6,41	6,61	6,00	3,03	2,62
Agriculture	0,00	0,00	0,00	0,00	0,00	0,00
Rest	0,04	0,04	0,05	0,05	0,05	0,05
Total	**55,08**	**53,44**	**47,82**	**47,40**	**44,66**	**40,20**

	1998	1999	2000	2001	2002	2003
Energy Supply	7,37	7,38	7,25	8,10	7,80	8,06
Smalls Scale Consumption	12,43	12,57	11,16	11,74	10,44	10,53
Industry	12,93	11,33	10,69	10,59	10,86	11,29
Traffic	2,81	2,53	2,50	2,56	2,47	2,45
Agriculture	0,00	0,00	0,00	0,00	0,00	0,00
Rest	0,05	0,06	0,06	0,06	0,06	0,06
Total	**35,60**	**33,86**	**31,67**	**33,05**	**31,63**	**32,39**

	2004	2005	2006	2007	2008
Energy Supply	7,42	6,97	8,00	6,01	3,33
Smalls Scale Consumption	9,48	8,33	7,71	6,30	6,95
Industry	10,38	11,84	12,20	12,02	11,78
Traffic	0,37	0,35	0,33	0,33	0,32
Agriculture	0,00	0,00	0,00	0,00	0,00
Rest	0,06	0,06	0,06	0,06	0,06
Total	**27,71**	**27,54**	**28,30**	**24,71**	**22,44**

Table 3.1: Sulphur dioxide emissions (provided by Umweltbundesamt)

Chapter 4

Vertical profile of sulphur dioxide

4.1 Vertical data points

The distribution of the sulphur dioxide in the Venusian lower atmosphere is discussed in chapter 2.3. Now the data, which will be used in all the calculations for the vertical profile, has to be selected wisely.

In the last few decades several data points have been measured, but sometimes they differ in abundance. In Chapter 2.3 the table 2.2 was shown and it should be discussed why these data point have been chosen.

Altitude (km)	Mixing Ratio (ppm)	Reference	Source
12	22 ± 3	Bertaux et al. 1996	Vega 1 & 2
22	38	Bertaux et al. 1996	Vega 1 & 2
35	130 ± 40	Bézard et al. 1993	Earth based IR spectrometry
42	130 ± 40	Bézard et al. 1993	Earth based IR spectrometry
52	110	Bertaux et al. 1996	Vega 1 & 2
69	0.5	Na et al. 1994	UV sounding rocket

Table 2.2: Sulphur dioxide mixing ratio obtained through various measurements. An overview is also given by de Bergh et al. 2006

These data points are given in the paper by de Bergh et al. 2006 and they show the vertical distribution of sulphur dioxide, obtained from different explorations. This data set was chosen, because these abundances were measured more than once and different explorations showed very similar mixing ratios. Three sources (Vega, IR spectrometry and UV sounding rockets) are shown here, but the mixing ratios have been acquired from Venera missions as well.

A more recent paper from Belyaev et al. (Belyaev et al. 2011) confirmed some of the mixing ratios shown in the table 2.2.

There are also some strong deviations from other explorations, but since they were measured only once they will be disregarded. Single deviations could be generated by active volcanoes during the landing phase or just are simple measurement errors.

The lowest 10 kilometers of the Venusian atmosphere are not explored good enough to create one single vertical profile. A strong decrease is obvious from the data points in the atmosphere, but the mixing ratios at ground level are not known at all. The only mixing ratios we can appoint to are the two measurement from the Vega mission.
One Vega lander measured a mixing ratio of 0 ppm and the other one a mixing ratio of 25 ppm.

The mixing ratio at ground level is very important for all calculations, because the density of the atmosphere is highest at ground level and so is the total amount of sulphur dioxide. Thus it is necessary to create two models and to compare them.

Model A uses the mixing ratio of 0 ppm, from the Vega 2 measurement, as a starting point and model B uses 25 ppm from the Vega 1 measurement. It also has to be pointed out that the measurement of the 25 ppm value is obtained even at a lower altitude than the 0 ppm measurement. The real value might be somewhere in between, but from now on we will use model A and model B for all calculations.

The table 2.2 is now corrected to

Altitude (km)	Mixing Ratio (ppm)	Reference	Source
0	0/25		Vega 1 & 2
12	22 ± 3	Bertaux et al. 1996	Vega 1 & 2
22	38	Bertaux et al. 1996	Vega 1 & 2
35	130 ± 40	Bézard et al. 1993	Earth based IR spectrometry
42	130 ± 40	Bézard et al. 1993	Earth based IR spectrometry
52	110	Bertaux et al. 1996	Vega 1 & 2
69	0.5	Na et al. 1994	UV sounding rocket

Table 4.1: Sulphur dioxide mixing ratio from de Bergh et al. 2006 including the mixing ratios at ground level obtained by Vega 1 & 2.

4.2 Model A and model B

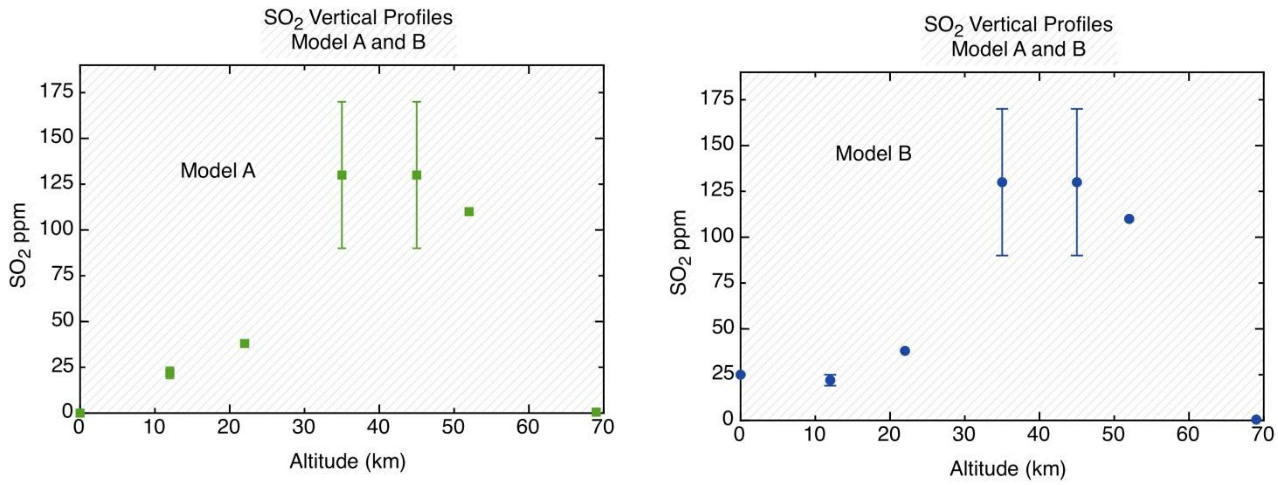

Figure 4.1: Model A and model B data points.

Functions have to be plotted through the data points to obtain the vertical profile of sulphur dioxide. A set of three function types, which produce three different progressions is chosen.

1) Linear functions
2) Exponential functions
3) Cubic Spline functions

The reason for choosing three different function types is to obtain a comparison and to better understand the progression of the mixing ratio of sulphur dioxide in the Venusian lower atmosphere. In further calculations it will give us a good estimation of the lower and upper boundaries of the total amount of sulphur dioxide, which is present on Venus.

In Figure 4.1 it is clear that the progression between the first three data points is pretty constant. The biggest difference is expected at the huge increase to data points 4 and 5, and the strong decrease to data point 7.

4.3 Linear vertical profile

The first vertical profile is obtained by fitting linear functions between the data points. These functions are written as:

$$f(x) = mx + b \tag{1.03}$$

The 7 data points produce 6 functions. They are calculated and plotted.

Model A

$$\begin{aligned}
f_1(x) &= \frac{11}{6}x \\
f_2(x) &= \frac{8}{5}x + \frac{14}{5} \\
f_3(x) &= \frac{92}{13}x - \frac{1530}{13} \\
f_4(x) &= 130 \\
f_5(x) &= -\frac{20}{17}x + \frac{1810}{7} \\
f_6(x) &= -\frac{219}{34}x + \frac{7564}{17}
\end{aligned} \tag{1.04}$$

Model B

$$\begin{aligned}
f_1(x) &= -\frac{1}{4}x + 25 \\
f_2(x) &= \frac{8}{5}x + \frac{14}{5} \\
f_3(x) &= \frac{92}{13}x - \frac{1530}{13} \\
f_4(x) &= 130 \\
f_5(x) &= -\frac{20}{17}x + \frac{1810}{7} \\
f_6(x) &= -\frac{219}{34}x + \frac{7564}{17}
\end{aligned} \tag{1.05}$$

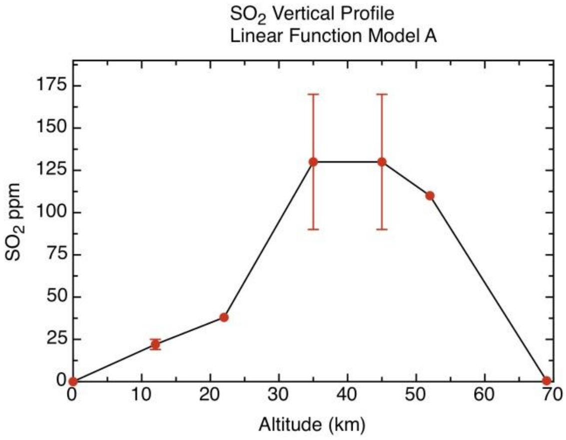

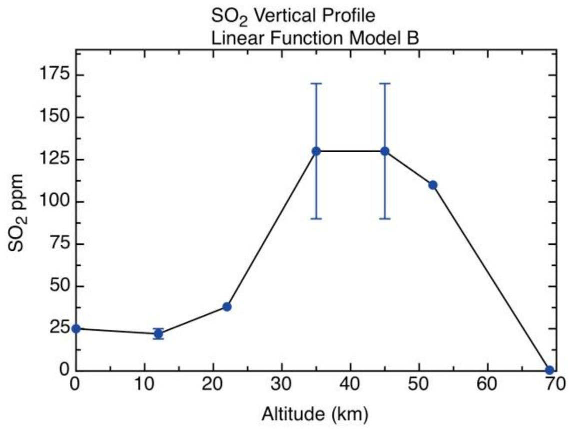

Figure 4.2: The vertical profile with linear functions

The linear functions are trivial functions, but they give a first good estimation of the vertical profile and in further consequence they allow fast calculations.

4.4 Exponential vertical profile

In this model the two big gaps in the vertical profile are fitted by an exponential function. This means that an exponential function is calculated from 12 km to 35 km altitude and a second one from 52 km to 69 km. The deviating data points are fitted by linear plots, because they would not make any sense with exponential plots.

Model B does have a third exponential function, which is calculated from 0 km to 22 km. The reason why a third exponential function is not possible for model A is that the value of model A at ground level is 0.

The linear functions are written as:

$$f(x) = mx + b \tag{1.06}$$

and the exponential functions are written as:

$$f(x) = a * e^{bx} \tag{1.07}$$

The two models are plotted with these functions:

Model A

$$\begin{aligned} f_1(x) &= \frac{11}{6}x \\ f_2(x) &= \frac{8}{5}x + \frac{14}{5} \\ f_3(x) &= 4.7405e^{0.0946x} \\ f_4(x) &= 130 \\ f_5(x) &= -\frac{20}{17}x + \frac{1810}{7} \\ f_6(x) &= 1608608269.8728e^{0.1728x} \end{aligned} \tag{1.08}$$

Model B

$$
\begin{aligned}
f_1(x) &= 25e^{0.019x} \\
f_2(x) &= \frac{8}{5}x + \frac{14}{5} \\
f_3(x) &= 4.7405e^{0.0946x} \\
f_4(x) &= 130 \\
f_5(x) &= -\frac{20}{17}x + \frac{1810}{7} \\
f_6(x) &= 1608608269.8728e^{0.1728x}
\end{aligned}
\qquad (1.09)
$$

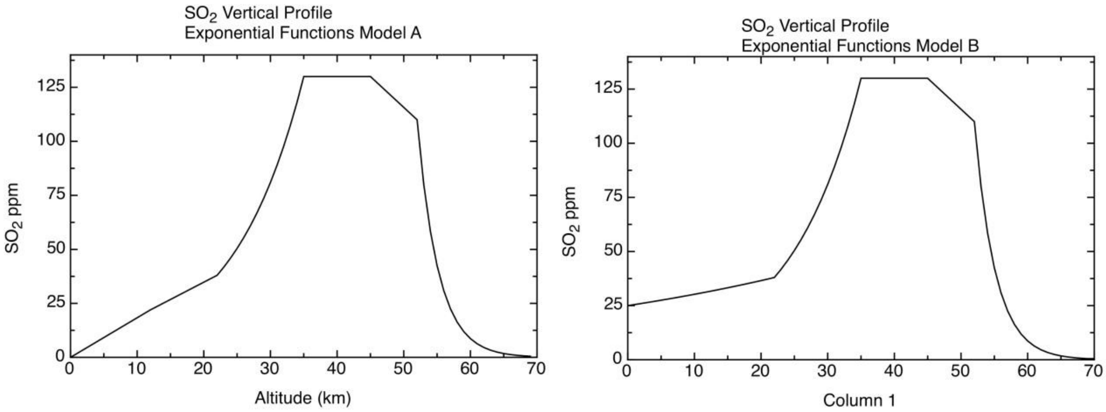

Figure 4.3: The vertical profile with exponential and linear functions

4.5 Cubic Spline vertical profile

A cubic Spline is a spline function, which is constructed of piecewise polynomial functions of third order and set through n points. A natural cubic Spline is given when the second derivative of each polynomial function is set to zero, to guarantee a system of n-2 equations, which can be solved easily and thus coefficients of the polynomials are calculated.

The cubic spline functions are calculated with the software ProFit from Quansoft for Macintosh computers.

It should be not forgotten that the functions have to fulfill some conditions when they are plotted. These major conditions are:

1) The values have to be positive
2) The plot should not have too large gaps, because the values should be realistic

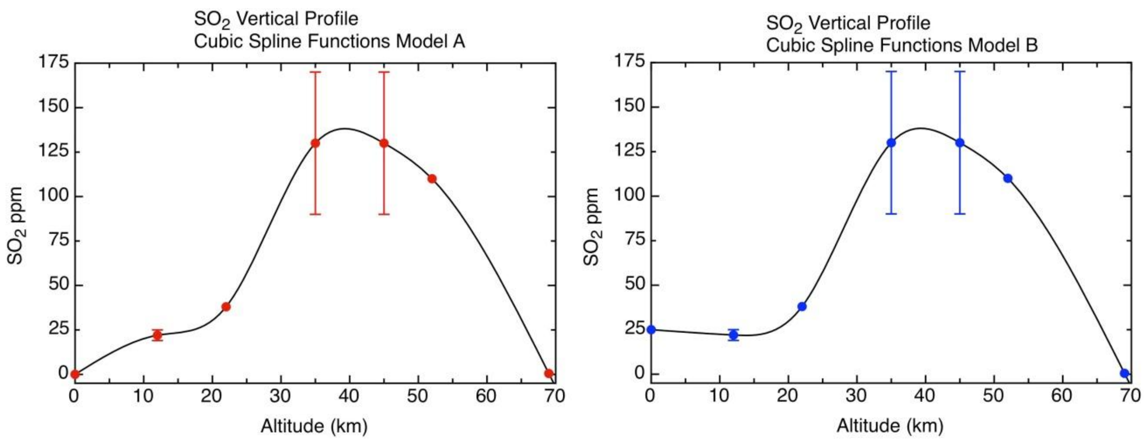

Figure 4.4: The vertical profile with cubic spline functions

The value at 70 kilometers altitude is -7.18 and cannot be considered in our models, since the values have to be positive.
The values at 70 kilometers are negligible for further investigations so they are set equal to the value at 69 kilometers. Now all values are positive and give a good model for the vertical profile of sulphur dioxide in the Venusian lower atmosphere.

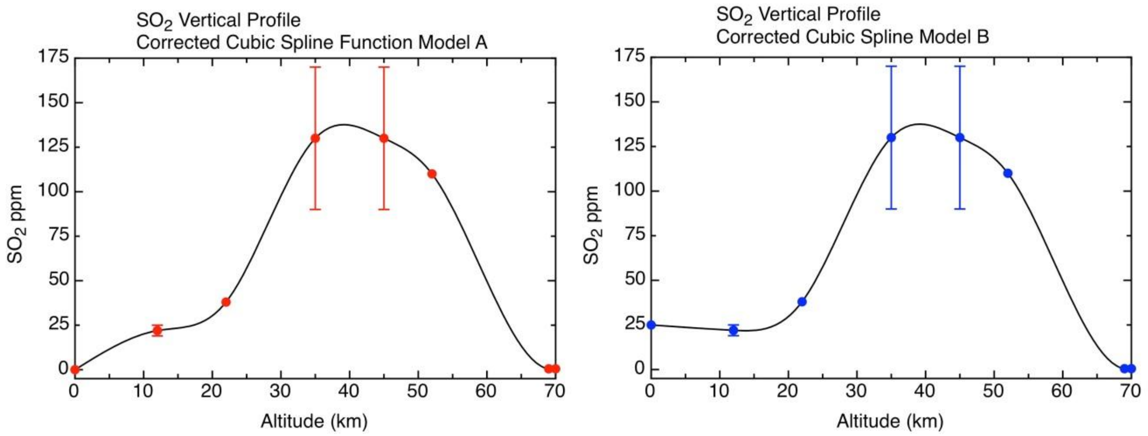

Figure 4.5: The corrected vertical profile obtained with cubic spline functions

The calculated and tabulated values from the cubic spline are given in Appendix 1.

Chapter 5

Calculations with the vertical profile

5.1 Plotting the density profile

For further calculations it is important to know the density at each altitude. There exists a published list (Landis et al. 2002), for the density of the Venusian atmosphere in 5 km altitude steps.

H, km	T, K	P, bar	ρ, kg/m³
0	735	92.10	64.79
5	697	66.65	49.87
10	658	47.39	37.72
15	621	33.04	27.95
20	581	22.52	20.39
25	539	14.93	14.57
30	497	9.851	10.15
35	455	5.917	6.831
40	418	3.501	4.404
45	385	1.979	2.693
50	350	1.066	1.594
55	302	0.5314	0.9207
60	263	0.2357	0.4694
65	243	0.09765	0.2086
70	230	0.03690	0.08393
75	215	0.01363	0.03298
80	197	0.004760	0.01186
85	181	0.001393	0.004007
90	169	0.0003736	0.001151
95	168	0.0001.016	0.0003155
100	175	0.00002660	0.00007890

Table 5.1: Temperature, Pressure and Density Profile (from Landis et al. 2002)

To obtain values for every single kilometer a cubic spline was fitted through all data points and calculated from 0 to 100 kilometers altitude. The software, which was used for the cubic spline is ProFit from Quansoft.

The tabulated calculations can be found in Appendix 2.

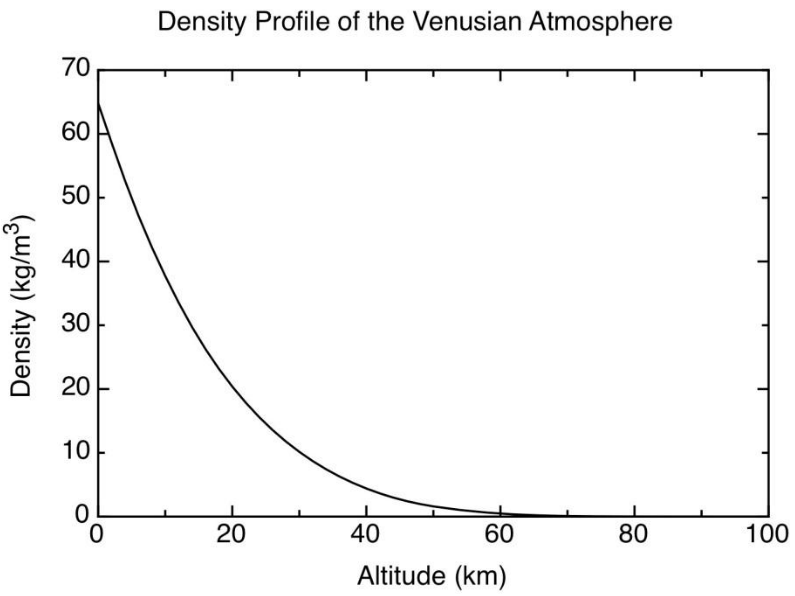

Figure 5.1: Density profile of the Venusian atmosphere

5.2 Plotting the temperature and pressure profile

The temperature and pressure profiles are obtained in the same way as the density profile. A Cubic spline is set through all data points and the values are calculated in 1 kilometer steps from 0 to 100 kilometers altitude.

The tabulated calculations can be found in Appendix 3.

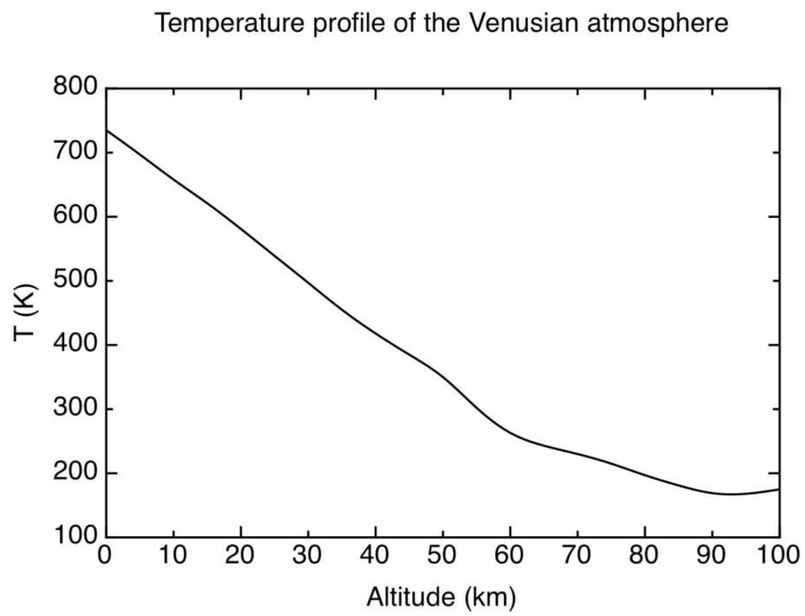

Figure 5.2: The temperature profile in Kelvin

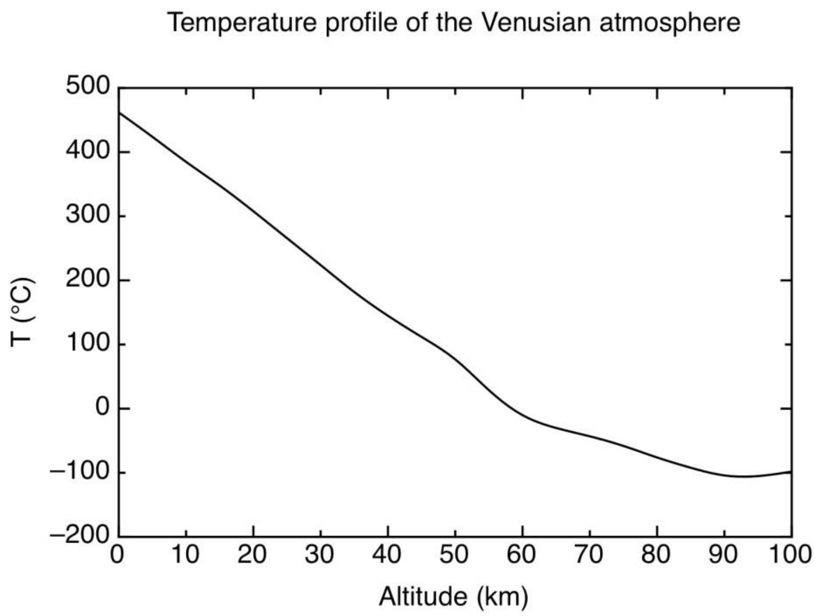

Figure 5.3: Temperature profile of the Venusian atmosphere in Celsius

The pressure profile is also calculated with a cubic spline for the first 100 kilometers of altitude.

All calculations needed for the density plot can be found in Appendix 4

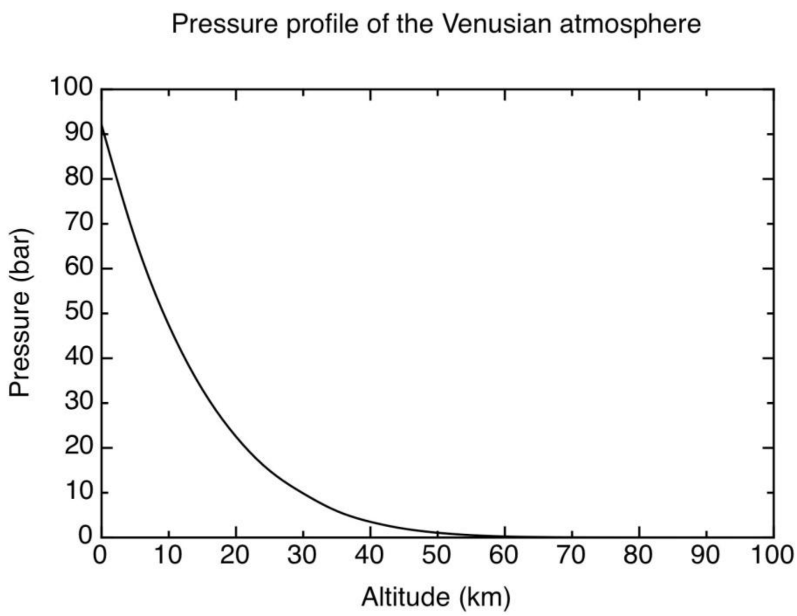

Figure 5.4: The pressure profile plotted against the altitude

5.3 Calculating the mass of the atmosphere

The main idea is to calculate the total amount of some elemental species in the lower atmosphere. To do so, an approximation has to be stepwise. The Venusian atmosphere is subdivided into shells and each shell has a radius of 1 kilometer. 70 shells represent the lower atmosphere up to a height of 70 kilometers. The volumes of these shells are calculated with the formula:

$$V_i = \frac{4}{3}\pi(r_1^3 - r_2^3) \quad (1.10)$$

And to calculate the total mass of each shell, the volumes have been multiplied with the density of each shell:

$$m_i = V_i * \rho_i \quad (1.11)$$

The density of each shell is known through the density profile from Figure 5.1 and the volume of each shell is calculated with the Formula (1.10).

The mass of each shell is also calculated for every kilometer and the 70 data points are also plotted in the following graph:

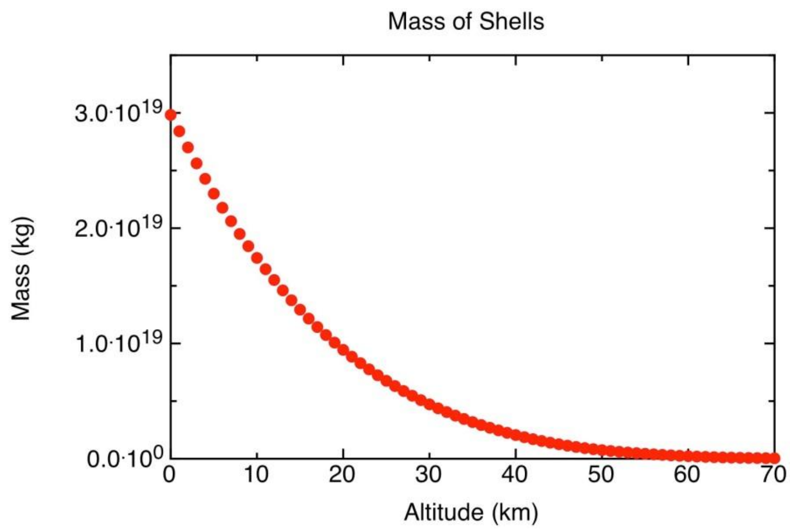

Figure 5.5: The mass of the shells plotted against the height

The calculated total mass of the Venusian atmosphere is about $4.98*10^{20}$ kg, which stands in good agreement with Fegley et al. (Fegley et al. (Fegley et al. 2006), who predicts that the mass of the whole atmosphere is $4.95*10^{20}$ kg. The mass of the atmosphere below 70 km altitude is about 99.96% of the total mass in these numerical calculations.

The numerical calculation can be found in Appendix 5.

5.4 Sulphur dioxide in the atmosphere

Now the mass of each spherical shell is known. Through the vertical profile it is possible to obtain the percentage of sulphur dioxide in each shell and the sum of all percentages in all spherical shells constitutes the total mass of sulphur dioxide present in the Venusian lower atmosphere.

Before it is possible to do so, the values in the Venusian sulphur dioxide vertical profile have to be be transformed. They all are given in ppm by Volume and they have to be transformed into ppm by Mass. The ppm by Volume values have to be multiplied with a factor k. This factor k is the molecular mass of sulphur dioxide divided by the mean molecular mass of the Venusian atmosphere.

$$k_{SO_2} = \frac{SO_2\ Molecular\ Mass}{Venus\ Mean\ Molecular\ Mass} \tag{1.12}$$

In this atmospheric model, the atmosphere consists out of 96.5% CO_2 and 3.5% N_2. To simplify the model it is presumed that the whole lower atmosphere is a uniform compound of these two constituents and other minor species are neglected, because they are very rare.

The molecular weight of CO_2 and N_2 is:

C = 12.0107 g/mole

O = 15.9994 g/mole

N = 14.0067 g/mole

$$CO_2 = C + 2 \times O = 12.0107 + 2 \times 15.9994 = 44.0095 \text{ g/mole} \quad (1.13)$$

$$N_2 = 2 \times N = 2 \times 14.0067 = 28.0134 \text{ g/mole} \quad (1.14)$$

$$0{,}965 \times CO_2 + 0{,}035 \times N_2 = 43.4496 \cong 43.45 \text{ g/mole} \quad (1.15)$$

The Venusian mean molecular mass of the atmosphere is 43.45 g/mole. This agrees perfectly with the NASA Factsheet Data (Appendix 16).

The molecular mass of SO_2 is:

$$SO_2 = S + 2 \times O = 32.065 + 2 \times 15.9994 = 64.0638 \cong 64.06 \text{ g/mole} \quad (1.16)$$

The factor k for SO_2 is:

$$k_{SO_2} = \frac{64.06}{43.45} \cong 1.47 \quad (1.17)$$

Table 4.1 shows the ppm by Volume values of sulphur dioxide. In table 5.2 they are transformed to ppm by Mass.

SO2	Model A	Model B	Model A	Model B
Altitude (km)	Mixing Ratio (ppm)	Mixing Ratio (ppm)	Mixing Ratio (ppm by Mass)	Mixing Ratio (ppm by Mass)
0	0	25	0	36.75
12	22 ± 3	22 ± 3	32.34 ± 4.41	32.34 ± 4.41
22	38	38	55.86	55.86
35	130 ± 40	130 ± 40	191.1 ± 58.8	191.1 ± 58.8
45	130 ± 40	130 ± 40	191.1 ± 58.8	191.1 ± 58.8
52	110	110	161.7	161.7
69	0.5	0.5	0.74	0.74

Table 5.6: Sulphur dioxide mixing ratio in ppm by Mass.

For further calculations all vertical profiles have to be transformed to mixing ratios in ppm by Mass and they are plotted in figure 5.3.

5.5 Vertical profiles with the transformed mixing ratio

The mixing ratios of sulphur dioxide are transformed from ppm by Volume to ppm by Mass. Furthermore all three types of vertical profiles, which were introduced before, have been calculated with the ppm by Mass values. With these vertical profiles it is possible to obtain the total mass of sulphur dioxide in the Venusian lower atmosphere.

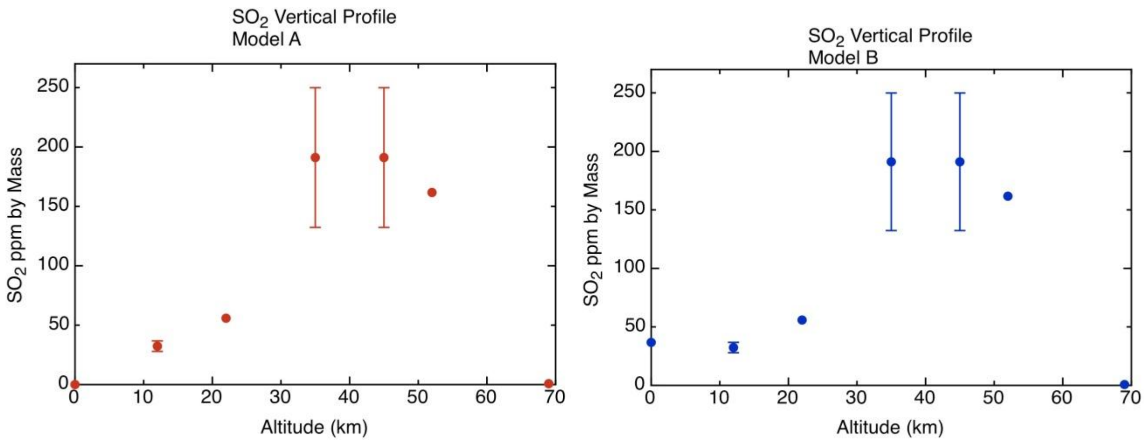

Figure 5.6: Sulphur dioxide vertical profiles with mixing ratios given in ppm by Mass.

The models displayed before are now adapted to the mixing ratio given in ppm by Mass.
Here are the vertical profiles with the linear functions.

Model A

$$
\begin{aligned}
f_1(x) &= \frac{539}{200}x \\
f_2(x) &= \frac{294}{125}x + \frac{1029}{250} \\
f_3(x) &= \frac{104031}{10000}x - \frac{1730077}{10000} \\
f_4(x) &= \frac{1911}{10} \\
f_5(x) &= -\frac{21}{5}x + \frac{3801}{10} \\
f_6(x) &= -\frac{47341}{5000}x + \frac{3270241}{5000}
\end{aligned} \tag{1.18}
$$

Model B

$$
\begin{aligned}
f_1(x) &= -\frac{147}{400}x + \frac{147}{4} \\
f_2(x) &= \frac{294}{125}x + \frac{1029}{250} \\
f_3(x) &= \frac{104031}{10000}x - \frac{1730077}{10000} \\
f_4(x) &= \frac{1911}{10} \\
f_5(x) &= -\frac{21}{5}x + \frac{3801}{10} \\
f_6(x) &= -\frac{47341}{5000}x + \frac{3270241}{5000}
\end{aligned} \tag{1.19}
$$

The vertical profile with the exponential functions is given with:

Model A

$$
\begin{aligned}
f_1(x) &= \frac{539}{200}x \\
f_2(x) &= \frac{294}{125}x + \frac{1029}{250} \\
f_3(x) &= 16.7844e^{0.0547x} \\
f_4(x) &= \frac{1911}{10} \\
f_5(x) &= -\frac{21}{5}x + \frac{3801}{10} \\
f_6(x) &= 2316121249.2918e^{-0.3169x}
\end{aligned} \tag{1.20}
$$

Model B

$$
\begin{aligned}
f_1(x) &= 36{,}75e^{-0.0107x} \\
f_2(x) &= \frac{294}{125}x + \frac{1029}{250} \\
f_3(x) &= 16.7844e^{0.0547x} \\
f_4(x) &= \frac{1911}{10} \\
f_5(x) &= -\frac{21}{5}x + \frac{3801}{10} \\
f_6(x) &= 2316121249.2918e^{-0.3169x}
\end{aligned} \tag{1.21}
$$

The cubic spline function is calculated with the ProFit Software again. The tabulated values can be found in Appendix 6.

Chapter 6

Calculating the total amount of sulphur dioxide

6.1 The numerical calculations

To obtain the total amount of one constituent in the Venusian lower atmosphere the atmosphere has to be split up into spherical shells.
For the first calculation the atmosphere is split up in to 70 spherical shells and the mass and the volume of each shell could be calculated with the formulas (1.10) and (1.11) given in chapter 5.

The density profile was calculated in chapter 5 and so the mass of each shell is known. This mass has to be multiplied with the mixing ratio (given in ppm by Mass) of sulphur dioxide at each height and the sum of the shells gives the total amount of sulphur dioxide present in the lower atmosphere.

$$\sum_{i=0}^{70} m_i * P_i \qquad (1.22)$$

P_i = mixing ratio in ppm by Mass at each altitude
All calculations were performed for all three types of vertical profiles (linear, exponential, cubic spline) and for both models model A and model B.

6.2 Using the linear vertical profile

The first calculations are performed with the linear vertical profile.
The numerical calculation is presented in the appendix 7.

The total amount of sulphur dioxide present in the Venusian lower atmosphere, which was calculated with a linear profile (model A) is:

$$2.236 * 10^{16} \pm 0.40 * 10^{16} \text{ kg} \tag{1.23}$$

The whole calculation for model B is analogue to model A. Now the linear vertical profile of model B is used.
The numerical calculations are presented in the appendix 8.

The total amount of the sulphur dioxide present in the Venusian lower atmosphere, corresponding to the model B, which is calculated with a linear profile is:

$$2.831 * 10^{16} \pm 0.40 * 10^{16} \text{ kg} \tag{1.24}$$

6.3 Using the exponential vertical profile

After the calculation with the linear density profile, the exponential profile is used to obtain the total amount of Sulphur dioxide.

All calculations are presented in the appendix 9.

For model A with an exponential vertical profile the total amount of sulphur dioxide amounts to:

$$2.104 * 10^{16} \pm 0.31 * 10^{16} \text{ kg} \quad (1.25)$$

Now the analogue calculation for model B is done and the calculation is shown in the appendix 10.

The total amount of sulphur dioxide calculated with the exponential vertical profile for model B is:

$$2.617 * 10^{16} \pm 0.39 * 10^{16} \text{ kg} \quad (1.26)$$

6.4 Using the cubic spline vertical profile

The numerical calculations for model A are presented in the appendix 11.

The total amount of sulphur dioxide according to the cubic spline for model A is:

$$2.267 * 10^{16} \pm 0.41 * 10^{16} \text{ kg} \quad (1.27)$$

For model B the analogue calculation is done and presented in the appendix 12.
The total amount of sulphur dioxide calculated with a cubic spline for model B is:

$$2.782 * 10^{16} \pm 0.41 * 10^{16} \text{ kg} \quad (1.28)$$

6.5 Comparing the results

Three different types of vertical profiles have been introduced (linear, exponential and cubic spline) and for all three types the calculation for the total amount of sulphur dioxide in the Venusian lower atmosphere is done.

The three results including their deviation are presented and it is remarkable that they do not vary much.

	Linear Profile (10^{16}kg)	Exponential Profile (10^{16}kg)	Cubic Spline Profile (10^{16}kg)
Model A	2.236±0.40	2.104±0.31	2.267±0.41
Model B	2.831±0.40	2.617±0.39	2.782±0.41

Table 6.7: The results of all calculations

To confirm the calculations it is needed to prove their accuracy. The number of the shells has to be increased and the results have to be compared with the ones from Table 6.7.

6.6 Proving the accuracy

To prove the accuracy of our results it is inevitable to make another calculation with an increased number of shells. In all calculations the number of shells is 70. That means that the shells are separated by one kilometer.

Now the shells will be separated by 0.25 kilometers and that means that the shell number is increased by a factor of 4. 280 shells are used in this calculation and the cubic spline model is used for the proof of accuracy.

At first the density, volumes, mass and the vertical profiles have to be calculated. The density profile and the vertical profile are calculated with a cubic spline and the volumes and the mass are calculated with the formulas (1.10) and (1.11).

The table for the density profile and the mixing ratio calculated with a cubic spline is given in the appendix 13.

For model A and model B the last 4 shells yield a negative value for the mixing ratio. Since negative values are not admitted in the calculation they are set equal to the shell 69. In chapter 4.5 this step is already discussed.

Now the calculation with model A and model B including their deviations is performed and the result gives us the total amount of sulphur dioxide.

The numerical calculation is presented in the appendix 14.
The result is:

$$2.268 * 10^{16} \pm 0.41 * 10^{16} \text{ kg} \tag{1.29}$$

Also the calculation with model B is done and after that the values should be compared with the ones from the calculation with only 70 shells. The appendix 15 includes all numerical calculations for model B.

The result for model B is:

$$2.740 * 10^{16} \pm 0.41 * 10^{16} \text{ kg} \tag{1.30}$$

The more accurate values have to be compared with the calculations before. The question is if there are crucial differences or not.

	Cubic Spline 70 shells (10^{16}kg)	Cubic Spline 280 shells (10^{16}kg)
Model A	2.267±0.41	2.268±0.41
Model B	2.782±0.41	2.740±0.41

Table 6.11: Comparison of the numerical calculations

The difference between the two calculations does not play a big role. The difference between the two model A calculations is about 0.04%.
The difference between the two model B calculations is just a bit higher with 1.5%.

The better numerical calculation does not deviate much from the calculation with 70 shells. It has to be noticed also that the differences between the linear, exponential and cubic spline calculation is far bigger than the 1.5% from above.

There is no need to accomplish more precise numerical calculations, because the values are certified and the accuracy is more than satisfying.

Chapter 7

Estimating the destruction rate

7.1 Weathering on Venus' surface

The foregoing chapters provided a good overview on the vertical profile of sulphur dioxide in the Venusian lower atmosphere. It was even possible to calculate the total amount of the sulphur dioxide present there. What is known about the sulfur cycle and what it is new with the calculations from this thesis?

Sulphur dioxide in the Venusian atmosphere is created from the large numbers of volcanoes on Venus. The present volcanic activity is not well known and we cannot estimate how much sulphur dioxide is produced daily.

500-1000 million years ago Venus was globally resurfaced (J. A. Wood 2003). This means that the entire crust was resurfaced by new volcanic output. From this time on, the surface interacted with the atmosphere.
It is not known what the atmosphere looked like before this global event, but it is known which reactions the rocks had undergone after the resurfacing event with the elemental species in the atmosphere.

For the understanding of the sulphur cycle one reaction is of major importance, because it is the only strong reaction with sulphur dioxide and the surface of Venus (Fegley et al. 1992)

$$\frac{d[CaSO_4]}{dt} = 10^{19.64(\pm 0.28)} e^{\frac{-15250(\pm 2970)}{T}} \text{ Molecules cm}^{-2} \text{ s}^{-1} \qquad (1.31)$$

Sulphur dioxide is highly reactive with the surface of Venus and it produces anhydrite. Other reactions are calculated and measured from experiments from Fegley and Prinn 1989 (Fegley and Prinn 1989) and they are far too slow to play a role in the sulfur cycle.
Formula (1.31) calculated with the temperature from the surface gives a global mean rate of

$$4.6 * 10^{10} \text{ Molecules cm}^{-2} \text{ s}^{-1} \quad (1.32)$$

This makes it possible to calculate how many grams of sulphur dioxide are lost to anhydrite yearly

$$6.67 * 10^{36} \text{ Molecules y}^{-1} \text{ at the global surface} \quad (1.33)$$

This makes

$$7.12 * 10^{14} \text{ g y}^{-1} \quad (1.34)$$

This means that in the last 500 – 1000 million years the surface has destroyed $3.56 * 10^{17}$ to $7.12 * 10^{17}$ tons of sulphur dioxide.

Other sulphur terminating reactions on the surface are just too slow and they can be neglected.
Also the reaction with other elemental species like acid sulphur is of minor rate and has not to be taken into the calculations. Acid sulphur is only available in the higher regions of the Venusian lower atmosphere and the abundance is only 0.1 – 10 ppmV and this is marginal.

$$SO_2 + O = SO_3 \quad (1.35)$$

$$SO_3 + H_20 = H_2SO_4 \quad (1.36)$$

This is the only reaction which is very fast in the Venusian lower atmosphere. Other reactions are even slower and do not play a role in our calculations.

Also the photolysis of sulphur dioxide plays only a role above the clouds. The vertical profile of sulphur dioxide shows us that the abundance at altitudes higher than 65 km is less than 1 ppm and the mass of the whole sulphur dioxide at high altitudes is almost zero.
This shows us that only the production of anhydrite is very fast and makes the biggest part of the destruction of sulphur dioxide.

In the calculations from chapter 4 it is known how much sulphur dioxide is present today. If we consider that since the last 500 – 1000 million years no global resurfacing took place it can be find out how strong the yearly production is.

The highest value of sulphur dioxide present in the Venusian atmosphere is the one from the calculations with model B.

$2.7 * 10^{16}$ kg are present today and in the last 500 – 1000 million years the surface destroyed $7.12 * 10^{20}$ kg sulphur dioxide.

Figure 7.1: The sulfur cycle in the last 500 – 1000 million years.

The production of sulphur dioxide can be calculated according to Figure 7.1 this way:

Figure 7.2: The calculation of the production of sulphur dioxide

Now it must be noted that the present value is smaller by a factor of 10^4 and this means that the production is pretty equal to the destruction rate. Not enough sulphur dioxide is still present and this is the reason why the production rate is just a little bigger than the destruction rate.

7.2 Discussing the results

What does a production rate of at least $7.12 * 10^{11}$ kg per year mean?

This is higher than the production rate of Earth!

In Chapter 3 the terrestrial volcanic outgassing is discussed and results from Stoiber et al (Stoiber et al. 1987) showed that the terrestrial sulphur dioxide production rate is approximately $1.3*10^{10}$ kg per year. On Venus the production rate is at least $7.12\ 10^{11}$ kg per year according to the annual destruction rate.

This is puzzling, because Venus is a geologically very inactive body compared to Earth.

The Vega 2 missions has shown that the S/Ca ratio is still very small, so today the anhydrite formation is still a topic and the reaction is still going on. (Fegley and Prinn 1997)

The solution of the problem is the fact that the destruction rate calculated by Fegley and Prinn 1989 (Fegley and Prinn 1989) is not constant over 500 - 1000 million years.

Fegley and Prinn (Fegley and Prinn 1997) calculated a yearly anhydrite deposition rate of 1 µm. On one hand they also mentioned that with a growing anhydrite layer the reaction may slow down, but on the other hand corresponding to Marshall et al. (Marshall et al. 1988) Aeolian weathering removes the fine anhydrite layer very fast and the reaction must not slow down.

Both sides may be correct but Aeolian weathering cannot remove the anhydrite layer for 500 – 1000 million years. The reaction must be slowed down at some timescale.

If the effect is not slowed down at some timescale this would mean that the present sulphur dioxide amount is a relict of a great event in the last one million years. The residence time of sulphur dioxide is very short on Venus. After Fegley et al (Fegley et al. 2006) the residence time is 1.9 million years at most.
Since the destruction is very rapid the volcanic event must have happened within this short timescale.

Appendix 1

The sulphur dioxide mixing ratio in ppmV tabulated with a cubic spline.

Altitude (km)	Model A (ppmV)	Model B (ppmV)
0	0	25
1	2.404	24.724
2	4.784	24.450
3	7.116	24.177
4	9.377	23.908
5	11.541	23.643
6	13.586	23.383
7	15.487	23.130
8	17.221	22.885
9	18.763	22.648
10	20.089	22.421
11	21.176	22.204
12	22	22
13	22.564	21.826
14	22.981	21.768
15	23.394	21.932
16	23.943	22.421
17	24.769	23.338
18	26.013	24.789
19	27.818	26.876
20	30.323	29.704
21	33.67	33.378

22	38	38
23	43.401	43.629
24	49.745	50.137
25	56.851	57.350
26	64.539	65.094
27	72.626	73.196
28	80.933	81.480
29	89.277	89.775
30	97.478	97.905
31	105.355	105.696
32	112.727	112.975
33	119.412	119.568
34	125.23	125.301
35	130	130
36	133.59	133.539
37	136.068	135.985
38	137.552	137.453
39	138.16	138.058
40	138.009	137.915
41	137.218	137.139
42	135.903	135.844
43	134.184	134.146
44	132.177	132.160
45	130	130.000
46	127.743	127.754
47	125.378	125.394
48	122.85	122.868
49	120.104	120.120
50	117.084	117.095

51	113.734	113.740
52	110	110
53	105.839	105.834
54	101.263	101.254
55	96.299	96.286
56	90.971	90.957
57	85.307	85.291
58	79.333	79.315
59	73.073	73.055
60	66.554	66.536
61	59.802	59.785
62	52.842	52.827
63	45.702	45.688
64	38.406	38.393
65	30.98	30.970
66	23.451	23.443
67	15.844	15.838
68	8.185	8.182
69	0.5	0.5
70	0.5	0.5

Appendix 2

The density profile tabulated with a cubic spline

Altitude (km)	Density (kg/m^3)
0	64.79
1	61.69
2	58.62
3	55.61
4	52.68
5	49.87
6	47.20
7	44.66
8	42.24
9	39.93
10	37.72
11	35.59
12	33.55
13	31.59
14	29.72
15	27.95
16	26.27
17	24.68
18	23.17
19	21.75
20	20.39
21	19.10

22	17.88
23	16.71
24	15.61
25	14.57
26	13.58
27	12.65
28	11.77
29	10.94
30	10.15
31	9.41
32	8.70
33	8.04
34	7.42
35	6.83
36	6.28
37	5.76
38	5.28
39	4.83
40	4.40
41	4.01
42	3.64
43	3.30
44	2.98
45	2.69
46	2.43
47	2.19
48	1.97
49	1.77

50	1.59
51	1.43
52	1.29
53	1.15
54	1.03
55	0.92
56	0.82
57	0.72
58	0.63
59	0.54
60	0.47
61	0.40
62	0.34
63	0.29
64	0.25
65	0.21
66	0.17
67	0.15
68	0.12
69	0.10
70	0.08
71	0.07
72	0.06
73	0.05
74	0.04
75	0.03
76	0.03
77	0.02

78	0.02
79	0.01
80	0.01
81	0.01
82	0.01
83	0.01
84	0.00
85	0.00
86	0.00
87	0.00
88	0.00
89	0.00
90	0.00
91	0.00
92	0.00
93	0.00
94	0.00
95	0.00
96	0.00
97	0.00
98	0.00
99	0.00
100	0.00

Appendix 3

The temperature profile tabulated with a cubic spline

Altitude (km)	Temperature (K)	Temperature (°C)
0	735	461.85
1	727.49	454.34
2	719.95	446.8
3	712.38	439.23
4	704.73	431.58
5	697	423.85
6	689.17	416.02
7	681.3	408.15
8	673.43	400.28
9	665.65	392.5
10	658	384.85
11	650.53	377.38
12	643.17	370.02
13	635.86	362.71
14	628.49	355.34
15	621	347.85
16	613.31	340.16
17	605.45	332.3
18	597.42	324.27
19	589.26	316.11
20	581	307.85
21	572.66	299.51

22	564.27	291.12
23	555.84	282.69
24	547.41	274.26
25	539	265.85
26	530.62	257.47
27	522.25	249.1
28	513.87	240.72
29	505.47	232.32
30	497	223.85
31	488.47	215.32
32	479.93	206.78
33	471.46	198.31
34	463.13	189.98
35	455	181.85
36	447.14	173.99
37	439.54	166.39
38	432.16	159.01
39	424.99	151.84
40	418	144.85
41	411.16	138.01
42	404.45	131.3
43	397.87	124.72
44	391.39	118.24
45	385	111.85
46	378.66	105.51
47	372.18	99.03
48	365.39	92.24
49	358.06	84.91

50	350	76.85
51	341.09	67.94
52	331.54	58.39
53	321.65	48.5
54	311.7	38.55
55	302	28.85
56	292.8	19.65
57	284.21	11.06
58	276.33	3.18
59	269.23	-3.92
60	263	-10.15
61	257.69	-15.46
62	253.18	-19.97
63	249.32	-23.83
64	245.98	-27.17
65	243	-30.15
66	240.25	-32.9
67	237.64	-35.51
68	235.1	-38.05
69	232.58	-40.57
70	230	-43.15
71	227.3	-45.85
72	224.46	-48.69
73	221.48	-51.67
74	218.32	-54.83
75	215	-58.15
76	211.5	-61.65
77	207.89	-65.26

78	204.22	-68.93
79	200.57	-72.58
80	197	-76.15
81	193.57	-79.58
82	190.27	-82.88
83	187.09	-86.06
84	184	-89.15
85	181	-92.15
86	178.08	-95.07
87	175.32	-97.83
88	172.82	-100.33
89	170.68	-102.47
90	169	-104.15
91	167.86	-105.29
92	167.23	-105.92
93	167.07	-106.08
94	167.34	-105.81
95	168	-105.15
96	168.99	-104.16
97	170.26	-102.89
98	171.72	-101.43
99	173.33	-99.82
100	175	-98.15

Appendix 4

The pressure profile tabulated with a cubic spline

Altitude (km)	Pressure (bar)
0	92.1
1	86.7474
2	81.4604
3	76.3048
4	71.3461
5	66.65
6	62.2661
7	58.1793
8	54.3584
9	50.7724
10	47.39
11	44.1849
12	41.1497
13	38.2822
14	35.5798
15	33.04
16	30.659
17	28.4274
18	26.3343
19	24.3688
20	22.52
21	20.7794

22	19.1474
23	17.6266
24	16.22
25	14.93
26	13.7557
27	12.6807
28	11.685
29	10.7485
30	9.851
31	8.9778
32	8.1357
33	7.3368
34	6.5932
35	5.917
36	5.3166
37	4.7853
38	4.3125
39	3.8879
40	3.501
41	3.143
42	2.8119
43	2.5077
44	2.2301
45	1.979
46	1.7538
47	1.5524
48	1.3723
49	1.211

50	1.066
51	0.9351
52	0.8171
53	0.7111
54	0.6162
55	0.5314
56	0.456
57	0.3892
58	0.3306
59	0.2797
60	0.2357
61	0.1982
62	0.1664
63	0.1396
64	0.1169
65	0.0977
66	0.0811
67	0.067
68	0.0551
69	0.0452
70	0.0369
71	0.0301
72	0.0246
73	0.0202
74	0.0166
75	0.0136
76	0.0112
77	0.0091

78	0.0074
79	0.0059
80	0.0048
81	0.0038
82	0.003
83	0.0023
84	0.0018
85	0.0014
86	0.0011
87	0.0008
88	0.0006
89	0.0005
90	0.0004
91	0.0003
92	0.0002
93	0.0002
94	0.0001
95	0.0001
96	0.0001
97	0.0001
98	0
99	0
100	0

Appendix 5

Gathering the mass of each spherical shells with numerical calculations.

Shellnumber	Volume (km^3)	Density (kg/m^3)	Mass (kg)
0	460310370.03	64.79	2.98235E+19
1	460462493.49	61.69	2.84057E+19
2	460614642.07	58.62	2.70004E+19
3	460766815.80	55.61	2.5621E+19
4	460919014.65	52.68	2.42809E+19
5	461071238.64	49.87	2.29936E+19
6	461223487.76	47.20	2.17694E+19
7	461375762.01	44.66	2.06057E+19
8	461528061.40	42.24	1.94968E+19
9	461680385.91	39.93	1.8437E+19
10	461832735.56	37.72	1.74203E+19
11	461985110.35	35.59	1.64423E+19
12	462137510.26	33.55	1.5503E+19
13	462289935.31	31.59	1.46037E+19
14	462442385.49	29.72	1.37454E+19
15	462594860.81	27.95	1.29295E+19
16	462747361.26	26.27	1.21566E+19
17	462899886.84	24.68	1.14246E+19
18	463052437.55	23.17	1.07309E+19
19	463205013.39	21.75	1.00729E+19
20	463357614.37	20.39	9.44786E+18
21	463510240.48	19.10	8.85351E+18

22	463662891.73	17.88	8.28864E+18
23	463815568.10	16.71	7.75239E+18
24	463968269.61	15.61	7.24388E+18
25	464120996.25	14.57	6.76224E+18
26	464273748.03	13.58	6.30654E+18
27	464426524.94	12.65	5.87557E+18
28	464579326.98	11.77	5.46809E+18
29	464732154.15	10.94	5.08285E+18
30	464885006.46	10.15	4.71858E+18
31	465037883.89	9.41	4.37414E+18
32	465190786.46	8.70	4.04878E+18
33	465343714.17	8.04	3.74187E+18
34	465496667.01	7.42	3.45278E+18
35	465649644.97	6.83	3.18085E+18
36	465802648.08	6.28	2.92544E+18
37	465955676.31	5.76	2.68582E+18
38	466108729.68	5.28	2.46122E+18
39	466261808.18	4.83	2.2509E+18
40	466414911.81	4.40	2.05409E+18
41	466568040.58	4.01	1.87014E+18
42	466721194.48	3.64	1.69876E+18
43	466874373.51	3.30	1.53975E+18
44	467027577.67	2.98	1.39294E+18
45	467180806.97	2.69	1.25812E+18
46	467334061.40	2.43	1.13501E+18
47	467487340.96	2.19	1.02297E+18
48	467640645.66	1.97	9.21266E+17
49	467793975.48	1.77	8.29157E+17

50	467947330.44	1.59	7.45908E+17
51	468100710.54	1.43	6.70739E+17
52	468254115.76	1.29	6.02705E+17
53	468407546.12	1.15	5.4082E+17
54	468561001.61	1.03	4.84096E+17
55	468714482.24	0.92	4.31545E+17
56	468867987.99	0.82	3.82366E+17
57	469021518.88	0.72	3.36513E+17
58	469175074.91	0.63	2.94134E+17
59	469328656.06	0.54	2.55372E+17
60	469482262.35	0.47	2.20375E+17
61	469635893.77	0.40	1.89217E+17
62	469789550.32	0.34	1.61689E+17
63	469943232.01	0.29	1.37513E+17
64	470096938.83	0.25	1.16408E+17
65	470250670.78	0.21	9.80943E+16
66	470404427.86	0.17	8.22992E+16
67	470558210.08	0.15	6.87804E+16
68	470712017.43	0.12	5.73032E+16
69	470865849.91	0.10	4.76324E+16
70	471019707.53	0.08	3.95327E+16
Sum			4.98071E+20

Appendix 6

The mixing ratio in ppm by Mass calculated for model A and model B with a cubic spline.

Altitude (km)	Model A (ppm by Mass)	Model B (ppm by Mass)
0	0	36.750
1	3.534	36.345
2	7.033	35.941
3	10.461	35.540
4	13.784	35.144
5	16.966	34.755
6	19.972	34.373
7	22.766	34.001
8	25.315	33.641
9	27.581	33.292
10	29.531	32.958
11	31.129	32.641
12	32.34	32.340
13	33.169	32.084
14	33.783	31.999
15	34.389	32.240
16	35.196	32.958
17	36.41	34.307
18	38.24	36.439
19	40.892	39.508
20	44.574	43.665

21	49.495	49.065
22	55.86	55.860
23	63.799	64.134
24	73.125	73.701
25	83.571	84.304
26	94.872	95.688
27	106.76	107.597
28	118.971	119.776
29	131.237	131.969
30	143.293	143.920
31	154.872	155.373
32	165.709	166.074
33	175.536	175.765
34	184.089	184.193
35	191.1	191.100
36	196.377	196.302
37	200.02	199.898
38	202.201	202.056
39	203.095	202.945
40	202.873	202.735
41	201.71	201.594
42	199.778	199.691
43	197.25	197.195
44	194.3	194.275
45	191.1	191.100
46	187.782	187.798

47	184.305	184.330
48	180.59	180.616
49	176.553	176.576
50	172.113	172.130
51	167.19	167.198
52	161.7	161.700
53	155.583	155.576
54	148.857	148.844
55	141.559	141.541
56	133.729	133.707
57	125.403	125.379
58	116.62	116.595
59	107.418	107.392
60	97.836	97.810
61	87.911	87.886
62	77.681	77.658
63	67.184	67.163
64	56.459	56.441
65	45.544	45.529
66	34.476	34.465
67	23.294	23.286
68	12.036	12.032
69	0.74	0.740
70	0.74	0.740

Appendix 7

Calculation of the total amount of sulphur dioxide for model A with linear functions.

Shell	Density (kg/m^3)	Mass (kg)	Linear Profile	Deviation 1	Deviation 2
0	64.790	2.982.E+19	0.000.E+00	0.000.E+00	0.000.E+00
1	61.690	2.841.E+19	7.655.E+13	8.699.E+13	6.611.E+13
2	58.618	2.700.E+19	1.455.E+14	1.654.E+14	1.257.E+14
3	55.605	2.562.E+19	2.071.E+14	2.354.E+14	1.789.E+14
4	52.679	2.428.E+19	2.617.E+14	2.974.E+14	2.261.E+14
5	49.870	2.299.E+19	3.098.E+14	3.521.E+14	2.676.E+14
6	47.199	2.177.E+19	3.520.E+14	4.000.E+14	3.040.E+14
7	44.662	2.061.E+19	3.887.E+14	4.417.E+14	3.357.E+14
8	42.244	1.950.E+19	4.204.E+14	4.777.E+14	3.630.E+14
9	39.934	1.844.E+19	4.472.E+14	5.082.E+14	3.862.E+14
10	37.720	1.742.E+19	4.695.E+14	5.335.E+14	4.055.E+14
11	35.591	1.644.E+19	4.874.E+14	5.539.E+14	4.210.E+14
12	33.546	1.550.E+19	5.014.E+14	5.697.E+14	4.330.E+14
13	31.590	1.460.E+19	5.066.E+14	5.646.E+14	4.487.E+14
14	29.724	1.375.E+19	5.092.E+14	5.577.E+14	4.607.E+14
15	27.950	1.293.E+19	5.094.E+14	5.493.E+14	4.695.E+14
16	26.270	1.216.E+19	5.075.E+14	5.397.E+14	4.753.E+14
17	24.680	1.142.E+19	5.038.E+14	5.290.E+14	4.786.E+14
18	23.174	1.073.E+19	4.985.E+14	5.174.E+14	4.795.E+14
19	21.746	1.007.E+19	4.916.E+14	5.049.E+14	4.783.E+14

20	20.390	9.448.E+18	4.833.E+14	4.916.E+14	4.750.E+14
21	19.101	8.854.E+18	4.737.E+14	4.776.E+14	4.698.E+14
22	17.876	8.289.E+18	4.630.E+14	4.630.E+14	4.630.E+14
23	16.714	7.752.E+18	5.137.E+14	5.487.E+14	4.786.E+14
24	15.613	7.244.E+18	5.553.E+14	6.208.E+14	4.898.E+14
25	14.570	6.762.E+18	5.888.E+14	6.805.E+14	4.970.E+14
26	13.584	6.307.E+18	6.147.E+14	7.288.E+14	5.006.E+14
27	12.651	5.876.E+18	6.338.E+14	7.667.E+14	5.010.E+14
28	11.770	5.468.E+18	6.467.E+14	7.951.E+14	4.984.E+14
29	10.937	5.083.E+18	6.540.E+14	8.150.E+14	4.931.E+14
30	10.150	4.719.E+18	6.563.E+14	8.270.E+14	4.855.E+14
31	9.406	4.374.E+18	6.539.E+14	8.319.E+14	4.758.E+14
32	8.703	4.049.E+18	6.473.E+14	8.305.E+14	4.642.E+14
33	8.041	3.742.E+18	6.372.E+14	8.234.E+14	4.510.E+14
34	7.417	3.453.E+18	6.239.E+14	8.113.E+14	4.365.E+14
35	6.831	3.181.E+18	6.079.E+14	7.949.E+14	4.208.E+14
36	6.280	2.925.E+18	5.591.E+14	7.311.E+14	3.870.E+14
37	5.764	2.686.E+18	5.133.E+14	6.712.E+14	3.553.E+14
38	5.280	2.461.E+18	4.703.E+14	6.151.E+14	3.256.E+14
39	4.828	2.251.E+18	4.301.E+14	5.625.E+14	2.978.E+14
40	4.404	2.054.E+18	3.925.E+14	5.133.E+14	2.718.E+14
41	4.008	1.870.E+18	3.574.E+14	4.673.E+14	2.474.E+14
42	3.640	1.699.E+18	3.246.E+14	4.245.E+14	2.247.E+14
43	3.298	1.540.E+18	2.942.E+14	3.848.E+14	2.037.E+14
44	2.983	1.393.E+18	2.662.E+14	3.481.E+14	1.843.E+14

45	2.693	1.258.E+18	2.404.E+14	3.144.E+14	1.664.E+14
46	2.429	1.135.E+18	2.121.E+14	2.693.E+14	1.549.E+14
47	2.188	1.023.E+18	1.869.E+14	2.299.E+14	1.439.E+14
48	1.970	9.213.E+17	1.644.E+14	1.954.E+14	1.335.E+14
49	1.772	8.292.E+17	1.445.E+14	1.654.E+14	1.236.E+14
50	1.594	7.459.E+17	1.269.E+14	1.394.E+14	1.143.E+14
51	1.433	6.707.E+17	1.113.E+14	1.169.E+14	1.056.E+14
52	1.287	6.027.E+17	9.746.E+13	9.746.E+13	9.746.E+13
53	1.155	5.408.E+17	8.233.E+13	8.233.E+13	8.233.E+13
54	1.033	4.841.E+17	6.911.E+13	6.911.E+13	6.911.E+13
55	0.921	4.315.E+17	5.752.E+13	5.752.E+13	5.752.E+13
56	0.816	3.824.E+17	4.735.E+13	4.735.E+13	4.735.E+13
57	0.717	3.365.E+17	3.848.E+13	3.848.E+13	3.848.E+13
58	0.627	2.941.E+17	3.085.E+13	3.085.E+13	3.085.E+13
59	0.544	2.554.E+17	2.437.E+13	2.437.E+13	2.437.E+13
60	0.469	2.204.E+17	1.894.E+13	1.894.E+13	1.894.E+13
61	0.403	1.892.E+17	1.447.E+13	1.447.E+13	1.447.E+13
62	0.344	1.617.E+17	1.084.E+13	1.084.E+13	1.084.E+13
63	0.293	1.375.E+17	7.914.E+12	7.914.E+12	7.914.E+12
64	0.248	1.164.E+17	5.597.E+12	5.597.E+12	5.597.E+12
65	0.209	9.809.E+16	3.788.E+12	3.788.E+12	3.788.E+12
66	0.175	8.230.E+16	2.399.E+12	2.399.E+12	2.399.E+12
67	0.146	6.878.E+16	1.354.E+12	1.354.E+12	1.354.E+12
68	0.122	5.730.E+16	5.852.E+11	5.852.E+11	5.852.E+11
69	0.101	4.763.E+16	3.525.E+10	3.525.E+10	3.525.E+10

70	0.084	3.953.E+16	2.925.E+10	2.925.E+10	2.925.E+10
Sum			2.23553E+16	2.63533E+16	1.83572E+16

Appendix 8

Calculation of the total amount of sulphur dioxide for model B with linear functions.

Shell	Density (kg/m^3)	Mass (kg)	Linear Profile	Deviation 1	Deviation 2
0	64.790	2.982E+19	1.096E+15	1.096E+15	1.096E+15
1	61.690	2.841E+19	1.033E+15	1.044E+15	1.023E+15
2	58.618	2.700E+19	9.724E+14	9.923E+14	9.526E+14
3	55.605	2.562E+19	9.133E+14	9.416E+14	8.851E+14
4	52.679	2.428E+19	8.566E+14	8.923E+14	8.209E+14
5	49.870	2.299E+19	8.028E+14	8.450E+14	7.605E+14
6	47.199	2.177E+19	7.520E+14	8.000E+14	7.040E+14
7	44.662	2.061E+19	7.043E+14	7.573E+14	6.512E+14
8	42.244	1.950E+19	6.592E+14	7.165E+14	6.019E+14
9	39.934	1.844E+19	6.166E+14	6.776E+14	5.556E+14
10	37.720	1.742E+19	5.762E+14	6.402E+14	5.122E+14
11	35.591	1.644E+19	5.378E+14	6.043E+14	4.713E+14
12	33.546	1.550E+19	5.014E+14	5.697E+14	4.330E+14
13	31.590	1.460E+19	5.066E+14	5.646E+14	4.487E+14
14	29.724	1.375E+19	5.092E+14	5.577E+14	4.607E+14
15	27.950	1.293E+19	5.094E+14	5.493E+14	4.695E+14
16	26.270	1.216E+19	5.075E+14	5.397E+14	4.753E+14
17	24.680	1.142E+19	5.038E+14	5.290E+14	4.786E+14
18	23.174	1.073E+19	4.985E+14	5.174E+14	4.795E+14
19	21.746	1.007E+19	4.916E+14	5.049E+14	4.783E+14

20	20.390	9.448E+18	4.833E+14	4.916E+14	4.750E+14
21	19.101	8.854E+18	4.737E+14	4.776E+14	4.698E+14
22	17.876	8.289E+18	4.630E+14	4.630E+14	4.630E+14
23	16.714	7.752E+18	5.137E+14	5.487E+14	4.786E+14
24	15.613	7.244E+18	5.553E+14	6.208E+14	4.898E+14
25	14.570	6.762E+18	5.888E+14	6.805E+14	4.970E+14
26	13.584	6.307E+18	6.147E+14	7.288E+14	5.006E+14
27	12.651	5.876E+18	6.338E+14	7.667E+14	5.010E+14
28	11.770	5.468E+18	6.467E+14	7.951E+14	4.984E+14
29	10.937	5.083E+18	6.540E+14	8.150E+14	4.931E+14
30	10.150	4.719E+18	6.563E+14	8.270E+14	4.855E+14
31	9.406	4.374E+18	6.539E+14	8.319E+14	4.758E+14
32	8.703	4.049E+18	6.473E+14	8.305E+14	4.642E+14
33	8.041	3.742E+18	6.372E+14	8.234E+14	4.510E+14
34	7.417	3.453E+18	6.239E+14	8.113E+14	4.365E+14
35	6.831	3.181E+18	6.079E+14	7.949E+14	4.208E+14
36	6.280	2.925E+18	5.591E+14	7.311E+14	3.870E+14
37	5.764	2.686E+18	5.133E+14	6.712E+14	3.553E+14
38	5.280	2.461E+18	4.703E+14	6.151E+14	3.256E+14
39	4.828	2.251E+18	4.301E+14	5.625E+14	2.978E+14
40	4.404	2.054E+18	3.925E+14	5.133E+14	2.718E+14
41	4.008	1.870E+18	3.574E+14	4.673E+14	2.474E+14
42	3.640	1.699E+18	3.246E+14	4.245E+14	2.247E+14
43	3.298	1.540E+18	2.942E+14	3.848E+14	2.037E+14
44	2.983	1.393E+18	2.662E+14	3.481E+14	1.843E+14

45	2.693	1.258E+18	2.404E+14	3.144E+14	1.664E+14
46	2.429	1.135E+18	2.121E+14	2.693E+14	1.549E+14
47	2.188	1.023E+18	1.869E+14	2.299E+14	1.439E+14
48	1.970	9.213E+17	1.644E+14	1.954E+14	1.335E+14
49	1.772	8.292E+17	1.445E+14	1.654E+14	1.236E+14
50	1.594	7.459E+17	1.269E+14	1.394E+14	1.143E+14
51	1.433	6.707E+17	1.113E+14	1.169E+14	1.056E+14
52	1.287	6.027E+17	9.746E+13	9.746E+13	9.746E+13
53	1.155	5.408E+17	8.233E+13	8.233E+13	8.233E+13
54	1.033	4.841E+17	6.911E+13	6.911E+13	6.911E+13
55	0.921	4.315E+17	5.752E+13	5.752E+13	5.752E+13
56	0.816	3.824E+17	4.735E+13	4.735E+13	4.735E+13
57	0.717	3.365E+17	3.848E+13	3.848E+13	3.848E+13
58	0.627	2.941E+17	3.085E+13	3.085E+13	3.085E+13
59	0.544	2.554E+17	2.437E+13	2.437E+13	2.437E+13
60	0.469	2.204E+17	1.894E+13	1.894E+13	1.894E+13
61	0.403	1.892E+17	1.447E+13	1.447E+13	1.447E+13
62	0.344	1.617E+17	1.084E+13	1.084E+13	1.084E+13
63	0.293	1.375E+17	7.914E+12	7.914E+12	7.914E+12
64	0.248	1.164E+17	5.597E+12	5.597E+12	5.597E+12
65	0.209	9.809E+16	3.788E+12	3.788E+12	3.788E+12
66	0.175	8.230E+16	2.399E+12	2.399E+12	2.399E+12
67	0.146	6.878E+16	1.354E+12	1.354E+12	1.354E+12
68	0.122	5.730E+16	5.852E+11	5.852E+11	5.852E+11
69	0.101	4.763E+16	3.525E+10	3.525E+10	3.525E+10

70	0.084	3.953E+16	2.925E+10	2.925E+10	2.925E+10
Sum			2.831E+16	3.231E+16	2.431E+16

Appendix 9

Calculation of the total amount of sulphur dioxide for model A with exponential functions.

Shell	Density (kg/m^3)	Mass (kg)	Exponential Profile	Deviation 1	Deviation 2
0	64.790	2.982E+19	0.000E+00	0.000E+00	0.000E+00
1	61.690	2.841E+19	7.655E+13	8.699E+13	6.611E+13
2	58.618	2.700E+19	1.455E+14	1.654E+14	1.257E+14
3	55.605	2.562E+19	2.071E+14	2.354E+14	1.789E+14
4	52.679	2.428E+19	2.617E+14	2.974E+14	2.261E+14
5	49.870	2.299E+19	3.098E+14	3.521E+14	2.676E+14
6	47.199	2.177E+19	3.520E+14	4.000E+14	3.040E+14
7	44.662	2.061E+19	3.887E+14	4.417E+14	3.357E+14
8	42.244	1.950E+19	4.204E+14	4.777E+14	3.630E+14
9	39.934	1.844E+19	4.472E+14	5.082E+14	3.862E+14
10	37.720	1.742E+19	4.695E+14	5.335E+14	4.055E+14
11	35.591	1.644E+19	4.874E+14	5.539E+14	4.210E+14
12	33.546	1.550E+19	5.014E+14	5.697E+14	4.330E+14
13	31.590	1.460E+19	4.991E+14	4.991E+14	4.991E+14
14	29.724	1.375E+19	4.962E+14	4.962E+14	4.962E+14
15	27.950	1.293E+19	4.930E+14	4.930E+14	4.930E+14
16	26.270	1.216E+19	4.896E+14	4.896E+14	4.896E+14
17	24.680	1.142E+19	4.859E+14	4.859E+14	4.859E+14

18	23.174	1.073E+19	4.821E+14	4.821E+14	4.821E+14
19	21.746	1.007E+19	4.780E+14	4.780E+14	4.780E+14
20	20.390	9.448E+18	4.735E+14	4.735E+14	4.735E+14
21	19.101	8.854E+18	4.687E+14	4.687E+14	4.687E+14
22	17.876	8.289E+18	4.630E+14	4.630E+14	4.630E+14
23	16.714	7.752E+18	4.759E+14	4.854E+14	4.625E+14
24	15.613	7.244E+18	4.888E+14	5.090E+14	4.618E+14
25	14.570	6.762E+18	5.016E+14	5.331E+14	4.606E+14
26	13.584	6.307E+18	5.142E+14	5.579E+14	4.590E+14
27	12.651	5.876E+18	5.266E+14	5.832E+14	4.570E+14
28	11.770	5.468E+18	5.387E+14	6.091E+14	4.544E+14
29	10.937	5.083E+18	5.504E+14	6.353E+14	4.514E+14
30	10.150	4.719E+18	5.617E+14	6.618E+14	4.477E+14
31	9.406	4.374E+18	5.723E+14	6.884E+14	4.435E+14
32	8.703	4.049E+18	5.823E+14	7.150E+14	4.387E+14
33	8.041	3.742E+18	5.916E+14	7.414E+14	4.332E+14
34	7.417	3.453E+18	6.000E+14	7.677E+14	4.271E+14
35	6.831	3.181E+18	6.079E+14	7.949E+14	4.208E+14
36	6.280	2.925E+18	5.591E+14	7.311E+14	3.870E+14
37	5.764	2.686E+18	5.133E+14	6.712E+14	3.553E+14
38	5.280	2.461E+18	4.703E+14	6.151E+14	3.256E+14
39	4.828	2.251E+18	4.301E+14	5.625E+14	2.978E+14
40	4.404	2.054E+18	3.925E+14	5.133E+14	2.718E+14

41	4.008	1.870E+18	3.574E+14	4.673E+14	2.474E+14
42	3.640	1.699E+18	3.246E+14	4.245E+14	2.247E+14
43	3.298	1.540E+18	2.942E+14	3.848E+14	2.037E+14
44	2.983	1.393E+18	2.662E+14	3.481E+14	1.843E+14
45	2.693	1.258E+18	2.404E+14	3.144E+14	1.664E+14
46	2.429	1.135E+18	2.105E+14	2.689E+14	1.548E+14
47	2.188	1.023E+18	1.852E+14	2.277E+14	1.435E+14
48	1.970	9.213E+17	1.628E+14	1.928E+14	1.330E+14
49	1.772	8.292E+17	1.431E+14	1.631E+14	1.232E+14
50	1.594	7.459E+17	1.257E+14	1.379E+14	1.141E+14
51	1.433	6.707E+17	1.103E+14	1.165E+14	1.056E+14
52	1.287	6.027E+17	9.746E+13	9.746E+13	9.746E+13
53	1.155	5.408E+17	5.397E+13	5.397E+13	5.397E+13
54	1.033	4.841E+17	3.508E+13	3.508E+13	3.508E+13
55	0.921	4.315E+17	2.271E+13	2.271E+13	2.271E+13
56	0.816	3.824E+17	1.461E+13	1.461E+13	1.461E+13
57	0.717	3.365E+17	9.338E+12	9.338E+12	9.338E+12
58	0.627	2.941E+17	5.927E+12	5.927E+12	5.927E+12
59	0.544	2.554E+17	3.736E+12	3.736E+12	3.736E+12
60	0.469	2.204E+17	2.341E+12	2.341E+12	2.341E+12
61	0.403	1.892E+17	1.460E+12	1.460E+12	1.460E+12
62	0.344	1.617E+17	9.058E+11	9.058E+11	9.058E+11
63	0.293	1.375E+17	5.594E+11	5.594E+11	5.594E+11

64	0.248	1.164E+17	3.439E+11	3.439E+11	3.439E+11
65	0.209	9.809E+16	2.104E+11	2.104E+11	2.104E+11
66	0.175	8.230E+16	1.282E+11	1.282E+11	1.282E+11
67	0.146	6.878E+16	7.780E+10	7.780E+10	7.780E+10
68	0.122	5.730E+16	4.706E+10	4.706E+10	4.706E+10
69	0.101	4.763E+16	3.525E+10	3.525E+10	3.525E+10
70	0.084	3.953E+16	2.925E+10	2.925E+10	2.925E+10
Sum			2.104E+16	2.412E+16	1.785E+16

Appendix 10

Calculation of the total amount of sulphur dioxide for model B with exponential functions.

Shell	Density (kg/m^3)	Mass (kg)	Exponential Profile	Deviation 1	Deviation 2
0	64.790	2.982E+19	1.096E+15	1.096E+15	1.096E+15
1	61.690	2.841E+19	1.016E+15	1.044E+15	9.876E+14
2	58.618	2.700E+19	9.388E+14	9.923E+14	8.853E+14
3	55.605	2.562E+19	8.654E+14	9.416E+14	7.893E+14
4	52.679	2.428E+19	7.961E+14	8.923E+14	6.999E+14
5	49.870	2.299E+19	7.311E+14	8.450E+14	6.173E+14
6	47.199	2.177E+19	6.707E+14	8.000E+14	5.413E+14
7	44.662	2.061E+19	6.144E+14	7.573E+14	4.715E+14
8	42.244	1.950E+19	5.620E+14	7.165E+14	4.076E+14
9	39.934	1.844E+19	5.132E+14	6.776E+14	3.489E+14
10	37.720	1.742E+19	4.677E+14	6.402E+14	2.951E+14
11	35.591	1.644E+19	4.251E+14	6.043E+14	2.460E+14
12	33.546	1.550E+19	5.014E+14	5.697E+14	4.330E+14
13	31.590	1.460E+19	4.991E+14	4.991E+14	4.991E+14
14	29.724	1.375E+19	4.962E+14	4.962E+14	4.962E+14
15	27.950	1.293E+19	4.930E+14	4.930E+14	4.930E+14
16	26.270	1.216E+19	4.896E+14	4.896E+14	4.896E+14
17	24.680	1.142E+19	4.859E+14	4.859E+14	4.859E+14

18	23.174	1.073E+19	4.821E+14	4.821E+14	4.821E+14
19	21.746	1.007E+19	4.780E+14	4.780E+14	4.780E+14
20	20.390	9.448E+18	4.735E+14	4.735E+14	4.735E+14
21	19.101	8.854E+18	4.687E+14	4.687E+14	4.687E+14
22	17.876	8.289E+18	4.630E+14	4.630E+14	4.630E+14
23	16.714	7.752E+18	4.759E+14	4.854E+14	4.625E+14
24	15.613	7.244E+18	4.888E+14	5.090E+14	4.618E+14
25	14.570	6.762E+18	5.016E+14	5.331E+14	4.606E+14
26	13.584	6.307E+18	5.142E+14	5.579E+14	4.590E+14
27	12.651	5.876E+18	5.266E+14	5.832E+14	4.570E+14
28	11.770	5.468E+18	5.387E+14	6.091E+14	4.544E+14
29	10.937	5.083E+18	5.504E+14	6.353E+14	4.514E+14
30	10.150	4.719E+18	5.617E+14	6.618E+14	4.477E+14
31	9.406	4.374E+18	5.723E+14	6.884E+14	4.435E+14
32	8.703	4.049E+18	5.823E+14	7.150E+14	4.387E+14
33	8.041	3.742E+18	5.916E+14	7.414E+14	4.332E+14
34	7.417	3.453E+18	6.000E+14	7.677E+14	4.271E+14
35	6.831	3.181E+18	6.079E+14	7.949E+14	4.208E+14
36	6.280	2.925E+18	5.591E+14	7.311E+14	3.870E+14
37	5.764	2.686E+18	5.133E+14	6.712E+14	3.553E+14
38	5.280	2.461E+18	4.703E+14	6.151E+14	3.256E+14
39	4.828	2.251E+18	4.301E+14	5.625E+14	2.978E+14
40	4.404	2.054E+18	3.925E+14	5.133E+14	2.718E+14

41	4.008	1.870E+18	3.574E+14	4.673E+14	2.474E+14
42	3.640	1.699E+18	3.246E+14	4.245E+14	2.247E+14
43	3.298	1.540E+18	2.942E+14	3.848E+14	2.037E+14
44	2.983	1.393E+18	2.662E+14	3.481E+14	1.843E+14
45	2.693	1.258E+18	2.404E+14	3.144E+14	1.664E+14
46	2.429	1.135E+18	2.105E+14	2.689E+14	1.548E+14
47	2.188	1.023E+18	1.852E+14	2.277E+14	1.435E+14
48	1.970	9.213E+17	1.628E+14	1.928E+14	1.330E+14
49	1.772	8.292E+17	1.431E+14	1.631E+14	1.232E+14
50	1.594	7.459E+17	1.257E+14	1.379E+14	1.141E+14
51	1.433	6.707E+17	1.103E+14	1.165E+14	1.056E+14
52	1.287	6.027E+17	9.746E+13	9.746E+13	9.746E+13
53	1.155	5.408E+17	5.397E+13	5.397E+13	5.397E+13
54	1.033	4.841E+17	3.508E+13	3.508E+13	3.508E+13
55	0.921	4.315E+17	2.271E+13	2.271E+13	2.271E+13
56	0.816	3.824E+17	1.461E+13	1.461E+13	1.461E+13
57	0.717	3.365E+17	9.338E+12	9.338E+12	9.338E+12
58	0.627	2.941E+17	5.927E+12	5.927E+12	5.927E+12
59	0.544	2.554E+17	3.736E+12	3.736E+12	3.736E+12
60	0.469	2.204E+17	2.341E+12	2.341E+12	2.341E+12
61	0.403	1.892E+17	1.460E+12	1.460E+12	1.460E+12
62	0.344	1.617E+17	9.058E+11	9.058E+11	9.058E+11
63	0.293	1.375E+17	5.594E+11	5.594E+11	5.594E+11

64	0.248	1.164E+17	3.439E+11	3.439E+11	3.439E+11
65	0.209	9.809E+16	2.104E+11	2.104E+11	2.104E+11
66	0.175	8.230E+16	1.282E+11	1.282E+11	1.282E+11
67	0.146	6.878E+16	7.780E+10	7.780E+10	7.780E+10
68	0.122	5.730E+16	4.706E+10	4.706E+10	4.706E+10
69	0.101	4.763E+16	3.525E+10	3.525E+10	3.525E+10
70	0.084	3.953E+16	2.925E+10	2.925E+10	2.925E+10
Sum			2.617E+16	3.008E+16	2.215E+16

Appendix 11

Calculation of the total amount of sulphur dioxide for model A with a cubic spline.

Shell	Density (kg/m^3)	Mass (kg)	Cubic Spline Profile	Deviation 1	Deviation 2
0	64.790	2.982E+19	0.000E+00	0.000E+00	0.000E+00
1	61.690	2.841E+19	1.004E+14	1.279E+14	7.283E+13
2	58.618	2.7E+19	1.899E+14	2.416E+14	1.382E+14
3	55.605	2.562E+19	2.680E+14	3.400E+14	1.961E+14
4	52.679	2.428E+19	3.347E+14	4.227E+14	2.466E+14
5	49.870	2.299E+19	3.901E+14	4.900E+14	2.902E+14
6	47.199	2.177E+19	4.348E+14	5.422E+14	3.273E+14
7	44.662	2.061E+19	4.691E+14	5.798E+14	3.584E+14
8	42.244	1.95E+19	4.936E+14	6.034E+14	3.837E+14
9	39.934	1.844E+19	5.085E+14	6.135E+14	4.035E+14
10	37.720	1.742E+19	5.144E+14	6.108E+14	4.181E+14
11	35.591	1.644E+19	5.118E+14	5.958E+14	4.278E+14
12	33.546	1.55E+19	5.014E+14	5.697E+14	4.330E+14
13	31.590	1.46E+19	4.844E+14	5.345E+14	4.343E+14
14	29.724	1.375E+19	4.644E+14	4.955E+14	4.332E+14
15	27.950	1.293E+19	4.446E+14	4.579E+14	4.314E+14
16	26.270	1.216E+19	4.279E+14	4.258E+14	4.299E+14
17	24.680	1.142E+19	4.160E+14	4.022E+14	4.298E+14
18	23.174	1.073E+19	4.103E+14	3.892E+14	4.315E+14
19	21.746	1.007E+19	4.119E+14	3.882E+14	4.356E+14
20	20.390	9.448E+18	4.211E+14	4.001E+14	4.421E+14
21	19.101	8.854E+18	4.382E+14	4.251E+14	4.513E+14

22	17.876	8.289E+18	4.630E+14	4.630E+14	4.630E+14
23	16.714	7.752E+18	4.946E+14	5.124E+14	4.768E+14
24	15.613	7.244E+18	5.297E+14	5.683E+14	4.911E+14
25	14.570	6.762E+18	5.651E+14	6.261E+14	5.042E+14
26	13.584	6.307E+18	5.983E+14	6.818E+14	5.148E+14
27	12.651	5.876E+18	6.273E+14	7.325E+14	5.221E+14
28	11.770	5.468E+18	6.505E+14	7.758E+14	5.253E+14
29	10.937	5.083E+18	6.671E+14	8.102E+14	5.240E+14
30	10.150	4.719E+18	6.761E+14	8.343E+14	5.180E+14
31	9.406	4.374E+18	6.774E+14	8.477E+14	5.072E+14
32	8.703	4.049E+18	6.709E+14	8.501E+14	4.917E+14
33	8.041	3.742E+18	6.568E+14	8.417E+14	4.719E+14
34	7.417	3.453E+18	6.356E+14	8.231E+14	4.481E+14
35	6.831	3.181E+18	6.079E+14	7.949E+14	4.208E+14
36	6.280	2.925E+18	5.745E+14	7.583E+14	3.907E+14
37	5.764	2.686E+18	5.372E+14	7.151E+14	3.593E+14
38	5.280	2.461E+18	4.977E+14	6.674E+14	3.279E+14
39	4.828	2.251E+18	4.571E+14	6.167E+14	2.976E+14
40	4.404	2.054E+18	4.167E+14	5.643E+14	2.692E+14
41	4.008	1.87E+18	3.772E+14	5.114E+14	2.430E+14
42	3.640	1.699E+18	3.394E+14	4.592E+14	2.195E+14
43	3.298	1.54E+18	3.037E+14	4.085E+14	1.989E+14
44	2.983	1.393E+18	2.706E+14	3.600E+14	1.813E+14
45	2.693	1.258E+18	2.404E+14	3.144E+14	1.664E+14
46	2.429	1.135E+18	2.131E+14	2.721E+14	1.542E+14
47	2.188	1.023E+18	1.885E+14	2.334E+14	1.437E+14
48	1.970	9.213E+17	1.664E+14	1.986E+14	1.341E+14
49	1.772	8.292E+17	1.464E+14	1.677E+14	1.250E+14

50	1.594	7.459E+17	1.284E+14	1.407E+14	1.160E+14
51	1.433	6.707E+17	1.121E+14	1.174E+14	1.069E+14
52	1.287	6.027E+17	9.746E+13	9.746E+13	9.746E+13
53	1.155	5.408E+17	8.414E+13	8.055E+13	8.774E+13
54	1.033	4.841E+17	7.206E+13	6.621E+13	7.791E+13
55	0.921	4.315E+17	6.109E+13	5.402E+13	6.816E+13
56	0.816	3.824E+17	5.113E+13	4.362E+13	5.864E+13
57	0.717	3.365E+17	4.220E+13	3.483E+13	4.957E+13
58	0.627	2.941E+17	3.430E+13	2.746E+13	4.114E+13
59	0.544	2.554E+17	2.743E+13	2.136E+13	3.351E+13
60	0.469	2.204E+17	2.156E+13	1.637E+13	2.675E+13
61	0.403	1.892E+17	1.663E+13	1.235E+13	2.092E+13
62	0.344	1.617E+17	1.256E+13	9.140E+12	1.598E+13
63	0.293	1.375E+17	9.239E+12	6.611E+12	1.187E+13
64	0.248	1.164E+17	6.572E+12	4.638E+12	8.507E+12
65	0.209	9.809E+16	4.468E+12	3.119E+12	5.816E+12
66	0.175	8.23E+16	2.837E+12	1.967E+12	3.708E+12
67	0.146	6.878E+16	1.602E+12	1.109E+12	2.096E+12
68	0.122	5.73E+16	6.897E+11	4.819E+11	8.975E+11
69	0.101	4.763E+16	3.525E+10	3.525E+10	3.525E+10
70	0.084	3.953E+16	2.925E+10	2.925E+10	2.925E+10
Sum			2.267E+16	2.680E+16	1.854E+16

Appendix 12

Calculation of the total amount of sulphur dioxide for model B with a cubic spline.

Shell	Density (kg/m^3)	Mass (kg)	Cubic Spline Profile	Deviation 1	Deviation 2
0	64.790	2.982E+19	1.096E+15	1.096E+15	1.096E+15
1	61.690	2.841E+19	1.032E+15	1.060E+15	1.005E+15
2	58.618	2.700E+19	9.704E+14	1.022E+15	9.187E+14
3	55.605	2.562E+19	9.106E+14	9.825E+14	8.386E+14
4	52.679	2.428E+19	8.533E+14	9.414E+14	7.653E+14
5	49.870	2.299E+19	7.991E+14	8.990E+14	6.993E+14
6	47.199	2.177E+19	7.483E+14	8.557E+14	6.409E+14
7	44.662	2.061E+19	7.006E+14	8.114E+14	5.899E+14
8	42.244	1.950E+19	6.559E+14	7.658E+14	5.460E+14
9	39.934	1.844E+19	6.138E+14	7.188E+14	5.088E+14
10	37.720	1.742E+19	5.741E+14	6.705E+14	4.778E+14
11	35.591	1.644E+19	5.367E+14	6.207E+14	4.527E+14
12	33.546	1.550E+19	5.014E+14	5.697E+14	4.330E+14
13	31.590	1.460E+19	4.685E+14	5.187E+14	4.184E+14
14	29.724	1.375E+19	4.398E+14	4.710E+14	4.087E+14
15	27.950	1.293E+19	4.168E+14	4.301E+14	4.036E+14
16	26.270	1.216E+19	4.007E+14	3.986E+14	4.027E+14
17	24.680	1.142E+19	3.919E+14	3.781E+14	4.057E+14
18	23.174	1.073E+19	3.910E+14	3.698E+14	4.122E+14
19	21.746	1.007E+19	3.980E+14	3.743E+14	4.216E+14
20	20.390	9.448E+18	4.125E+14	3.915E+14	4.336E+14
21	19.101	8.854E+18	4.344E+14	4.213E+14	4.475E+14

22	17.876	8.289E+18	4.630E+14	4.630E+14	4.630E+14
23	16.714	7.752E+18	4.972E+14	5.150E+14	4.794E+14
24	15.613	7.244E+18	5.339E+14	5.725E+14	4.953E+14
25	14.570	6.762E+18	5.701E+14	6.311E+14	5.091E+14
26	13.584	6.307E+18	6.035E+14	6.870E+14	5.199E+14
27	12.651	5.876E+18	6.322E+14	7.374E+14	5.270E+14
28	11.770	5.468E+18	6.549E+14	7.802E+14	5.297E+14
29	10.937	5.083E+18	6.708E+14	8.139E+14	5.277E+14
30	10.150	4.719E+18	6.791E+14	8.373E+14	5.209E+14
31	9.406	4.374E+18	6.796E+14	8.499E+14	5.093E+14
32	8.703	4.049E+18	6.724E+14	8.516E+14	4.932E+14
33	8.041	3.742E+18	6.577E+14	8.426E+14	4.728E+14
34	7.417	3.453E+18	6.360E+14	8.235E+14	4.485E+14
35	6.831	3.181E+18	6.079E+14	7.949E+14	4.208E+14
36	6.280	2.925E+18	5.743E+14	7.580E+14	3.905E+14
37	5.764	2.686E+18	5.369E+14	7.148E+14	3.590E+14
38	5.280	2.461E+18	4.973E+14	6.670E+14	3.276E+14
39	4.828	2.251E+18	4.568E+14	6.163E+14	2.973E+14
40	4.404	2.054E+18	4.164E+14	5.640E+14	2.689E+14
41	4.008	1.870E+18	3.770E+14	5.112E+14	2.428E+14
42	3.640	1.699E+18	3.392E+14	4.591E+14	2.194E+14
43	3.298	1.540E+18	3.036E+14	4.084E+14	1.989E+14
44	2.983	1.393E+18	2.706E+14	3.600E+14	1.812E+14
45	2.693	1.258E+18	2.404E+14	3.144E+14	1.664E+14
46	2.429	1.135E+18	2.132E+14	2.721E+14	1.542E+14
47	2.188	1.023E+18	1.886E+14	2.334E+14	1.437E+14
48	1.970	9.213E+17	1.664E+14	1.986E+14	1.342E+14
49	1.772	8.292E+17	1.464E+14	1.678E+14	1.251E+14

50	1.594	7.459E+17	1.284E+14	1.408E+14	1.160E+14
51	1.433	6.707E+17	1.121E+14	1.174E+14	1.069E+14
52	1.287	6.027E+17	9.746E+13	9.746E+13	9.746E+13
53	1.155	5.408E+17	8.414E+13	8.054E+13	8.773E+13
54	1.033	4.841E+17	7.205E+13	6.620E+13	7.791E+13
55	0.921	4.315E+17	6.108E+13	5.401E+13	6.816E+13
56	0.816	3.824E+17	5.113E+13	4.362E+13	5.863E+13
57	0.717	3.365E+17	4.219E+13	3.482E+13	4.956E+13
58	0.627	2.941E+17	3.429E+13	2.745E+13	4.114E+13
59	0.544	2.554E+17	2.743E+13	2.135E+13	3.350E+13
60	0.469	2.204E+17	2.155E+13	1.636E+13	2.675E+13
61	0.403	1.892E+17	1.663E+13	1.234E+13	2.092E+13
62	0.344	1.617E+17	1.256E+13	9.137E+12	1.598E+13
63	0.293	1.375E+17	9.236E+12	6.608E+12	1.186E+13
64	0.248	1.164E+17	6.570E+12	4.636E+12	8.505E+12
65	0.209	9.809E+16	4.466E+12	3.118E+12	5.815E+12
66	0.175	8.230E+16	2.836E+12	1.966E+12	3.707E+12
67	0.146	6.878E+16	1.602E+12	1.108E+12	2.095E+12
68	0.122	5.730E+16	6.895E+11	4.817E+11	8.972E+11
69	0.101	4.763E+16	3.525E+10	3.525E+10	3.525E+10
70	0.084	3.953E+16	2.925E+10	2.925E+10	2.925E+10
			2.782E+16	3.195E+16	2.369E+16

Appendix 13

The density profile tabulated with a cubic spline and calculated in 0.25 km altitude steps.

Shell	Density	Model A	Model B
0	64.790	0.000	36.750
0.25	64.014	0.885	36.649
0.5	63.238	1.769	36.547
0.75	62.463	2.652	36.446
1	61.690	3.534	36.345
1.25	60.918	4.413	36.243
1.5	60.148	5.290	36.142
1.75	59.382	6.163	36.042
2	58.618	7.033	35.941
2.25	57.858	7.898	35.840
2.5	57.103	8.758	35.740
2.75	56.351	9.612	35.640
3	55.605	10.461	35.540
3.25	54.864	11.303	35.441
3.5	54.129	12.138	35.342
3.75	53.401	12.965	35.243
4	52.679	13.784	35.144
4.25	51.965	14.594	35.046
4.5	51.258	15.394	34.949
4.75	50.560	16.185	34.852
5	49.870	16.966	34.755
5.25	49.189	17.735	34.659

5.5	48.517	18.493	34.563
5.75	47.854	19.239	34.468
6	47.199	19.972	34.373
6.25	46.553	20.691	34.279
6.5	45.915	21.398	34.186
6.75	45.284	22.089	34.093
7	44.662	22.766	34.001
7.25	44.046	23.428	33.910
7.5	43.439	24.073	33.819
7.75	42.838	24.703	33.730
8	42.244	25.315	33.641
8.25	41.657	25.909	33.552
8.5	41.077	26.485	33.465
8.75	40.502	27.043	33.378
9	39.934	27.581	33.292
9.25	39.372	28.100	33.207
9.5	38.816	28.598	33.124
9.75	38.265	29.075	33.041
10	37.720	29.531	32.958
10.25	37.180	29.965	32.877
10.5	36.645	30.376	32.797
10.75	36.115	30.765	32.718
11	35.591	31.129	32.641
11.25	35.071	31.470	32.564
11.5	34.558	31.785	32.488
11.75	34.049	32.076	32.413
12	33.546	32.340	32.340
12.25	33.049	32.579	32.268

12.5	32.557	32.794	32.200
12.75	32.071	32.990	32.138
13	31.590	33.169	32.084
13.25	31.115	33.334	32.041
13.5	30.645	33.490	32.011
13.75	30.181	33.638	31.996
14	29.724	33.783	31.999
14.25	29.271	33.927	32.023
14.5	28.825	34.074	32.070
14.75	28.385	34.227	32.141
15	27.950	34.389	32.240
15.25	27.521	34.564	32.369
15.5	27.099	34.755	32.530
15.75	26.682	34.964	32.726
16	26.270	35.196	32.958
16.25	25.865	35.453	33.230
16.5	25.465	35.739	33.544
16.75	25.070	36.057	33.902
17	24.680	36.410	34.307
17.25	24.296	36.802	34.761
17.5	23.917	37.235	35.266
17.75	23.543	37.713	35.824
18	23.174	38.240	36.439
18.25	22.810	38.818	37.113
18.5	22.451	39.450	37.847
18.75	22.096	40.140	38.644
19	21.746	40.892	39.508
19.25	21.400	41.708	40.439

19.5	21.059	42.591	41.441
19.75	20.723	43.546	42.516
20	20.390	44.574	43.665
20.25	20.062	45.680	44.893
20.5	19.737	46.867	46.201
20.75	19.417	48.137	47.591
21	19.101	49.495	49.065
21.25	18.789	50.942	50.627
21.5	18.481	52.484	52.279
21.75	18.177	54.122	54.022
22	17.876	55.860	55.860
22.25	17.580	57.700	57.793
22.5	17.288	59.640	59.820
22.75	16.999	61.674	61.935
23	16.714	63.799	64.134
23.25	16.433	66.011	66.415
23.5	16.156	68.305	68.772
23.75	15.883	70.678	71.202
24	15.613	73.125	73.701
24.25	15.347	75.642	76.265
24.5	15.084	78.225	78.889
24.75	14.825	80.869	81.570
25	14.570	83.571	84.304
25.25	14.318	86.327	87.087
25.5	14.070	89.131	89.915
25.75	13.825	91.981	92.783
26	13.584	94.872	95.688
26.25	13.346	97.799	98.626

26.5	13.111	100.759	101.593
26.75	12.879	103.748	104.585
27	12.651	106.760	107.597
27.25	12.426	109.793	110.627
27.5	12.204	112.842	113.669
27.75	11.986	115.903	116.720
28	11.770	118.971	119.776
28.25	11.557	122.043	122.833
28.5	11.348	125.114	125.887
28.75	11.141	128.180	128.933
29	10.937	131.237	131.969
29.25	10.736	134.281	134.989
29.5	10.538	137.308	137.990
29.75	10.343	140.313	140.969
30	10.150	143.293	143.920
30.25	9.960	146.243	146.840
30.5	9.773	149.159	149.725
30.75	9.588	152.037	152.570
31	9.406	154.872	155.373
31.25	9.227	157.661	158.129
31.5	9.050	160.400	160.834
31.75	8.875	163.084	163.483
32	8.703	165.709	166.074
32.25	8.534	168.271	168.601
32.5	8.367	170.765	171.062
32.75	8.203	173.189	173.451
33	8.041	175.536	175.765
33.25	7.882	177.804	178.001

33.5	7.725	179.989	180.153
33.75	7.570	182.085	182.218
34	7.417	184.089	184.193
34.25	7.267	185.996	186.072
34.5	7.120	187.804	187.852
34.75	6.974	189.506	189.530
35	6.831	191.100	191.100
35.25	6.690	192.582	192.560
35.5	6.551	193.954	193.913
35.75	6.415	195.218	195.159
36	6.280	196.377	196.302
36.25	6.148	197.434	197.345
36.5	6.018	198.392	198.291
36.75	5.890	199.253	199.141
37	5.764	200.020	199.898
37.25	5.640	200.695	200.566
37.5	5.518	201.282	201.146
37.75	5.398	201.783	201.642
38	5.280	202.201	202.056
38.25	5.164	202.539	202.391
38.5	5.050	202.798	202.649
38.75	4.938	202.983	202.833
39	4.828	203.095	202.945
39.25	4.719	203.137	202.989
39.5	4.612	203.113	202.967
39.75	4.507	203.024	202.881
40	4.404	202.873	202.735
40.25	4.302	202.664	202.530

40.5	4.203	202.398	202.270
40.75	4.105	202.080	201.957
41	4.008	201.710	201.594
41.25	3.914	201.292	201.183
41.5	3.821	200.829	200.727
41.75	3.729	200.323	200.228
42	3.640	199.778	199.691
42.25	3.552	199.195	199.116
42.5	3.466	198.577	198.506
42.75	3.381	197.928	197.865
43	3.298	197.250	197.195
43.25	3.217	196.545	196.498
43.5	3.137	195.817	195.777
43.75	3.059	195.067	195.035
44	2.983	194.300	194.275
44.25	2.908	193.516	193.498
44.5	2.835	192.720	192.709
44.75	2.763	191.914	191.908
45	2.693	191.100	191.100
45.25	2.625	190.281	190.286
45.5	2.558	189.455	189.465
45.75	2.492	188.623	188.636
46	2.429	187.782	187.798
46.25	2.366	186.930	186.950
46.5	2.306	186.068	186.090
46.75	2.246	185.194	185.217
47	2.188	184.305	184.330
47.25	2.132	183.402	183.427

47.5	2.076	182.482	182.509
47.75	2.023	181.545	181.572
48	1.970	180.590	180.616
48.25	1.919	179.614	179.639
48.5	1.869	178.616	178.642
48.75	1.820	177.596	177.621
49	1.772	176.553	176.576
49.25	1.726	175.484	175.505
49.5	1.681	174.388	174.409
49.75	1.637	173.265	173.284
50	1.594	172.113	172.130
50.25	1.552	170.931	170.946
50.5	1.511	169.717	169.730
50.75	1.472	168.470	168.481
51	1.433	167.190	167.198
51.25	1.395	165.873	165.880
51.5	1.358	164.521	164.525
51.75	1.322	163.130	163.132
52	1.287	161.700	161.700
52.25	1.253	160.230	160.228
52.5	1.219	158.720	158.716
52.75	1.187	157.171	157.165
53	1.155	155.583	155.576
53.25	1.123	153.957	153.948
53.5	1.093	152.294	152.283
53.75	1.063	150.593	150.582
54	1.033	148.857	148.844
54.25	1.004	147.084	147.070

54.5	0.976	145.277	145.261
54.75	0.948	143.435	143.418
55	0.921	141.559	141.541
55.25	0.894	139.650	139.631
55.5	0.867	137.708	137.688
55.75	0.841	135.734	135.713
56	0.816	133.729	133.707
56.25	0.790	131.692	131.670
56.5	0.766	129.625	129.602
56.75	0.741	127.529	127.505
57	0.717	125.403	125.379
57.25	0.694	123.248	123.224
57.5	0.671	121.066	121.041
57.75	0.649	118.856	118.831
58	0.627	116.620	116.595
58.25	0.605	114.357	114.332
58.5	0.585	112.069	112.043
58.75	0.564	109.756	109.730
59	0.544	107.418	107.392
59.25	0.525	105.057	105.031
59.5	0.506	102.672	102.646
59.75	0.487	100.265	100.239
60	0.469	97.836	97.810
60.25	0.452	95.385	95.360
60.5	0.435	92.914	92.888
60.75	0.419	90.422	90.397
61	0.403	87.911	87.886
61.25	0.388	85.380	85.356

61.5	0.373	82.831	82.807
61.75	0.358	80.265	80.241
62	0.344	77.681	77.658
62.25	0.331	75.080	75.058
62.5	0.318	72.463	72.441
62.75	0.305	69.831	69.810
63	0.293	67.184	67.163
63.25	0.281	64.523	64.503
63.5	0.269	61.848	61.828
63.75	0.258	59.160	59.141
64	0.248	56.459	56.441
64.25	0.237	53.747	53.729
64.5	0.227	51.023	51.006
64.75	0.218	48.289	48.273
65	0.209	45.544	45.529
65.25	0.200	42.790	42.776
65.5	0.191	40.027	40.013
65.75	0.183	37.255	37.243
66	0.175	34.476	34.465
66.25	0.167	31.690	31.679
66.5	0.160	28.897	28.887
66.75	0.153	26.098	26.090
67	0.146	23.294	23.286
67.25	0.140	20.485	20.479
67.5	0.133	17.672	17.666
67.75	0.127	14.856	14.851
68	0.122	12.036	12.032
68.25	0.116	9.214	9.211

68.5	0.111	6.390	6.388
68.75	0.106	3.566	3.565
69	0.101	0.740	0.740
69.25	0.097	0.740	0.740
69.5	0.092	0.740	0.740
69.75	0.088	0.740	0.740
70	0.084	0.740	0.740

Appendix 14

The cubic spline calculations with 280 shells. This is the result for model A:

Shell	Volume (km^3)	Density (kg/m^3)	Mass	Model A	Deviation 1	Deviation 2
0	115063332.3	64.790	7.455E+18	0.000E+00	0.000E+00	0.000E+00
0.25	115072838.8	64.014	7.366E+18	6.518E+12	8.311E+12	4.725E+12
0.5	115082345.8	63.238	7.278E+18	1.288E+13	1.642E+13	9.335E+12
0.75	115091853.1	62.463	7.189E+18	1.907E+13	2.431E+13	1.383E+13
1	115101360.8	61.690	7.101E+18	2.509E+13	3.198E+13	1.821E+13
1.25	115110868.9	60.918	7.012E+18	3.095E+13	3.943E+13	2.247E+13
1.5	115120377.4	60.148	6.924E+18	3.663E+13	4.665E+13	2.661E+13
1.75	115129886.3	59.382	6.837E+18	4.214E+13	5.364E+13	3.064E+13
2	115139395.6	58.618	6.749E+18	4.747E+13	6.039E+13	3.454E+13
2.25	115148905.3	57.858	6.662E+18	5.262E+13	6.690E+13	3.834E+13
2.5	115158415.4	57.103	6.576E+18	5.759E+13	7.317E+13	4.201E+13
2.75	115167925.8	56.351	6.490E+18	6.238E+13	7.920E+13	4.557E+13
3	115177436.7	55.605	6.404E+18	6.700E+13	8.498E+13	4.901E+13
3.25	115186947.9	54.864	6.320E+18	7.143E+13	9.052E+13	5.234E+13
3.5	115196459.6	54.129	6.236E+18	7.569E+13	9.582E+13	5.555E+13
3.75	115205971.6	53.401	6.152E+18	7.976E+13	1.009E+14	5.866E+13
4	115215484	52.679	6.069E+18	8.366E+13	1.057E+14	6.165E+13
4.25	115224996.9	51.965	5.988E+18	8.738E+13	1.102E+14	6.453E+13
4.5	115234510.1	51.258	5.907E+18	9.093E+13	1.146E+14	6.731E+13
4.75	115244023.7	50.560	5.827E+18	9.431E+13	1.186E+14	6.998E+13
5	115253537.7	49.870	5.748E+18	9.751E+13	1.225E+14	7.255E+13

5.25	115263052.1	49.189	5.670E+18	1.006E+14	1.261E+14	7.501E+13
5.5	115272566.9	48.517	5.593E+18	1.034E+14	1.295E+14	7.738E+13
5.75	115282082	47.854	5.517E+18	1.061E+14	1.326E+14	7.965E+13
6	115291597.6	47.199	5.442E+18	1.087E+14	1.355E+14	8.183E+13
6.25	115301113.6	46.553	5.368E+18	1.111E+14	1.382E+14	8.391E+13
6.5	115310629.9	45.915	5.294E+18	1.133E+14	1.407E+14	8.589E+13
6.75	115320146.7	45.284	5.222E+18	1.154E+14	1.429E+14	8.778E+13
7	115329663.8	44.662	5.151E+18	1.173E+14	1.449E+14	8.959E+13
7.25	115339181.3	44.046	5.080E+18	1.190E+14	1.467E+14	9.130E+13
7.5	115348699.3	43.439	5.011E+18	1.206E+14	1.483E+14	9.292E+13
7.75	115358217.6	42.838	4.942E+18	1.221E+14	1.497E+14	9.446E+13
8	115367736.3	42.244	4.874E+18	1.234E+14	1.508E+14	9.591E+13
8.25	115377255.4	41.657	4.806E+18	1.245E+14	1.518E+14	9.727E+13
8.5	115386774.9	41.077	4.740E+18	1.255E+14	1.525E+14	9.855E+13
8.75	115396294.8	40.502	4.674E+18	1.264E+14	1.530E+14	9.975E+13
9	115405815.1	39.934	4.609E+18	1.271E+14	1.534E+14	1.009E+14
9.25	115415335.7	39.372	4.544E+18	1.277E+14	1.535E+14	1.019E+14
9.5	115424856.8	38.816	4.480E+18	1.281E+14	1.534E+14	1.029E+14
9.75	115434378.3	38.265	4.417E+18	1.284E+14	1.531E+14	1.037E+14
10	115443900.1	37.720	4.355E+18	1.286E+14	1.527E+14	1.045E+14
10.25	115453422.4	37.180	4.293E+18	1.286E+14	1.520E+14	1.052E+14
10.5	115462945	36.645	4.231E+18	1.285E+14	1.512E+14	1.059E+14
10.75	115472468	36.115	4.170E+18	1.283E+14	1.501E+14	1.065E+14
11	115481991.5	35.591	4.110E+18	1.279E+14	1.489E+14	1.069E+14
11.25	115491515.3	35.071	4.050E+18	1.275E+14	1.476E+14	1.074E+14
11.5	115501039.5	34.558	3.991E+18	1.269E+14	1.460E+14	1.077E+14
11.75	115510564.1	34.049	3.933E+18	1.262E+14	1.443E+14	1.080E+14
12	115520089.1	33.546	3.875E+18	1.253E+14	1.424E+14	1.082E+14

12.25	115529614.5	33.049	3.818E+18	1.244E+14	1.404E+14	1.084E+14
12.5	115539140.3	32.557	3.762E+18	1.234E+14	1.382E+14	1.085E+14
12.75	115548666.4	32.071	3.706E+18	1.223E+14	1.360E+14	1.085E+14
13	115558193	31.590	3.650E+18	1.211E+14	1.336E+14	1.086E+14
13.25	115567720	31.115	3.596E+18	1.199E+14	1.312E+14	1.085E+14
13.5	115577247.3	30.645	3.542E+18	1.186E+14	1.288E+14	1.085E+14
13.75	115586775.1	30.181	3.489E+18	1.173E+14	1.263E+14	1.084E+14
14	115596303.2	29.724	3.436E+18	1.161E+14	1.239E+14	1.083E+14
14.25	115605831.7	29.271	3.384E+18	1.148E+14	1.214E+14	1.082E+14
14.5	115615360.6	28.825	3.333E+18	1.136E+14	1.190E+14	1.081E+14
14.75	115624890	28.385	3.282E+18	1.123E+14	1.167E+14	1.079E+14
15	115634419.7	27.950	3.232E+18	1.111E+14	1.145E+14	1.078E+14
15.25	115643949.8	27.521	3.183E+18	1.100E+14	1.123E+14	1.077E+14
15.5	115653480.3	27.099	3.134E+18	1.089E+14	1.102E+14	1.076E+14
15.75	115663011.1	26.682	3.086E+18	1.079E+14	1.083E+14	1.075E+14
16	115672542.4	26.270	3.039E+18	1.070E+14	1.064E+14	1.075E+14
16.25	115682074.1	25.865	2.992E+18	1.061E+14	1.047E+14	1.074E+14
16.5	115691606.1	25.465	2.946E+18	1.053E+14	1.032E+14	1.074E+14
16.75	115701138.6	25.070	2.901E+18	1.046E+14	1.018E+14	1.074E+14
17	115710671.5	24.680	2.856E+18	1.040E+14	1.005E+14	1.074E+14
17.25	115720204.7	24.296	2.812E+18	1.035E+14	9.945E+13	1.075E+14
17.5	115729738.3	23.917	2.768E+18	1.031E+14	9.855E+13	1.076E+14
17.75	115739272.4	23.543	2.725E+18	1.028E+14	9.782E+13	1.077E+14
18	115748806.8	23.174	2.682E+18	1.026E+14	9.728E+13	1.079E+14
18.25	115758341.6	22.810	2.640E+18	1.025E+14	9.693E+13	1.081E+14
18.5	115767876.8	22.451	2.599E+18	1.025E+14	9.677E+13	1.083E+14
18.75	115777412.4	22.096	2.558E+18	1.027E+14	9.681E+13	1.086E+14
19	115786948.4	21.746	2.518E+18	1.030E+14	9.704E+13	1.089E+14

19.25	115796484.8	21.400	2.478E+18	1.034E+14	9.748E+13	1.092E+14
19.5	115806021.5	21.059	2.439E+18	1.039E+14	9.812E+13	1.096E+14
19.75	115815558.7	20.723	2.400E+18	1.045E+14	9.897E+13	1.101E+14
20	115825096.3	20.390	2.362E+18	1.053E+14	1.000E+14	1.105E+14
20.25	115834634.2	20.062	2.324E+18	1.062E+14	1.013E+14	1.110E+14
20.5	115844172.6	19.737	2.286E+18	1.072E+14	1.027E+14	1.116E+14
20.75	115853711.3	19.417	2.250E+18	1.083E+14	1.044E+14	1.122E+14
21	115863250.4	19.101	2.213E+18	1.095E+14	1.063E+14	1.128E+14
21.25	115872790	18.789	2.177E+18	1.109E+14	1.083E+14	1.135E+14
21.5	115882329.9	18.481	2.142E+18	1.124E+14	1.106E+14	1.142E+14
21.75	115891870.2	18.177	2.107E+18	1.140E+14	1.131E+14	1.149E+14
22	115901410.9	17.876	2.072E+18	1.157E+14	1.157E+14	1.157E+14
22.25	115910952	17.580	2.038E+18	1.176E+14	1.186E+14	1.166E+14
22.5	115920493.5	17.288	2.004E+18	1.195E+14	1.216E+14	1.174E+14
22.75	115930035.4	16.999	1.971E+18	1.215E+14	1.248E+14	1.183E+14
23	115939577.6	16.714	1.938E+18	1.236E+14	1.281E+14	1.192E+14
23.25	115949120.3	16.433	1.905E+18	1.258E+14	1.315E+14	1.201E+14
23.5	115958663.4	16.156	1.873E+18	1.280E+14	1.349E+14	1.210E+14
23.75	115968206.8	15.883	1.842E+18	1.302E+14	1.385E+14	1.219E+14
24	115977750.7	15.613	1.811E+18	1.324E+14	1.421E+14	1.228E+14
24.25	115987294.9	15.347	1.780E+18	1.346E+14	1.457E+14	1.236E+14
24.5	115996839.5	15.084	1.750E+18	1.369E+14	1.493E+14	1.244E+14
24.75	116006384.5	14.825	1.720E+18	1.391E+14	1.529E+14	1.253E+14
25	116015930	14.570	1.690E+18	1.413E+14	1.565E+14	1.260E+14
25.25	116025475.8	14.318	1.661E+18	1.434E+14	1.601E+14	1.268E+14
25.5	116035022	14.070	1.633E+18	1.455E+14	1.636E+14	1.274E+14
25.75	116044568.6	13.825	1.604E+18	1.476E+14	1.670E+14	1.281E+14
26	116054115.5	13.584	1.576E+18	1.496E+14	1.704E+14	1.287E+14

26.25	116063662.9	13.346	1.549E+18	1.515E+14	1.737E+14	1.292E+14
26.5	116073210.7	13.111	1.522E+18	1.533E+14	1.770E+14	1.297E+14
26.75	116082758.9	12.879	1.495E+18	1.551E+14	1.801E+14	1.301E+14
27	116092307.4	12.651	1.469E+18	1.568E+14	1.831E+14	1.305E+14
27.25	116101856.4	12.426	1.443E+18	1.584E+14	1.860E+14	1.308E+14
27.5	116111405.7	12.204	1.417E+18	1.599E+14	1.888E+14	1.310E+14
27.75	116120955.4	11.986	1.392E+18	1.613E+14	1.914E+14	1.312E+14
28	116130505.6	11.770	1.367E+18	1.626E+14	1.939E+14	1.313E+14
28.25	116140056.1	11.557	1.342E+18	1.638E+14	1.963E+14	1.313E+14
28.5	116149607	11.348	1.318E+18	1.649E+14	1.985E+14	1.313E+14
28.75	116159158.3	11.141	1.294E+18	1.659E+14	2.006E+14	1.312E+14
29	116168710	10.937	1.271E+18	1.667E+14	2.025E+14	1.310E+14
29.25	116178262.1	10.736	1.247E+18	1.675E+14	2.043E+14	1.307E+14
29.5	116187814.6	10.538	1.224E+18	1.681E+14	2.059E+14	1.304E+14
29.75	116197367.5	10.343	1.202E+18	1.686E+14	2.073E+14	1.300E+14
30	116206920.7	10.150	1.180E+18	1.690E+14	2.086E+14	1.295E+14
30.25	116216474.4	9.960	1.158E+18	1.693E+14	2.096E+14	1.289E+14
30.5	116226028.4	9.773	1.136E+18	1.694E+14	2.106E+14	1.283E+14
30.75	116235582.9	9.588	1.114E+18	1.694E+14	2.113E+14	1.276E+14
31	116245137.7	9.406	1.093E+18	1.693E+14	2.119E+14	1.268E+14
31.25	116254693	9.227	1.073E+18	1.691E+14	2.123E+14	1.259E+14
31.5	116264248.6	9.050	1.052E+18	1.688E+14	2.125E+14	1.250E+14
31.75	116273804.6	8.875	1.032E+18	1.683E+14	2.126E+14	1.240E+14
32	116283361	8.703	1.012E+18	1.677E+14	2.125E+14	1.229E+14
32.25	116292917.8	8.534	9.925E+17	1.670E+14	2.122E+14	1.218E+14
32.5	116302475	8.367	9.731E+17	1.662E+14	2.118E+14	1.206E+14
32.75	116312032.6	8.203	9.541E+17	1.652E+14	2.112E+14	1.193E+14
33	116321590.6	8.041	9.354E+17	1.642E+14	2.104E+14	1.180E+14

33.25	116331149	7.882	9.169E+17	1.630E+14	2.095E+14	1.166E+14
33.5	116340707.7	7.725	8.987E+17	1.618E+14	2.084E+14	1.151E+14
33.75	116350266.9	7.570	8.807E+17	1.604E+14	2.071E+14	1.136E+14
34	116359826.4	7.417	8.631E+17	1.589E+14	2.057E+14	1.120E+14
34.25	116369386.4	7.267	8.457E+17	1.573E+14	2.042E+14	1.104E+14
34.5	116378946.7	7.120	8.286E+17	1.556E+14	2.025E+14	1.087E+14
34.75	116388507.5	6.974	8.117E+17	1.538E+14	2.007E+14	1.070E+14
35	116398068.6	6.831	7.951E+17	1.519E+14	1.987E+14	1.052E+14
35.25	116407630.1	6.690	7.788E+17	1.500E+14	1.966E+14	1.034E+14
35.5	116417192	6.551	7.627E+17	1.479E+14	1.944E+14	1.015E+14
35.75	116426754.3	6.415	7.469E+17	1.458E+14	1.920E+14	9.959E+13
36	116436317	6.280	7.313E+17	1.436E+14	1.895E+14	9.767E+13
36.25	116445880.1	6.148	7.159E+17	1.413E+14	1.870E+14	9.572E+13
36.5	116455443.6	6.018	7.008E+17	1.390E+14	1.843E+14	9.376E+13
36.75	116465007.4	5.890	6.860E+17	1.367E+14	1.816E+14	9.179E+13
37	116474571.7	5.764	6.714E+17	1.343E+14	1.788E+14	8.981E+13
37.25	116484136.4	5.640	6.570E+17	1.319E+14	1.759E+14	8.784E+13
37.5	116493701.4	5.518	6.428E+17	1.294E+14	1.729E+14	8.587E+13
37.75	116503266.8	5.398	6.289E+17	1.269E+14	1.699E+14	8.391E+13
38	116512832.7	5.280	6.152E+17	1.244E+14	1.668E+14	8.197E+13
38.25	116522398.9	5.164	6.018E+17	1.219E+14	1.637E+14	8.004E+13
38.5	116531965.5	5.050	5.885E+17	1.193E+14	1.606E+14	7.814E+13
38.75	116541532.5	4.938	5.755E+17	1.168E+14	1.574E+14	7.625E+13
39	116551100	4.828	5.627E+17	1.143E+14	1.541E+14	7.440E+13
39.25	116560667.8	4.719	5.500E+17	1.117E+14	1.509E+14	7.257E+13
39.5	116570235.9	4.612	5.376E+17	1.092E+14	1.476E+14	7.077E+13
39.75	116579804.5	4.507	5.255E+17	1.067E+14	1.443E+14	6.901E+13
40	116589373.5	4.404	5.135E+17	1.042E+14	1.411E+14	6.728E+13

40.25	116598942.9	4.302	5.017E+17	1.017E+14	1.378E+14	6.559E+13
40.5	116608512.6	4.203	4.901E+17	9.919E+13	1.344E+14	6.393E+13
40.75	116618082.8	4.105	4.787E+17	9.673E+13	1.311E+14	6.232E+13
41	116627653.3	4.008	4.675E+17	9.429E+13	1.278E+14	6.075E+13
41.25	116637224.3	3.914	4.565E+17	9.188E+13	1.246E+14	5.921E+13
41.5	116646795.6	3.821	4.457E+17	8.950E+13	1.213E+14	5.772E+13
41.75	116656367.3	3.729	4.351E+17	8.715E+13	1.180E+14	5.628E+13
42	116665939.5	3.640	4.246E+17	8.483E+13	1.148E+14	5.488E+13
42.25	116675512	3.552	4.144E+17	8.255E+13	1.116E+14	5.352E+13
42.5	116685084.9	3.466	4.044E+17	8.030E+13	1.084E+14	5.221E+13
42.75	116694658.2	3.381	3.945E+17	7.809E+13	1.052E+14	5.095E+13
43	116704231.9	3.298	3.849E+17	7.592E+13	1.021E+14	4.973E+13
43.25	116713805.9	3.217	3.754E+17	7.379E+13	9.902E+13	4.856E+13
43.5	116723380.4	3.137	3.662E+17	7.170E+13	9.597E+13	4.743E+13
43.75	116732955.3	3.059	3.571E+17	6.966E+13	9.296E+13	4.635E+13
44	116742530.5	2.983	3.482E+17	6.765E+13	9.000E+13	4.531E+13
44.25	116752106.2	2.908	3.395E+17	6.570E+13	8.707E+13	4.432E+13
44.5	116761682.2	2.835	3.310E+17	6.378E+13	8.420E+13	4.337E+13
44.75	116771258.7	2.763	3.226E+17	6.192E+13	8.137E+13	4.247E+13
45	116780835.5	2.693	3.145E+17	6.010E+13	7.859E+13	4.161E+13
45.25	116790412.7	2.625	3.065E+17	5.833E+13	7.586E+13	4.079E+13
45.5	116799990.4	2.558	2.987E+17	5.660E+13	7.319E+13	4.001E+13
45.75	116809568.4	2.492	2.911E+17	5.492E+13	7.057E+13	3.926E+13
46	116819146.8	2.429	2.837E+17	5.328E+13	6.801E+13	3.855E+13
46.25	116828725.6	2.366	2.765E+17	5.168E+13	6.550E+13	3.786E+13
46.5	116838304.7	2.306	2.694E+17	5.012E+13	6.305E+13	3.719E+13
46.75	116847884.3	2.246	2.625E+17	4.861E+13	6.067E+13	3.655E+13
47	116857464.3	2.188	2.557E+17	4.713E+13	5.834E+13	3.592E+13

47.25	116867044.7	2.132	2.491E+17	4.569E+13	5.607E+13	3.531E+13
47.5	116876625.4	2.076	2.427E+17	4.429E+13	5.387E+13	3.471E+13
47.75	116886206.6	2.023	2.364E+17	4.292E+13	5.172E+13	3.412E+13
48	116895788.1	1.970	2.303E+17	4.159E+13	4.964E+13	3.353E+13
48.25	116905370.1	1.919	2.243E+17	4.029E+13	4.762E+13	3.296E+13
48.5	116914952.4	1.869	2.185E+17	3.903E+13	4.566E+13	3.239E+13
48.75	116924535.1	1.820	2.128E+17	3.779E+13	4.377E+13	3.182E+13
49	116934118.2	1.772	2.073E+17	3.659E+13	4.193E+13	3.126E+13
49.25	116943701.7	1.726	2.019E+17	3.542E+13	4.015E+13	3.069E+13
49.5	116953285.6	1.681	1.966E+17	3.428E+13	3.844E+13	3.013E+13
49.75	116962869.9	1.637	1.915E+17	3.317E+13	3.678E+13	2.957E+13
50	116972454.6	1.594	1.865E+17	3.209E+13	3.518E+13	2.900E+13
50.25	116982039.7	1.552	1.816E+17	3.104E+13	3.364E+13	2.843E+13
50.5	116991625.1	1.511	1.768E+17	3.001E+13	3.215E+13	2.787E+13
50.75	117001211	1.472	1.722E+17	2.901E+13	3.072E+13	2.729E+13
51	117010797.3	1.433	1.677E+17	2.803E+13	2.935E+13	2.672E+13
51.25	117020383.9	1.395	1.633E+17	2.708E+13	2.802E+13	2.613E+13
51.5	117029971	1.358	1.590E+17	2.615E+13	2.675E+13	2.555E+13
51.75	117039558.4	1.322	1.548E+17	2.525E+13	2.553E+13	2.496E+13
52	117049146.2	1.287	1.507E+17	2.436E+13	2.436E+13	2.436E+13
52.25	117058734.4	1.253	1.467E+17	2.350E+13	2.324E+13	2.376E+13
52.5	117068323.1	1.219	1.427E+17	2.266E+13	2.216E+13	2.315E+13
52.75	117077912.1	1.187	1.389E+17	2.183E+13	2.113E+13	2.254E+13
53	117087501.5	1.155	1.352E+17	2.103E+13	2.013E+13	2.193E+13
53.25	117097091.2	1.123	1.315E+17	2.025E+13	1.918E+13	2.132E+13
53.5	117106681.4	1.093	1.280E+17	1.949E+13	1.827E+13	2.070E+13
53.75	117116272	1.063	1.244E+17	1.874E+13	1.739E+13	2.009E+13
54	117125863	1.033	1.210E+17	1.801E+13	1.655E+13	1.948E+13

54.25	117135454.3	1.004	1.176E+17	1.730E+13	1.574E+13	1.886E+13
54.5	117145046.1	0.976	1.143E+17	1.661E+13	1.497E+13	1.825E+13
54.75	117154638.2	0.948	1.111E+17	1.593E+13	1.422E+13	1.764E+13
55	117164230.8	0.921	1.079E+17	1.527E+13	1.350E+13	1.704E+13
55.25	117173823.7	0.894	1.047E+17	1.462E+13	1.281E+13	1.644E+13
55.5	117183417	0.867	1.016E+17	1.399E+13	1.215E+13	1.584E+13
55.75	117193010.7	0.841	9.858E+16	1.338E+13	1.151E+13	1.525E+13
56	117202604.9	0.816	9.558E+16	1.278E+13	1.090E+13	1.466E+13
56.25	117212199.4	0.790	9.263E+16	1.220E+13	1.032E+13	1.408E+13
56.5	117221794.2	0.766	8.974E+16	1.163E+13	9.758E+12	1.351E+13
56.75	117231389.5	0.741	8.690E+16	1.108E+13	9.221E+12	1.294E+13
57	117240985.2	0.717	8.412E+16	1.055E+13	8.706E+12	1.239E+13
57.25	117250581.3	0.694	8.139E+16	1.003E+13	8.214E+12	1.185E+13
57.5	117260177.8	0.671	7.871E+16	9.529E+12	7.743E+12	1.132E+13
57.75	117269774.6	0.649	7.609E+16	9.044E+12	7.293E+12	1.079E+13
58	117279371.9	0.627	7.352E+16	8.574E+12	6.864E+12	1.028E+13
58.25	117288969.5	0.605	7.102E+16	8.121E+12	6.454E+12	9.788E+12
58.5	117298567.5	0.585	6.856E+16	7.684E+12	6.064E+12	9.304E+12
58.75	117308166	0.564	6.617E+16	7.263E+12	5.692E+12	8.833E+12
59	117317764.8	0.544	6.384E+16	6.857E+12	5.338E+12	8.376E+12
59.25	117327364	0.525	6.156E+16	6.467E+12	5.002E+12	7.933E+12
59.5	117336963.6	0.506	5.934E+16	6.093E+12	4.682E+12	7.503E+12
59.75	117346563.6	0.487	5.718E+16	5.734E+12	4.379E+12	7.088E+12
60	117356164	0.469	5.509E+16	5.389E+12	4.091E+12	6.688E+12
60.25	117365764.8	0.452	5.305E+16	5.060E+12	3.819E+12	6.302E+12
60.5	117375366	0.435	5.107E+16	4.746E+12	3.561E+12	5.930E+12
60.75	117384967.6	0.419	4.916E+16	4.445E+12	3.317E+12	5.573E+12
61	117394569.5	0.403	4.730E+16	4.158E+12	3.086E+12	5.230E+12

61.25	117404171.9	0.388	4.550E+16	3.884E+12	2.868E+12	4.901E+12
61.5	117413774.6	0.373	4.375E+16	3.624E+12	2.662E+12	4.585E+12
61.75	117423377.8	0.358	4.206E+16	3.376E+12	2.468E+12	4.283E+12
62	117432981.3	0.344	4.042E+16	3.140E+12	2.285E+12	3.994E+12
62.25	117442585.2	0.331	3.883E+16	2.915E+12	2.112E+12	3.719E+12
62.5	117452189.5	0.318	3.730E+16	2.703E+12	1.949E+12	3.456E+12
62.75	117461794.3	0.305	3.581E+16	2.501E+12	1.796E+12	3.205E+12
63	117471399.4	0.293	3.437E+16	2.309E+12	1.652E+12	2.966E+12
63.25	117481004.9	0.281	3.299E+16	2.128E+12	1.517E+12	2.739E+12
63.5	117490610.8	0.269	3.164E+16	1.957E+12	1.390E+12	2.524E+12
63.75	117500217	0.258	3.035E+16	1.795E+12	1.271E+12	2.320E+12
64	117509823.7	0.248	2.910E+16	1.643E+12	1.159E+12	2.126E+12
64.25	117519430.8	0.237	2.789E+16	1.499E+12	1.055E+12	1.943E+12
64.5	117529038.2	0.227	2.673E+16	1.364E+12	9.568E+11	1.771E+12
64.75	117538646.1	0.218	2.560E+16	1.236E+12	8.652E+11	1.608E+12
65	117548254.3	0.209	2.452E+16	1.117E+12	7.797E+11	1.454E+12
65.25	117557863	0.200	2.348E+16	1.005E+12	6.999E+11	1.309E+12
65.5	117567472	0.191	2.247E+16	8.995E+11	6.254E+11	1.173E+12
65.75	117577081.4	0.183	2.150E+16	8.011E+11	5.562E+11	1.046E+12
66	117586691.3	0.175	2.057E+16	7.093E+11	4.917E+11	9.268E+11
66.25	117596301.5	0.167	1.968E+16	6.235E+11	4.318E+11	8.153E+11
66.5	117605912.1	0.160	1.882E+16	5.437E+11	3.763E+11	7.111E+11
66.75	117615523.1	0.153	1.799E+16	4.695E+11	3.248E+11	6.141E+11
67	117625134.5	0.146	1.719E+16	4.005E+11	2.771E+11	5.239E+11
67.25	117634746.2	0.140	1.643E+16	3.366E+11	2.331E+11	4.401E+11
67.5	117644358.4	0.133	1.570E+16	2.774E+11	1.924E+11	3.624E+11
67.75	117653971	0.127	1.500E+16	2.228E+11	1.550E+11	2.906E+11
68	117663583.9	0.122	1.432E+16	1.724E+11	1.205E+11	2.243E+11

68.25	117673197.3	0.116	1.368E+16	1.260E+11	8.879E+10	1.633E+11
68.5	117682811	0.111	1.306E+16	8.348E+10	5.973E+10	1.072E+11
68.75	117692425.2	0.106	1.247E+16	4.447E+10	3.313E+10	5.581E+10
69	117702039.7	0.101	1.191E+16	8.811E+09	8.811E+09	8.811E+09
69.25	117711654.6	0.097	1.137E+16	8.411E+09	8.411E+09	8.411E+09
69.5	117721269.9	0.092	1.085E+16	8.028E+09	8.028E+09	8.028E+09
69.75	117730885.6	0.088	1.035E+16	7.662E+09	7.662E+09	7.662E+09
70	117740501.7	0.084	9.882E+15	7.313E+09	7.313E+09	7.313E+09
Sum				2.268E+16	2.681E+16	1.854E+16

Appendix 15

The cubic spline calculations with 280 shells. This is the result for model B:

Shell	Volume (km^3)	Density (kg/m^3)	Mass	Model B	Deviation 1	Deviation 2
0	115063332	64.790	7.455E+18	2.740E+14	2.740E+14	2.740E+14
0.25	115072839	64.014	7.366E+18	2.700E+14	2.718E+14	2.682E+14
0.5	115082346	63.238	7.278E+18	2.660E+14	2.695E+14	2.624E+14
0.75	115091853	62.463	7.189E+18	2.620E+14	2.672E+14	2.568E+14
1	115101361	61.690	7.101E+18	2.581E+14	2.650E+14	2.512E+14
1.25	115110869	60.918	7.012E+18	2.542E+14	2.626E+14	2.457E+14
1.5	115120377	60.148	6.924E+18	2.503E+14	2.603E+14	2.402E+14
1.75	115129886	59.382	6.837E+18	2.464E+14	2.579E+14	2.349E+14
2	115139396	58.618	6.749E+18	2.426E+14	2.555E+14	2.297E+14
2.25	115148905	57.858	6.662E+18	2.388E+14	2.531E+14	2.245E+14
2.5	115158415	57.103	6.576E+18	2.350E+14	2.506E+14	2.194E+14
2.75	115167926	56.351	6.490E+18	2.313E+14	2.481E+14	2.145E+14
3	115177437	55.605	6.404E+18	2.276E+14	2.456E+14	2.096E+14
3.25	115186948	54.864	6.320E+18	2.240E+14	2.431E+14	2.049E+14
3.5	115196460	54.129	6.236E+18	2.204E+14	2.405E+14	2.002E+14
3.75	115205972	53.401	6.152E+18	2.168E+14	2.379E+14	1.957E+14
4	115215484	52.679	6.069E+18	2.133E+14	2.353E+14	1.913E+14
4.25	115224997	51.965	5.988E+18	2.098E+14	2.327E+14	1.870E+14
4.5	115234510	51.258	5.907E+18	2.064E+14	2.301E+14	1.828E+14
4.75	115244024	50.560	5.827E+18	2.031E+14	2.274E+14	1.787E+14
5	115253538	49.870	5.748E+18	1.998E+14	2.247E+14	1.748E+14

5.25	115263052	49.189	5.670E+18	1.965E+14	2.220E+14	1.710E+14
5.5	115272567	48.517	5.593E+18	1.933E+14	2.193E+14	1.673E+14
5.75	115282082	47.854	5.517E+18	1.901E+14	2.166E+14	1.637E+14
6	115291598	47.199	5.442E+18	1.870E+14	2.139E+14	1.602E+14
6.25	115301114	46.553	5.368E+18	1.840E+14	2.112E+14	1.568E+14
6.5	115310630	45.915	5.294E+18	1.810E+14	2.084E+14	1.536E+14
6.75	115320147	45.284	5.222E+18	1.780E+14	2.056E+14	1.505E+14
7	115329664	44.662	5.151E+18	1.751E+14	2.028E+14	1.475E+14
7.25	115339181	44.046	5.080E+18	1.723E+14	2.000E+14	1.446E+14
7.5	115348699	43.439	5.011E+18	1.695E+14	1.972E+14	1.418E+14
7.75	115358218	42.838	4.942E+18	1.667E+14	1.943E+14	1.391E+14
8	115367736	42.244	4.874E+18	1.640E+14	1.914E+14	1.365E+14
8.25	115377255	41.657	4.806E+18	1.613E+14	1.885E+14	1.340E+14
8.5	115386775	41.077	4.740E+18	1.586E+14	1.856E+14	1.316E+14
8.75	115396295	40.502	4.674E+18	1.560E+14	1.827E+14	1.294E+14
9	115405815	39.934	4.609E+18	1.534E+14	1.797E+14	1.272E+14
9.25	115415336	39.372	4.544E+18	1.509E+14	1.767E+14	1.251E+14
9.5	115424857	38.816	4.480E+18	1.484E+14	1.737E+14	1.231E+14
9.75	115434378	38.265	4.417E+18	1.459E+14	1.706E+14	1.212E+14
10	115443900	37.720	4.355E+18	1.435E+14	1.676E+14	1.194E+14
10.25	115453422	37.180	4.293E+18	1.411E+14	1.645E+14	1.177E+14
10.5	115462945	36.645	4.231E+18	1.388E+14	1.614E+14	1.161E+14
10.75	115472468	36.115	4.170E+18	1.364E+14	1.583E+14	1.146E+14
11	115481991	35.591	4.110E+18	1.342E+14	1.552E+14	1.132E+14
11.25	115491515	35.071	4.050E+18	1.319E+14	1.520E+14	1.118E+14
11.5	115501039	34.558	3.991E+18	1.297E+14	1.488E+14	1.105E+14
11.75	115510564	34.049	3.933E+18	1.275E+14	1.456E+14	1.093E+14
12	115520089	33.546	3.875E+18	1.253E+14	1.424E+14	1.082E+14

12.25	115529614	33.049	3.818E+18	1.232E+14	1.392E+14	1.072E+14
12.5	115539140	32.557	3.762E+18	1.211E+14	1.360E+14	1.063E+14
12.75	115548666	32.071	3.706E+18	1.191E+14	1.328E+14	1.054E+14
13	115558193	31.590	3.650E+18	1.171E+14	1.296E+14	1.046E+14
13.25	115567720	31.115	3.596E+18	1.152E+14	1.266E+14	1.039E+14
13.5	115577247	30.645	3.542E+18	1.134E+14	1.235E+14	1.032E+14
13.75	115586775	30.181	3.489E+18	1.116E+14	1.206E+14	1.027E+14
14	115596303	29.724	3.436E+18	1.099E+14	1.177E+14	1.022E+14
14.25	115605832	29.271	3.384E+18	1.084E+14	1.150E+14	1.017E+14
14.5	115615361	28.825	3.333E+18	1.069E+14	1.124E+14	1.014E+14
14.75	115624890	28.385	3.282E+18	1.055E+14	1.099E+14	1.011E+14
15	115634420	27.950	3.232E+18	1.042E+14	1.075E+14	1.009E+14
15.25	115643950	27.521	3.183E+18	1.030E+14	1.053E+14	1.007E+14
15.5	115653480	27.099	3.134E+18	1.020E+14	1.033E+14	1.006E+14
15.75	115663011	26.682	3.086E+18	1.010E+14	1.014E+14	1.006E+14
16	115672542	26.270	3.039E+18	1.002E+14	9.964E+13	1.007E+14
16.25	115682074	25.865	2.992E+18	9.943E+13	9.809E+13	1.008E+14
16.5	115691606	25.465	2.946E+18	9.882E+13	9.671E+13	1.009E+14
16.75	115701139	25.070	2.901E+18	9.834E+13	9.553E+13	1.011E+14
17	115710671	24.680	2.856E+18	9.797E+13	9.452E+13	1.014E+14
17.25	115720205	24.296	2.812E+18	9.773E+13	9.371E+13	1.018E+14
17.5	115729738	23.917	2.768E+18	9.761E+13	9.310E+13	1.021E+14
17.75	115739272	23.543	2.725E+18	9.762E+13	9.267E+13	1.026E+14
18	115748807	23.174	2.682E+18	9.774E+13	9.245E+13	1.030E+14
18.25	115758342	22.810	2.640E+18	9.799E+13	9.243E+13	1.036E+14
18.5	115767877	22.451	2.599E+18	9.837E+13	9.260E+13	1.041E+14
18.75	115777412	22.096	2.558E+18	9.886E+13	9.298E+13	1.047E+14
19	115786948	21.746	2.518E+18	9.948E+13	9.356E+13	1.054E+14

19.25	115796485	21.400	2.478E+18	1.002E+14	9.434E+13	1.061E+14
19.5	115806022	21.059	2.439E+18	1.011E+14	9.532E+13	1.068E+14
19.75	115815559	20.723	2.400E+18	1.020E+14	9.649E+13	1.076E+14
20	115825096	20.390	2.362E+18	1.031E+14	9.787E+13	1.084E+14
20.25	115834634	20.062	2.324E+18	1.043E+14	9.944E+13	1.092E+14
20.5	115844173	19.737	2.286E+18	1.056E+14	1.012E+14	1.101E+14
20.75	115853711	19.417	2.250E+18	1.071E+14	1.032E+14	1.109E+14
21	115863250	19.101	2.213E+18	1.086E+14	1.053E+14	1.119E+14
21.25	115872790	18.789	2.177E+18	1.102E+14	1.076E+14	1.128E+14
21.5	115882330	18.481	2.142E+18	1.120E+14	1.102E+14	1.138E+14
21.75	115891870	18.177	2.107E+18	1.138E+14	1.129E+14	1.147E+14
22	115901411	17.876	2.072E+18	1.157E+14	1.157E+14	1.157E+14
22.25	115910952	17.580	2.038E+18	1.178E+14	1.188E+14	1.168E+14
22.5	115920493	17.288	2.004E+18	1.199E+14	1.220E+14	1.178E+14
22.75	115930035	16.999	1.971E+18	1.221E+14	1.253E+14	1.188E+14
23	115939578	16.714	1.938E+18	1.243E+14	1.287E+14	1.198E+14
23.25	115949120	16.433	1.905E+18	1.265E+14	1.322E+14	1.209E+14
23.5	115958663	16.156	1.873E+18	1.288E+14	1.358E+14	1.219E+14
23.75	115968207	15.883	1.842E+18	1.311E+14	1.394E+14	1.228E+14
24	115977751	15.613	1.811E+18	1.335E+14	1.431E+14	1.238E+14
24.25	115987295	15.347	1.780E+18	1.358E+14	1.468E+14	1.247E+14
24.5	115996840	15.084	1.750E+18	1.380E+14	1.505E+14	1.256E+14
24.75	116006385	14.825	1.720E+18	1.403E+14	1.541E+14	1.265E+14
25	116015930	14.570	1.690E+18	1.425E+14	1.577E+14	1.273E+14
25.25	116025476	14.318	1.661E+18	1.447E+14	1.613E+14	1.280E+14
25.5	116035022	14.070	1.633E+18	1.468E+14	1.649E+14	1.287E+14
25.75	116044569	13.825	1.604E+18	1.489E+14	1.683E+14	1.294E+14
26	116054116	13.584	1.576E+18	1.508E+14	1.717E+14	1.300E+14

26.25	116063663	13.346	1.549E+18	1.528E+14	1.750E+14	1.305E+14
26.5	116073211	13.111	1.522E+18	1.546E+14	1.782E+14	1.310E+14
26.75	116082759	12.879	1.495E+18	1.564E+14	1.813E+14	1.314E+14
27	116092307	12.651	1.469E+18	1.580E+14	1.843E+14	1.317E+14
27.25	116101856	12.426	1.443E+18	1.596E+14	1.872E+14	1.320E+14
27.5	116111406	12.204	1.417E+18	1.611E+14	1.899E+14	1.322E+14
27.75	116120955	11.986	1.392E+18	1.624E+14	1.926E+14	1.323E+14
28	116130506	11.770	1.367E+18	1.637E+14	1.950E+14	1.324E+14
28.25	116140056	11.557	1.342E+18	1.649E+14	1.974E+14	1.324E+14
28.5	116149607	11.348	1.318E+18	1.659E+14	1.995E+14	1.323E+14
28.75	116159158	11.141	1.294E+18	1.669E+14	2.016E+14	1.321E+14
29	116168710	10.937	1.271E+18	1.677E+14	2.034E+14	1.319E+14
29.25	116178262	10.736	1.247E+18	1.684E+14	2.052E+14	1.316E+14
29.5	116187815	10.538	1.224E+18	1.690E+14	2.067E+14	1.312E+14
29.75	116197367	10.343	1.202E+18	1.694E+14	2.081E+14	1.307E+14
30	116206921	10.150	1.180E+18	1.698E+14	2.093E+14	1.302E+14
30.25	116216474	9.960	1.158E+18	1.700E+14	2.103E+14	1.296E+14
30.5	116226028	9.773	1.136E+18	1.701E+14	2.112E+14	1.289E+14
30.75	116235583	9.588	1.114E+18	1.700E+14	2.119E+14	1.282E+14
31	116245138	9.406	1.093E+18	1.699E+14	2.124E+14	1.273E+14
31.25	116254693	9.227	1.073E+18	1.696E+14	2.128E+14	1.264E+14
31.5	116264249	9.050	1.052E+18	1.692E+14	2.130E+14	1.254E+14
31.75	116273805	8.875	1.032E+18	1.687E+14	2.130E+14	1.244E+14
32	116283361	8.703	1.012E+18	1.681E+14	2.129E+14	1.233E+14
32.25	116292918	8.534	9.925E+17	1.673E+14	2.126E+14	1.221E+14
32.5	116302475	8.367	9.731E+17	1.665E+14	2.121E+14	1.209E+14
32.75	116312033	8.203	9.541E+17	1.655E+14	2.114E+14	1.196E+14
33	116321591	8.041	9.354E+17	1.644E+14	2.106E+14	1.182E+14

33.25	116331149	7.882	9.169E+17	1.632E+14	2.097E+14	1.167E+14
33.5	116340708	7.725	8.987E+17	1.619E+14	2.085E+14	1.153E+14
33.75	116350267	7.570	8.807E+17	1.605E+14	2.073E+14	1.137E+14
34	116359826	7.417	8.631E+17	1.590E+14	2.058E+14	1.121E+14
34.25	116369386	7.267	8.457E+17	1.574E+14	2.043E+14	1.105E+14
34.5	116378947	7.120	8.286E+17	1.556E+14	2.025E+14	1.088E+14
34.75	116388507	6.974	8.117E+17	1.538E+14	2.007E+14	1.070E+14
35	116398069	6.831	7.951E+17	1.519E+14	1.987E+14	1.052E+14
35.25	116407630	6.690	7.788E+17	1.500E+14	1.966E+14	1.033E+14
35.5	116417192	6.551	7.627E+17	1.479E+14	1.943E+14	1.015E+14
35.75	116426754	6.415	7.469E+17	1.458E+14	1.920E+14	9.955E+13
36	116436317	6.280	7.313E+17	1.436E+14	1.895E+14	9.761E+13
36.25	116445880	6.148	7.159E+17	1.413E+14	1.869E+14	9.566E+13
36.5	116455444	6.018	7.008E+17	1.390E+14	1.843E+14	9.369E+13
36.75	116465007	5.890	6.860E+17	1.366E+14	1.815E+14	9.171E+13
37	116474572	5.764	6.714E+17	1.342E+14	1.787E+14	8.973E+13
37.25	116484136	5.640	6.570E+17	1.318E+14	1.758E+14	8.775E+13
37.5	116493701	5.518	6.428E+17	1.293E+14	1.728E+14	8.578E+13
37.75	116503267	5.398	6.289E+17	1.268E+14	1.698E+14	8.383E+13
38	116512833	5.280	6.152E+17	1.243E+14	1.667E+14	8.188E+13
38.25	116522399	5.164	6.018E+17	1.218E+14	1.636E+14	7.995E+13
38.5	116531966	5.050	5.885E+17	1.193E+14	1.605E+14	7.805E+13
38.75	116541533	4.938	5.755E+17	1.167E+14	1.573E+14	7.617E+13
39	116551100	4.828	5.627E+17	1.142E+14	1.541E+14	7.431E+13
39.25	116560668	4.719	5.500E+17	1.117E+14	1.508E+14	7.249E+13
39.5	116570236	4.612	5.376E+17	1.091E+14	1.476E+14	7.070E+13
39.75	116579805	4.507	5.255E+17	1.066E+14	1.443E+14	6.893E+13
40	116589374	4.404	5.135E+17	1.041E+14	1.410E+14	6.721E+13

40.25	116598943	4.302	5.017E+17	1.016E+14	1.377E+14	6.552E+13
40.5	116608513	4.203	4.901E+17	9.913E+13	1.344E+14	6.387E+13
40.75	116618083	4.105	4.787E+17	9.667E+13	1.311E+14	6.226E+13
41	116627653	4.008	4.675E+17	9.424E+13	1.278E+14	6.069E+13
41.25	116637224	3.914	4.565E+17	9.183E+13	1.245E+14	5.916E+13
41.5	116646796	3.821	4.457E+17	8.946E+13	1.212E+14	5.768E+13
41.75	116656367	3.729	4.351E+17	8.711E+13	1.180E+14	5.624E+13
42	116665939	3.640	4.246E+17	8.480E+13	1.147E+14	5.484E+13
42.25	116675512	3.552	4.144E+17	8.252E+13	1.115E+14	5.349E+13
42.5	116685085	3.466	4.044E+17	8.027E+13	1.084E+14	5.218E+13
42.75	116694658	3.381	3.945E+17	7.807E+13	1.052E+14	5.092E+13
43	116704232	3.298	3.849E+17	7.590E+13	1.021E+14	4.971E+13
43.25	116713806	3.217	3.754E+17	7.377E+13	9.900E+13	4.854E+13
43.5	116723380	3.137	3.662E+17	7.169E+13	9.596E+13	4.741E+13
43.75	116732955	3.059	3.571E+17	6.964E+13	9.295E+13	4.634E+13
44	116742531	2.983	3.482E+17	6.764E+13	8.999E+13	4.530E+13
44.25	116752106	2.908	3.395E+17	6.569E+13	8.707E+13	4.431E+13
44.5	116761682	2.835	3.310E+17	6.378E+13	8.419E+13	4.337E+13
44.75	116771259	2.763	3.226E+17	6.192E+13	8.137E+13	4.247E+13
45	116780836	2.693	3.145E+17	6.010E+13	7.859E+13	4.161E+13
45.25	116790413	2.625	3.065E+17	5.833E+13	7.587E+13	4.079E+13
45.5	116799990	2.558	2.987E+17	5.660E+13	7.319E+13	4.001E+13
45.75	116809568	2.492	2.911E+17	5.492E+13	7.057E+13	3.927E+13
46	116819147	2.429	2.837E+17	5.328E+13	6.801E+13	3.855E+13
46.25	116828726	2.366	2.765E+17	5.168E+13	6.551E+13	3.786E+13
46.5	116838305	2.306	2.694E+17	5.013E+13	6.306E+13	3.720E+13
46.75	116847884	2.246	2.625E+17	4.861E+13	6.067E+13	3.655E+13
47	116857464	2.188	2.557E+17	4.714E+13	5.834E+13	3.593E+13

47.25	116867045	2.132	2.491E+17	4.570E+13	5.608E+13	3.531E+13
47.5	116876625	2.076	2.427E+17	4.429E+13	5.387E+13	3.471E+13
47.75	116886207	2.023	2.364E+17	4.293E+13	5.173E+13	3.412E+13
48	116895788	1.970	2.303E+17	4.159E+13	4.965E+13	3.354E+13
48.25	116905370	1.919	2.243E+17	4.030E+13	4.763E+13	3.296E+13
48.5	116914952	1.869	2.185E+17	3.903E+13	4.567E+13	3.239E+13
48.75	116924535	1.820	2.128E+17	3.780E+13	4.377E+13	3.183E+13
49	116934118	1.772	2.073E+17	3.660E+13	4.193E+13	3.126E+13
49.25	116943702	1.726	2.019E+17	3.543E+13	4.016E+13	3.070E+13
49.5	116953286	1.681	1.966E+17	3.429E+13	3.844E+13	3.013E+13
49.75	116962870	1.637	1.915E+17	3.318E+13	3.678E+13	2.957E+13
50	116972455	1.594	1.865E+17	3.209E+13	3.518E+13	2.900E+13
50.25	116982040	1.552	1.816E+17	3.104E+13	3.364E+13	2.844E+13
50.5	116991625	1.511	1.768E+17	3.001E+13	3.216E+13	2.787E+13
50.75	117001211	1.472	1.722E+17	2.901E+13	3.073E+13	2.729E+13
51	117010797	1.433	1.677E+17	2.803E+13	2.935E+13	2.672E+13
51.25	117020384	1.395	1.633E+17	2.708E+13	2.803E+13	2.614E+13
51.5	117029971	1.358	1.590E+17	2.615E+13	2.675E+13	2.555E+13
51.75	117039558	1.322	1.548E+17	2.525E+13	2.553E+13	2.496E+13
52	117049146	1.287	1.507E+17	2.436E+13	2.436E+13	2.436E+13
52.25	117058734	1.253	1.467E+17	2.350E+13	2.324E+13	2.376E+13
52.5	117068323	1.219	1.427E+17	2.266E+13	2.216E+13	2.315E+13
52.75	117077912	1.187	1.389E+17	2.183E+13	2.113E+13	2.254E+13
53	117087501	1.155	1.352E+17	2.103E+13	2.013E+13	2.193E+13
53.25	117097091	1.123	1.315E+17	2.025E+13	1.918E+13	2.132E+13
53.5	117106681	1.093	1.280E+17	1.949E+13	1.827E+13	2.070E+13
53.75	117116272	1.063	1.244E+17	1.874E+13	1.739E+13	2.009E+13
54	117125863	1.033	1.210E+17	1.801E+13	1.655E+13	1.947E+13

54.25	117135454	1.004	1.176E+17	1.730E+13	1.574E+13	1.886E+13
54.5	117145046	0.976	1.143E+17	1.661E+13	1.496E+13	1.825E+13
54.75	117154638	0.948	1.111E+17	1.593E+13	1.422E+13	1.764E+13
55	117164231	0.921	1.079E+17	1.527E+13	1.350E+13	1.704E+13
55.25	117173824	0.894	1.047E+17	1.462E+13	1.281E+13	1.643E+13
55.5	117183417	0.867	1.016E+17	1.399E+13	1.215E+13	1.584E+13
55.75	117193011	0.841	9.858E+16	1.338E+13	1.151E+13	1.524E+13
56	117202605	0.816	9.558E+16	1.278E+13	1.090E+13	1.466E+13
56.25	117212199	0.790	9.263E+16	1.220E+13	1.032E+13	1.408E+13
56.5	117221794	0.766	8.974E+16	1.163E+13	9.756E+12	1.351E+13
56.75	117231390	0.741	8.690E+16	1.108E+13	9.219E+12	1.294E+13
57	117240985	0.717	8.412E+16	1.055E+13	8.704E+12	1.239E+13
57.25	117250581	0.694	8.139E+16	1.003E+13	8.212E+12	1.185E+13
57.5	117260178	0.671	7.871E+16	9.527E+12	7.741E+12	1.131E+13
57.75	117269775	0.649	7.609E+16	9.042E+12	7.291E+12	1.079E+13
58	117279372	0.627	7.352E+16	8.573E+12	6.862E+12	1.028E+13
58.25	117288970	0.605	7.102E+16	8.119E+12	6.452E+12	9.786E+12
58.5	117298568	0.585	6.856E+16	7.682E+12	6.062E+12	9.302E+12
58.75	117308166	0.564	6.617E+16	7.261E+12	5.690E+12	8.831E+12
59	117317765	0.544	6.384E+16	6.855E+12	5.337E+12	8.374E+12
59.25	117327364	0.525	6.156E+16	6.466E+12	5.000E+12	7.931E+12
59.5	117336964	0.506	5.934E+16	6.091E+12	4.681E+12	7.502E+12
59.75	117346564	0.487	5.718E+16	5.732E+12	4.377E+12	7.087E+12
60	117356164	0.469	5.509E+16	5.388E+12	4.090E+12	6.686E+12
60.25	117365765	0.452	5.305E+16	5.059E+12	3.817E+12	6.300E+12
60.5	117375366	0.435	5.107E+16	4.744E+12	3.560E+12	5.929E+12
60.75	117384968	0.419	4.916E+16	4.444E+12	3.316E+12	5.572E+12
61	117394570	0.403	4.730E+16	4.157E+12	3.085E+12	5.229E+12

61.25	117404172	0.388	4.550E+16	3.883E+12	2.867E+12	4.900E+12
61.5	117413775	0.373	4.375E+16	3.623E+12	2.661E+12	4.584E+12
61.75	117423378	0.358	4.206E+16	3.375E+12	2.467E+12	4.282E+12
62	117432981	0.344	4.042E+16	3.139E+12	2.284E+12	3.994E+12
62.25	117442585	0.331	3.883E+16	2.915E+12	2.111E+12	3.718E+12
62.5	117452190	0.318	3.730E+16	2.702E+12	1.949E+12	3.455E+12
62.75	117461794	0.305	3.581E+16	2.500E+12	1.796E+12	3.204E+12
63	117471399	0.293	3.437E+16	2.309E+12	1.652E+12	2.966E+12
63.25	117481005	0.281	3.299E+16	2.128E+12	1.517E+12	2.739E+12
63.5	117490611	0.269	3.164E+16	1.957E+12	1.390E+12	2.523E+12
63.75	117500217	0.258	3.035E+16	1.795E+12	1.270E+12	2.319E+12
64	117509824	0.248	2.910E+16	1.642E+12	1.159E+12	2.126E+12
64.25	117519431	0.237	2.789E+16	1.499E+12	1.054E+12	1.943E+12
64.5	117529038	0.227	2.673E+16	1.363E+12	9.563E+11	1.770E+12
64.75	117538646	0.218	2.560E+16	1.236E+12	8.648E+11	1.607E+12
65	117548254	0.209	2.452E+16	1.116E+12	7.793E+11	1.453E+12
65.25	117557863	0.200	2.348E+16	1.004E+12	6.995E+11	1.309E+12
65.5	117567472	0.191	2.247E+16	8.992E+11	6.251E+11	1.173E+12
65.75	117577081	0.183	2.150E+16	8.009E+11	5.559E+11	1.046E+12
66	117586691	0.175	2.057E+16	7.090E+11	4.915E+11	9.266E+11
66.25	117596301	0.167	1.968E+16	6.233E+11	4.316E+11	8.151E+11
66.5	117605912	0.160	1.882E+16	5.435E+11	3.761E+11	7.110E+11
66.75	117615523	0.153	1.799E+16	4.693E+11	3.246E+11	6.140E+11
67	117625134	0.146	1.719E+16	4.004E+11	2.770E+11	5.237E+11
67.25	117634746	0.140	1.643E+16	3.365E+11	2.330E+11	4.400E+11
67.5	117644358	0.133	1.570E+16	2.773E+11	1.923E+11	3.623E+11
67.75	117653971	0.127	1.500E+16	2.227E+11	1.549E+11	2.905E+11
68	117663584	0.122	1.432E+16	1.724E+11	1.204E+11	2.243E+11

68.25	117673197	0.116	1.368E+16	1.260E+11	8.875E+10	1.633E+11
68.5	117682811	0.111	1.306E+16	8.345E+10	5.971E+10	1.072E+11
68.75	117692425	0.106	1.247E+16	4.446E+10	3.311E+10	5.580E+10
69	117702040	0.101	1.191E+16	8.811E+09	8.811E+09	8.811E+09
69.25	117711655	0.097	1.137E+16	8.411E+09	8.411E+09	8.411E+09
69.5	117721270	0.092	1.085E+16	8.028E+09	8.028E+09	8.028E+09
69.75	117730886	0.088	1.035E+16	7.662E+09	7.662E+09	7.662E+09
70	117740502	0.084	9.882E+15	7.313E+09	7.313E+09	7.313E+09
Sum				2.740E+16	3.153E+16	2.326E+16

Appendix 16

NASA Factsheet (http://nssdc.gsfc.nasa.gov/planetary/factsheet/venusfact.html)

Bulk Parameters	Venus	Earth
Mass (10^{24} kg)	48.685	59.736
Volume (10^{10} km^3)	92.843	108.321
Equatorial radius (km)	6051.8	6378.1
Polar radius (km)	6051.8	6356.8
Mean density (kg/m^3)	5243	5515
Surface gravity (m/s^2)	8,87	9,8
Escape velocity (km/s)	10,36	11,19
Atmosphere	Venus	Earth
Surface pressure (bars)	92	1.014
Surface density (kg/m^3)	65	1.217
Scale height (km)	15,9	8,5
Total mass of atmosphere (10^{18} kg)	480	5,1
Average temperature (K)	737	288
Wind speeds at the surface (m/s)	0,3 - 1	0 - 100
Mean molecular weight (g/mole)	43.45	28.97

Reference List

1. Barker E. S. 1979, Detection of SO2 in the UV Spectrum of Venus, Geophysical Research Letters, vol. 6 (2), 117

2. Basilevsky A. et al. 1993, Magellan observations of the Venera and Vega landing site regions, Journal of Geophysical Research, vol. 98, 17069 – 17097

3. Basilevsky A. and Head J. 2003, The surface of Venus, Reports on Progress in Physics, vol. 66, 1699 – 1734

4. Bell J. et al. 1991, Spectroscopic observations of bright and dark emission features on the night side of Venus, Science, vol. 252, 1293 - 1296

5. Belyaev D. et al 2011, Sulphur oxides in Venus mesosphere detected from SPICAV/SOIR VEX solar occultation, European Planetary Science Congress, vol. 6, 1856

6. BertauxJ. L. et al. 1996, Vega 1 and Vega 2 entry probes, J. Geophys. Research, vol. 101, No. E5, 12709 – 12745

7. BezardB. et al. 1993, The abundance of sulphur dioxide below the clouds of Venus, Geophysical Research Letters, vol. 20, 1587 – 1590

8. Bluth G. J. et al. 1993, The contribution of explosive volcanism to global atmospheric sulphur dioxide concentrations, Nature, vol. 366, 327

9. Crisp D. et al. 1991, The dark side of Venus: Near infrared images and spectra from the Anglo American Observatory, Science, vol. 253, 1263 - 1266

10. Collard A. D. et al. 1993, Latitudinal distribution of carbon monoxide in the deep atmosphere of Venus, Astrophysical Journal, vol. 147, 1230 - 1237

11. De Bergh C. et al. 1991, Deuterium on Venus: Observations from Earth, Science, vol. 251, 547 - 549

12. De Bergh C. et al. 2006, The composition of the atmosphere of Venus below 100 km altitude: an overview, Planetary and Space Science, vol. 54, 1389 – 1397

13. Esposito L. W. et al, 1997 Chemistry of Lower Atmosphere and Clouds, Venus II : Geology, Geophysics, Atmosphere, and Solar Wind Environment, Tucson, AZ : University of Arizona Press, 415

14. Esposito L. W. et al. 1984, Sulfur dioxide shows evidence for Venus volcanism, Science, vol. 223, 1072

15. Esposito L. W. et al. 1979, Sulfur dioxide in the Venus atmosphere: Distribution and implications, Geophysical Research Letters, vol. 6, 601 – 604

16. Esposito L. W. et al. 1980, Ultraviolet contrasts and the absorbers near the Venus cloud tops, Journal Geophysical Research, vol. 85, 194 - 216

17. FederovaA. et al. 2008, HDO and H2O vertical distribution and isotopic ratio in the Venus mesosphere by Solar Occultation at Infrared spectrometer on board Venus Express, J. Geophys. Res., vol. 113

18. FegleyB. et al. 1988, Thermochemical kinetics of SO2 reactions with possible Venus crustal minerals: First data for calcite, Lunar Planet Science Conference XIX, 315 – 316

19. FegleyB. et al. 1989, Estimation of the rate of volcanism on Venus from reaction rate measurements, Nature, vol. 337, 55 – 58

20. FegleyB. et al. 1992, Venus surface mineralogy: observational and theoretical constraints. Lunar Planetary Science Conference XXII, 3 – 20

21. FegleyB. et al. 1995, The rate of pyrite decomposition the surface of Venus, Icarus, vol. 115, 159 – 180

22. FegleyB. et al 1995, Basalt oxidation and hematite formation on the surface of Venus, Icarus, vol. 188, 373 - 383

23. FegleyB. et al. 1997, Geochemistry of surface-atmosphere interaction, Venus II : Geology, Geophysics, Atmosphere, and Solar Wind Environment, Tucson, AZ : University of Arizona Press, 591

24. Fegley B. and Schaefer L. 2006, Thermal Outgassing of Ordinary Chondritic Material – I. nominal Model Results, Meteoritics& Planetary Scienc, vol. 41, 5275

25. Graf H. F. et al. 1997, Volcanic sulfur emissions: Estimates of source strength and its contribution to global sulfate distribution, Journal of Geophysical Research, vol. 102, 10727 - 10738

26. Haulet R. et al. 1977, Sulphur dioxide discharge from Mt. Etna, Nature, vol. 268, 715 - 717

27. HuntenD. m. et al. 1989, Escape of atmosphere and loss of water, Origin and Evolution of Planetary and Satellite Atmospheres, Tucson University of Arizona Press, 386 - 422

28. Imamura T. 2002, H2SO4 cycle in the Venusian tropical atmosphere as constrained by a microphysical cloud model, Advances in Space Research, vol. 29 (2), 249 -254

29. IwagamiN. et al. 2008, Hemispheric distribution of HCl above and below the Venus' clouds by ground based 1.7 µm spectroscopy, Planetary and Space Science, vol. 56 (10), 1424 – 1434

30. Krasnopolsky V. A. and Parshev V. A. 1983, Photochemistry of the Venus atmosphere, Venus I, Tucson, AZ : University of Arizona Press, 431 - 458

31. KrasnopolskyV. A. et al. 1985, Chemical compositions of Venus' clouds, Planetary Space Science, vol. 33, 109 - 117

32. KrasnopolskyV. A. and Pollack J. B. 1994, H20 – H2SO4 system in Venus' clouds and OCS, CO, and H2SO4 profiles in Venus' troposphere, Lunar and Planetary Inst, vol. 25, 747

33. KrasnopolskyV. A. 2007, Chemical kinetic model for the lower atmosphere of Venus, Icarus, vol. 191, 25 -37

34. Kulikov Y. et al. 2006, Atmospheric and water loss from early Venus, Planetary and Space Science, vol. 54, 1425 – 1444

35. Lambert G. et al. 1988, Volcanic output of SO_2 and trace metals: A new approach, Geochemica et CosmochemicaActa, vol. 52, 39 - 42

36. Landis G. et al. 2002, Atmospheric Flight on Venus, AIAA–2002–0819, NASA/TM—2002-211467

37. Lee Y. J. et al. 2009, Vertical structure of the Venus cloud tops from the joint analysis of the VeRa and VIRTIS observations onboard Venus Express, European Planetary Science Congress, 729

38. MarcqE. et al. 2005, Latitudinal variations of CO and OCS in the lower atmosphere of Venus from near-infrared nightsidespectro-imaging, Icarus, vol. 179, 375 – 386

39. MarcqE. et al. 2009, Composition of the Venusian atmosphere after Venus Express, European Planetary Science Congress, 448

40. MarcqE. et al. 2008, A latitudinal survey of CO, OCS, H2O and SO2 in the lower atmosphere of Venus, J. Geophys. Res., vol. 113

41. Markiewicz W. J. et al. 2009, Morphology and droplet sizes of the upper clouds of Venus, European Planetary Science Congress, 720

42. Marov M. Y., 2005, Transits of Venus: New Views of the Solar System and Galaxy, Proceedings of IAU Colloquium #196, Cambridge University Press, 209-219

43. Marshall J. R. et al. 1988, Aeolian weathering of Venus surface materials: Preliminary results from laboratory simulations, Icarus, vol. 74, 495 – 515

44. Möller D. et al. 1984, Estimation of man-made global sulfur emissions, Atmospheric Environment, vol. 18, 19 - 27

45. MorozV. et al. 1979, Spectrophotometric experiment on the Venera 11 and 12 descent modules, Cosmic Research, vol. 17, 61 – 614

46. Murdin P. 2000, Encyclopedia of Astronomy and Astrophysics, Bristol: Institute of Physics Publishing, article 3736

47. Na C. Y. et al. 1990, IUE observations of Venus SO2 and SO, J. Geophysical Research, vol. 95, 7485

48. Na C.Y. 1992, Sulfur Oxides in the Middle Atmosphere of Venus, Ph.D Thesis, Univ. of Colorado

49. Na C. Y. et al. 1994, Sulfur dioxide in the atmosphere of Venus: Modeling results, Icarus, vol. 112, 389-395

50. Na C. Y. et al. 1993, SO2 on Venus: IUE, HST and ground-based measurements and the active volcanism connection, LPSC XXIV, 1403-1404

51. Nicholson S. B., 1961, Publications of the Astronomical Society of the Pacific, Vol. 73, No. 432, 182

52. Pollack J. B. et al. 1993, Near infrared light from Venus' nightside: a spectroscopic analysis, Icarus, vol. 103, 1 - 42

53. PrinnR. G. et al. 1985, The photochemistry of the atmosphere of Venus, The photochemistry of Atmosphere, New York Academic Press, 281 – 336

54. Smith S. J. et al. 2011, Anthropogenic sulfur dioxide emissions: 1850 – 2000, Atmospheric Chemistry and Physics, vol. 11, 1101 – 1116

55. Stoiber R. et al. 1987, Annual contribution of sulfur dioxide to the atmosphere by volcanoes, Journal of Volcanology and Geothermal Research, vol. 33, 1

56. SurkovY. A. et al. 1986, Venus rock compositions at the Vega 2 landing site, Lunar Planetary Science Conference XVII, 215 – 218

57. Symonds R. B. et al 1994, Volcanic gas studies: methods, results and applications, Volatiles in Magma, Mineralogical Society of America Reviews in Mineralogy, v. 30,1-66.

58. Taylor F. W. 2010, Venus: Not evil, just a bit unfortunate, Astronomy and Geophysics, vol. 51, 26

59. Titov D. V. et al. 1983, On the possibility of aerosol formation by the reaction between SO2 and NH3 in Venus' atmosphere, Cosmic Research, vol. 21, 401

60. Tsang C. et al. 2009, Variability of CO concentrations in the Venus troposphere from Venus Express/VIRTIS using a band ratio technique, Icarus, vol. 201, 432 - 443

61. Tsang C. et al. 2010, Correlations between cloud thickness and sub-cloud water abundance on Venus, Geophysical Research Letters, vol. 37, 02202

62. Whittaker I. et al. 2009, The effect of solar wind conditions upon the atmospheric boundary layers at Venus, European Planetary Science Congress, 734

63. Wickramasinghe N. C. 2008, On the possibility of microbiota transfer from Venus to Earth, Astrophysical Space Science, vol. 37, 133 – 137

64. ZasovaL.et al. 2007, Structure of the Venus atmosphere, Planetary and Space Science, vol. 55, 1712 – 1728

65. Zhang T. L. et al. 2007, Little or no solar wind enters Venus‘ atmosphere at solar minimum, Nature, vol. 450, 654 – 656

66. Zolotov M. et al. 1996, A model of thermochemical equilibrium in the near surface atmosphere of Venus, Geochemistry Intl., vol. 33, 80 – 100

Picture Reference List

Figure 1.1: http://www.theosophy-nw.org/theosnw/world/mideast/49-99-0-mi-wtst-tablet-xi.jpg

Figure 1.2: http://mentallandscape.com/Venera_9.jpg

Figure 1.3: http://www.lunarplanner.com/Images/Venus/Venus-Express/VE-DoubleVortex.jpg

Figure 1.4: http://library.thinkquest.org/18652/gal_venus_nims_37221.jpg

Figure 2.2:Basilevsky A. and Head J. 2003, The surface of Venus, Reports on Progress in Physics, vol. 66, 1699 – 1734

Figure 2.3: http://www.realclimate.org/wp-content/uploads/airglowcartoon.gif
Figure 2.4: http://physics.uoregon.edu/~jimbrau/BrauImNew/Chap09/FG09_19.jpg

Figure 2.5: Esposito L. W. et al. 1979, Sulfur dioxide in the Venus atmosphere: Distribution and implications, Geophysical Reasearch Letters, vol. 6, 601 – 604

Figure 2.6: Bertaux J. L. et al. 1996, Vega 1 and Vega 2 entry probes, J. Geophys. Research, Vol. 101, No. E5, 12709 – 12745

Figure 2.7: Bertaux J. L. et al. 1996, Vega 1 and Vega 2 entry probes, J. Geophys. Research, Vol. 101, No. E5, 12709 – 12745

Figure 2.8: Tsang C. et al. 2009, Variability of CO concentrations in the Venus troposphere from Venus Express/VIRTIS using a band ratio technique, Icarus, vol. 201, 432 - 443

Figure 3.1: Bluth G. J. et al. 1993, The contribution of explosive volcanism to global atmospheric sulphur dioxide concentrations, Nature, vol. 366, 327

Curriculum Vitae

General
Name: Alen Đuričić, Bakk.
Adress: Hetzendorferstrasse 93/4/1, 1120 Vienna
Day of Birth: 12.12.1983
Place of Birth: Sarajevo, Bosnia & Hercegovina
Nationality: Austria
Parents: Mirsada Đuričić (Džeko) deceased, Ranko Đuričić

Education
1990 – 1992: elementary school in Sarajevo, Bosnia & Hercegovina
1992 – 1994: elementary school, Steinlechnergasse, in Vienna, Austria
1994 – 2002: gymnasium, Fichtnergasse BRG XIII, in Vienna, Austria
2002: start of university studies in Astronomy, University of Vienna

Jobs
Schülerhilfe Humer Wien – Mathematics Teacher (2004 – up to present)
Schülerhilfe Humer Wien – Mathematics Teacher & Coach (2008 – up to present)
VHS ISIS Project (State Award for Integration 2011) Wien – Mathematics Teacher (2010 – up to present)

Languages
Fluent in Bosnian/Croatian/Serbian (spoken and written)
Fluent in German (spoken and written)
Fluent in English (spoken and written)
French (Basic knowledge)

National/International Scientifc Membership
EOG – Eclipse Observing Group, Institute for Astronomy, University of Vienna (since 2006)
Research Platform – Exolife, University of Vienna (since 2009)

National/International Activity/Awards
Mathematical Olympiad (1999-2002) + 2nd Place in the National Competition (2000)
ESA Summer School Alpbach (2008)

National/International Conferences (active participation)
Europlanet, Potsdam, Germany (2009)
EGU, Vienna, Austria (2010)

National/International Conferences (passive participation)
ArchEnviron: Peering into the Cradle of Life: Processes and Habitats on the Archean Earth, Vienna, Austria (2008)

Additional Qualifications
Endorsement by Ibanez Guitars

Publications

- **Duricic A**., Firneis M., Leitner J.J. (2009), *SO2 in the Venusian lower atmosphere*, presented to the European Planetary Science Congress 2009, held 14-18 September in Potsdam, Germany, p. 308
- **Duricic A**., Leitner J. J., Firneis M. (2010), *SO2 vertical profile on Venus*, presented to the EGU General Assembly 2010, held 2-7 May, 2010 in Vienna, Austria, p. 6948
- Duffard R., **Duricic A**. et al. (2011), *A multiple-rendezvous, sample-return mission to two near-Earth asteroids*, Advances in Space Research, vol. 48, issue 1, p. 120 - 132

Additional Publications

- Music LP: Journey Saturnine – Ecliptica – Rebeat GmbH (2012)
- Music LP: The Longest Night – Dragony (2012)
- Music LP: (to be announced) – Dignity – Napalm Records (to be released in 2012)